

Unitarity Methods for Scattering Amplitudes in Perturbative Gauge Theories

by
MASSIMILIANO VINCON

A report presented for the examination
for the transfer of status to the degree of
Doctor of Philosophy of the University of London

Thesis Supervisor
DR ANDREAS BRANDHUBER

Centre for Research in String Theory
Department of Physics
Queen Mary University of London
Mile End Road
London E1 4NS
United Kingdom

*The strong do what they want and the weak suffer as they must.*¹

¹Thucydides.

Declaration

I hereby declare that the material presented in this thesis is a representation of my own personal work unless otherwise stated and is a result of collaborations with Andreas Brandhuber and Gabriele Travaglini.

Massimiliano Vincon

Abstract

In this thesis, we discuss novel techniques used to compute perturbative scattering amplitudes in gauge theories. In particular, we focus on the use of complex momenta and generalised unitarity as efficient and elegant tools, as opposed to standard textbook Feynman rules, to compute one-loop amplitudes in gauge theories. We consider scattering amplitudes in non-supersymmetric and supersymmetric Yang-Mills theories (SYM). After introducing some of the required mathematical machinery, we give concrete examples as to how generalised unitarity works in practice and we correctly reproduce the n -gluon one-loop MHV amplitude in non-supersymmetric Yang-Mills theory with a scalar running in the loop, thus confirming an earlier result obtained using MHV diagrams: no independent check of this result had been carried out yet. Non-supersymmetric scattering amplitudes are the most difficult to compute and are of great importance as they are part of background processes at the LHC. Lastly, we explore an alluring and fascinating relation between colour-ordered amplitudes in $\mathcal{N} = 4$ SYM and amplitudes in supersymmetric Quantum Electrodynamics (SQED) at the one-loop level. Furthermore, we consider the possibility of recursive structures of two-loop amplitudes in maximally SQED similar to the ones discovered for the $\mathcal{N} = 4$ SYM theory.

Contents

1	Prolegomenon	7
1.1	Outline	10
2	Some Preliminaries	13
2.1	Colour Ordering	13
2.2	Spinor Helicity Notation	16
2.3	Tree-Level Amplitudes	18
2.3.1	Complex Momenta and MHV Tree-Level Amplitudes	18
2.3.2	Supersymmetry at Tree Level	21
2.4	Supersymmetric Decomposition	23
2.5	Modern Methods	24
2.5.1	The CSW construction	25
2.5.2	CSW Extended: Fermions and Massless Scalars	27
2.5.3	The BCFW Recursion Relations	28
2.5.4	The MHV Amplitude as a Solution of the BCF Recursion Relation	30
3	Unitarity	32

<i>CONTENTS</i>	2
3.1 The Optical Theorem	33
3.2 Cutkosky Rules	34
3.2.1 One Step Backward, Two forward	35
3.3 Generalised Unitarity in $D = 4$	38
3.3.1 The Box Example	38
3.4 Generalised Unitarity in $D = 4 - 2\epsilon$	42
4 Scalar One-Loop Amplitudes	46
4.1 The MHV Scalar Amplitude: The Adjacent Case	49
4.2 The MHV Scalar Amplitude: The General Case	53
4.3 NMHV Scalar amplitudes	58
4.3.1 An Example: Coefficient of Three-Mass Triangle	60
5 Hidden Structures in (S)QED	66
5.1 In Search of the (S)QED-(S)QCD Correspondence	69
5.2 Approximate Iterative Structures in $\mathcal{N} = 2$ SQED	75
6 An <i>Antipasto</i> of Wilson Loop-$\mathcal{N} = 4$ SYM Duality	81
6.1 Collinear Limit of Gluon Amplitudes	83
6.2 One-Loop Splitting Amplitudes from Light-like Wilson Loops	85
7 Conclusions and Outlook	92
A Spinor and Dirac Traces Identities	94
A.1 Spinor Identities	94

<i>CONTENTS</i>	3
A.2 Dirac Traces	96
B Feynman Rules for a $SU(N_c)$ Gauge Theory	98
B.1 Feynman Rules	98
B.2 Feynman Rules in the Spinor Helicity Formalism	100
B.2.1 Wavefunctions	100
B.2.2 Propagators	101
B.3 Vertices	101
C Tensor Integrals	102
C.1 Bubble Integrals	102
C.2 Triangle Integrals	103
C.3 Box Integrals	103
D Passarino-Veltman Reduction	104
E Twistor Space	107

List of Figures

2.1	<i>Examples of application of complex momenta: three-point amplitude and generalised unitarity cuts.</i>	19
2.2	<i>The five-gluon tree level amplitude computed in a Feynman fashion.</i>	25
2.3	<i>The four allowed diagrams contributing to $\mathcal{A}_5(1^-, 2^-, 3^-, 4^+, 5^+)$. Observe how all vertices are MHV.</i>	27
2.4	<i>The four allowed diagrams contributing to $\mathcal{A}_5(1_q^-, 2^-, 3^-, 4^+, 5_q^+)$. We point to the fact that helicity conservation is respected and all the vertices are still MHV.</i>	28
2.5	<i>A diagrammatic representation of (2.5.11).</i>	30
2.6	<i>The only diagram contributing to $\mathcal{A}_n(1^-, 2^+, \dots, m^-, \dots, n^+)$ for $m > 3$. Notice that the vertex on the left is a googly MHV amplitude.</i>	31
3.1	<i>The optical theorem (3.1.7): the imaginary part of the forward scattering amplitude given as a sum of intermediate states.</i>	34
3.2	<i>A pictorial representation of (3.2.6).</i>	36
3.3	<i>The two possibilities: either i and j on the same side of the cut or on opposite sides.</i>	37
3.4	<i>A possible quadruple-cut contributing to the $1^- 2^- 3^+ 4^+ 5^+$ amplitude. The remaining quadruple-cuts are obtained by a colour-ordered cyclic permutations of the external states.</i>	39

- 3.5 *The remaining quadruple-cuts contributing to the one-loop $1^-2^-3^+4^+5^+$ amplitude.* 41
- 3.6 *One of the two possible quadruple cuts contributing to the $1^+2^+3^+4^+$ amplitude. The other diagram, which is identical to the one depicted here, is obtained by flipping the internal helicities so that the final result is achieved by doubling the contribution coming from the diagram in this Figure.* 43
- 3.7 *The triple-cut diagram contributing to the $1^+2^+3^+4^+$ amplitude. There are four such diagrams obtained by cyclic permutations of the external particles.* 44
- 4.1 *The three-particle cut diagram contributing to the n -gluon amplitude in the case of adjacent negative-helicity gluons* 50
- 4.2 *One of the two possible triple cut diagrams contributing to the n -gluon amplitude in the general case. The other triple cut diagram is obtained by swapping i and j through the replacements $m_1 - 1 \rightarrow m_1$ and $m_2 \leftrightarrow m_1$. 53*
- 4.3 *A quadruple cut diagram contributing to the n -gluon amplitude in the general case.* 57
- 4.4 *The triple-cut diagrams contributing to the n -gluon one-loop NMHV scalar amplitude $\mathcal{A}_{scalar}^n(1^+, \dots, i^-, j^-, \dots, k^-, \dots, n^+)$* 59
- 4.5 *The triple-cut diagram contributing to the n -gluon scalar NMHV amplitude $\mathcal{A}_n(1^+, \dots, i^-, \dots, j^-, \dots, k^-, \dots, n^+)$* 62
- 5.1 *The two-mass easy box function appearing in (5.1.1). The momenta $p = k_3$ and $q = k_4$ are null, whereas $P := k_1 + k_5 + \dots + k_m$ and $Q := k_2 + k_{m+1} + \dots + k_n$ are massive. The one-mass box function in (5.1.1) is obtained by setting $m = n$, so that the top right corner becomes massless (and contains only the momentum k_2).* 71
- 5.2 *In this Figure we plot (the real part of) the right-hand side of (5.2.10), representing the four-point two-loop MHV amplitude in $\mathcal{N} = 2$ SQED, together with our ansatz (5.2.6), with $y = -u/s$ given by set I. The two overlapping functions are hardly distinguishable in this plot.* 79

- 5.3 *This figure shows a plot of the $\mathcal{N} = 2$ SQED remainder function, constructed as the difference between the two-loop MHV amplitude in $\mathcal{N} = 2$ SQED and (5.2.6). 80*
- 6.1 *A one-loop correction to the Wilson loop, where the gluon stretches between two non-adjacent segments (left) which, in the collinear limit (right) gives rise to finite and IR contributions to $r_1^{[1]}(z)$ and IR contributions to $\mathcal{M}_{n-1}^{1-loop}$ 86*
- 6.2 *A one-loop correction to the Wilson loop, where the gluon stretches between two lightlike momenta meeting at a cusp both (case a) or only one (case b) going collinear. This kind of diagrams contributes to $r_1^{[1]}(z)$ by providing infrared-divergent terms of the form given in (6.2.3). 90*
- 6.3 *A one-loop correction to the Wilson loop, where the gluon stretches between either two adjacent lightlike momenta $p, q \neq 1, 2$ meeting at a cusp (case a) providing IR divergences to $\mathcal{M}_{n-1}^{1-loop}$ or two non-adjacent lightlike momenta with $q \neq 3, n$ (case b) contributing to the finite part of $\mathcal{M}_{n-1}^{1-loop}$. 91*
- E.1 *Pictorial representation in twistor space of a MHV amplitude (left) and NMHV amplitude (right). 110*

Chapter 1

Prolegomenon

Although we have long left behind the *a-tom* of Democritus, we are nevertheless struggling to understand and describe our modern version of atom. Particle physics as we are taught, and as we in turn try to teach, is concerned with the study of objects so infinitesimally smaller than Democritus' atoms that the only viable method to probe them is to collide¹ them and describe their behaviour after the collision. Thankfully, a proportion of mankind is inclined toward a thorough understanding of the universe through every means at its disposal, and it has managed to define a physical quantity that describes the behaviour of such a particle collision: the scattering cross section which is proportional to the probability that the process will indeed occur. We interpret the probability as the absolute value squared of a quantum mechanical amplitude.

Scattering amplitudes are computed in an expansion in power series of coupling constants. At the leading order (LO), many methods both numerical MADGRAPH [1], CompHEP [2] and analytical (see rest of the thesis) are available. However, there are some instances in which a next-to-next-to-leading order (NNLO) enhances the scattering amplitude by several orders of magnitude. At the LHC, statistical evidence for the scalar Higgs boson responsible for generating mass in electro-weak (EW) symmetry breaking, is expected to be found. A NNLO calculation for the Higgs boson would boost its cross section by a factor of two [3–6]. Additionally, a whole host of supersymmetric partners of the known particles is awaited with much trepidation. Below, we show a table representing some sort of “priority” wishlist of next-to-leading (NLO) processes expected to take place at the LHC which the experimental particle physics community has addressed to the attention of the theoretical community. Be that as it may, the signatures for new physics will be so intertwined with the physics we already know that

¹Our most favourite particle collider is the Large Hadron Collider (LHC), which is currently out of order and scheduled to resume in November 2009.

process ($V \in \{Z, W, \gamma\}$)	relevant for
1. $pp \rightarrow V V$ jet	$t\bar{t}H$, new physics
2. $pp \rightarrow t\bar{t}b\bar{b}$	$t\bar{t}H$
3. $pp \rightarrow t\bar{t} + 2$ jets	$t\bar{t}H$
4. $pp \rightarrow V V b\bar{b}$	VBF $\rightarrow H \rightarrow VV$, $t\bar{t}H$, new physics
5. $pp \rightarrow V V + 2$ jets	VBF $\rightarrow H \rightarrow VV$
6. $pp \rightarrow V + 3$ jets	various new physics signatures
7. $pp \rightarrow V V V$	SUSY trilepton

Table 1.1: The LHC “priority” wishlist, extracted from [7].

calculations at least at NLO order will be required in order to separate the new and interesting events from the known background.

Theory hand-in-hand with experiment have given to mankind a somewhat comprehensive and accurate description of the realm of particle physics, the *standard model* (SM). It purports to happily nest three of the four known fundamental forces of nature, *i.e.* electro-weak theory and quantum chromodynamics (QCD), next to each other in a quantum gauge field theory with gauge group $SU(3) \times SU(2) \times U(1)$. However, the story is not all flowers and roses in that, for instance, gravity is not incorporated into the SM. Also, one of the problems that mostly affects the SM is its incapacity to explain the *hierarchy problem*, the discrepancy between the energy scale of EW theory $m_{\text{EW}} \sim 10^3$ GeV and grand unified theory (GUT) or Planck scale $M_{\text{Pl}} = G_{\text{N}}^{-1/2} \sim 10^{18}$ GeV, *i.e.* the discrepancy between the mass of the Higgs boson and the GUT scale or the Planck mass. It is thought that the SM should be coming naturally from a GUT with gauge groups $SU(5)$ or $SO(10)$ that spontaneously breaks to $SU(3) \times SU(2) \times U(1)$ at energies $M_{\text{GUT}} \sim 10^{14} - 10^{16}$ GeV.

Traditionally, scattering amplitudes in gauge theories are computed using Feynman rules, which are derived from an action. Alas, although the result is generally simple and elegant, the number of diagrams grows factorially as the number of external particles involved in the scattering process increases. Inevitably, one is led to develop alternative and more efficient ways of calculating scattering amplitudes by exploring as many and diverse roads as possible.

One such road was undertaken in [8] where a duality was found between type IIB string theory residing in the product space of 5-dimensional anti-de-Sitter space (AdS) and a 5-sphere, $\text{AdS}_5 \times \mathbb{S}^5$, and conformal $\mathcal{N} = 4$ super-Yang-Mills (SYM) theory in

Minkowski space with gauge group $SU(N_c)$, where the number of colours $N_c \rightarrow \infty$ [9]. The duality, generally known as the AdS/CFT correspondence, relates a weakly-coupled string theory to a strongly-coupled four-dimensional gauge theory.

In [10], another remarkable duality was found between weakly-coupled $\mathcal{N} = 4$ SYM in Minkowski space and weakly-coupled topological string theory on a Calabi-Yau $\mathbb{CP}^{3|4}$. In the same paper, a geometrical property of amplitudes in $\mathcal{N} = 4$ SYM was evinced, namely that tree-level² scattering amplitudes in $\mathcal{N} = 4$ SYM localise on curves in twistor space [11]. For example, the simplest of such scattering amplitudes, the maximally helicity violating (MHV) amplitudes, localise on algebraic curves of degree 1 in twistor space. This observation explained the simplicity of tree-level scattering amplitudes computed in a Feynman manner. The geometrical interpretation of amplitudes in twistor space led to a novel diagrammatic approach [12] for computing tree amplitudes in which the MHV amplitudes are employed as vertices, which are in turn glued by scalar propagators. In [13–15], a mathematical justification for these rules in terms of a light-cone Lagrangian formulation was given.

In spite of the situation at one loop being initially less clear, the diagrammatic approach of [12] was extended in [16] to compute one-loop MHV amplitudes in $\mathcal{N} = 4$ SYM, confirming earlier results of [17]. Subsequently, MHV amplitudes in $\mathcal{N} = 1$ SYM and pure Yang-Mills were given in [18, 19] and [20] respectively, confirming earlier work [21] and presenting for the first time the infinite sequence of MHV amplitudes in pure Yang-Mills theory. However, it was realised that the MHV diagrammatic approach only computes the *cut-constructible* part of an amplitude, thus missing³ certain rational contributions to the amplitude. In [22], the rational terms for the MHV amplitudes in pure Yang-Mills were presented, thus providing the complete n -gluon MHV amplitude in QCD using a supersymmetric decomposition of one-loop amplitudes in QCD.

In [23, 24], an entirely different road was followed which led to certain on-shell recursion relations for tree-level amplitudes in gauge theory. Based on the existence of relations between tree and one-loop amplitudes in $\mathcal{N} = 4$ SYM [25–28] and using complex momenta and complex analysis, recursion relations were found which allow one to construct *all* n -point scattering amplitudes starting from complex three-point amplitudes. Similar recursive structures were later discovered for tree-level amplitudes in gravity [29, 30]. At one loop, these on-shell recursive relations were applied to construct the rational parts of MHV scattering amplitudes in QCD [31–36]. On the gravity side, use of on-shell recursive relations yielded some one-loop results in [37].

²The tree-level amplitudes arise from a one-instanton computation which leads to a formalism similar to that introduced in [184].

³Rational terms are present in both supersymmetric and non-supersymmetric amplitudes. However, in supersymmetric theories the rational terms are uniquely linked to the cut-constructible parts [17, 21].

A study of collinear limits of maximally supersymmetric gauge theories amplitudes [38], led to the discovery of intriguing iterative structures of amplitudes in planar $\mathcal{N} = 4$ SYM. Namely, it was shown how the two-loop four-point MHV amplitude in $\mathcal{N} = 4$ SYM could be expressed in terms of one-loop amplitudes. This observation prompted speculation that the same iterative structure should hold for n -point MHV amplitudes for any number of loops and, to this end, an impressive three-loop calculation of the four-point MHV amplitude in $\mathcal{N} = 4$ SYM was carried out in [39]. There, an all-loop resummed formula for the n -point MHV amplitude was conjectured according to which multi-loop amplitudes could be recast in terms of one-loop amplitudes together with some kinematic-independent quantities. A two-loop calculation of the five-point amplitude [40] further confirmed the conjecture of [39].

The profound implications of the AdS/CFT correspondence were put to work in a seminal paper [41] in which the calculation of the four-point amplitude reproduced the strong-coupling limit of the all-loop *ansatz* proposed in [39]. This new finding suggested that a polygonal n -sided Wilson loop, this time evaluated at weak-coupling, could be related to the perturbative n -point MHV amplitude in $\mathcal{N} = 4$ SYM. The latter conjecture was successfully shown to hold at one-loop for the four-point [42] and n -point [43] amplitude. A two-loop calculation for the four- [44] and five-sided [45] Wilson loop, gave more evidence to the Wilson loop conjecture and at the same time testified favourably for the proposal of [39]. However, while a computation of the two-loop six-point MHV amplitude in $\mathcal{N} = 4$ SYM [46] revealed an incompleteness of the *ansatz* whereby the addition of a function (called remainder function) was needed, a parallel computation of the six-sided Wilson loop at two loops [47, 48] confirmed both the results of [46] and the correctness of the Wilson loop/MHV amplitude duality.

1.1 Outline

The thesis focuses on twistor string inspired methods to compute perturbative scattering amplitudes. In particular, the use of complex momenta and a novel approach to (generalised) unitarity will play a fundamental role throughout this thesis. In Chapter 2 we introduce the reader to some necessary machinery, which will be helpful (hopefully) to understand later chapters. Specifically, we review the spinor helicity formalism and the use of complex momenta to compute scattering amplitudes together with the simplest example of MHV amplitude, the three-point gluon amplitude. We present supersymmetric Ward identities (SWI), which are essential in computing scattering amplitudes with fermions or scalars running in the loop. Furthermore, we introduce the CSW construction by sketching the derivation of a five-point Next-to-MHV (NMHV) amplitude

which has three negative-helicity gluons. We end the chapter by recalling on-shell recursion relations which, based on the use of complex analysis, allow the construction of n -point tree-level amplitudes in terms of $n - 1$ -point and lower-point amplitudes.

Much of what lies at the heart of this thesis goes back to the S-matrix programme developed in the sixties. Although initially incepted as a theory for the strong interaction, it gradually lost momentum and allure due to the development of QCD, which was emerging as the correct theory describing the strong interaction. However, in the nineties it was taken up again, refined and, with the introduction of dimensional regularisation which was alien to the original formulation of the S-matrix programme, put to work to produce results which were unthinkable to obtain with Feynman graph techniques. In Chapter 3 we witness the revival of the S-matrix programme by working through simple examples.

In Chapter 4 we, based on the original work [49] of the author of this thesis, offer a complete rederivation of the n -point one-loop MHV amplitude in pure Yang-Mills by means of generalised unitarity. Due to a supersymmetric decomposition of QCD amplitudes (shown in Chapter 2) in terms of $\mathcal{N} = 4$, $\mathcal{N} = 1$ and pure Yang-Mills contributions, the knowledge of the scalar contribution to a QCD amplitude provides the last bit of information toward the full one-loop QCD amplitude⁴. Most of the calculation is found in the chapter, although we defer the nitty gritty to Appendix C and D. We conclude the chapter by considering NMHV pure Yang-Mills one-loop amplitudes. We stress the difficulties arising in computing such an amplitude and we offer a detailed and original⁵ calculation of the coefficient of the three-mass triangle integral function. Having the reader mastered Chapter 2 and Chapter 3, she/he will find Chapter 4 extremely digestible.

Since much of the thesis is focussed on gluon amplitudes, we felt obliged to pay tribute to (supersymmetric) quantum electrodynamics (SQED). In Chapter 5 we prove a relation between coefficients of certain integral functions in (S)QED and the correspondent integral functions in (S)YM. We then proceed to conclude the chapter by exploring the possibility of hidden recursive structures of two-loop amplitudes in $\mathcal{N} = 2$ SQED similar to the ones discovered in $\mathcal{N} = 4$ SYM. Although not on the same footing as those in $\mathcal{N} = 4$ SYM, we nevertheless manage to expose an approximate recursive structure for $\mathcal{N} = 2$ SQED which deserves to be more deeply explored. All of the chapter is based on the original work [51] of the author of this thesis.

Nearing the end of the thesis, we could not have finished without mentioning the

⁴Up to some rational coefficients. See discussions in Chapter 3 and Chapter 4.

⁵The coefficient of the NMHV three-mass triangle function in pure Yang-Mills was computed by the author of this thesis in an unpublished work. Much later on, it was published by other authors in [50].

duality between Wilson loop diagrams and $\mathcal{N} = 4$ SYM scattering amplitudes. By switching back to gluons, in Chapter 6 we introduce the reader to this remarkable duality and use it to compute⁶ the one-loop splitting amplitude from light-like Wilson loops finding agreement with a previous version of the calculation by means of unitarity.

In Chapter 7 we conclude the thesis with a summary of the work done and we discuss what the future may hold. A series of Appendices on spinors and Dirac traces, on Feynman rules, on tensor integrals and twistor space follows suit.

⁶This result was first arrived at by the author of this thesis in an unpublished work. It was subsequently published by others in [52].

Chapter 2

Some Preliminaries

It is common and unfortunate knowledge that computing scattering amplitudes in gauge theories by means of Feynman rules is a rather tedious and lengthy procedure. The complexity of the calculation of the amplitudes grows beyond control as the number of both external and internal particles increases. Nevertheless, the final result is often quite simple and neat. Why? Scattering amplitudes are functions of several variables which describe colour quantum numbers, polarisation states and kinematics. All this redundant information comes from employing Feynman rules. In order to disentangle all of the information and render the computation more manageable, it has become common to express the polarisation states by recurring to the spinor helicity formalism and to organise the colour dependence of the scattering amplitude in colour ordered subamplitudes, or primitive amplitudes. In § 2.1 we describe what colour ordering an amplitude means while we postpone the spinor helicity formalism to § 2.2. The use of complex momenta to deal with the kinematics of scattering amplitudes is given in § 2.3.1 of this chapter. Rudiments of supersymmetry are elucidated in § 2.3.2.

2.1 Colour Ordering

We may begin this section by recalling that colour decomposition dates back in time to the early formulation of string theory as a theory for Quantum Chromodynamics (QCD) [53–57]. The basic idea behind colour ordering is to divide a scattering amplitude into smaller gauge invariant pieces by using group theory arguments. We take our gauge group to be $SU(N_c)$ as it is the most commonly studied. Quarks and antiquarks transform in the fundamental \mathbf{N}_c and antifundamental $\bar{\mathbf{N}}_c$ representations respectively, carrying indices $i, \bar{j} = 1, 2, \dots, N_c$, whilst gluons carry an adjoint colour index $a =$

$1, 2, \dots, N_c^2 - 1$. The colour structure is encoded in the gauge group structure constants, which may be written in terms of traces of products of Hermitian $N_c \times N_c$ fundamental representation matrices, the $SU(N_c)$ generators $(T_a)_i^{\bar{j}}$, with $a = 1, 2, \dots, N_c^2 - 1$, as

$$f^{abc} = -\frac{i}{\sqrt{2}} \text{Tr}[[T^a, T^b], T^c], \quad (2.1.1)$$

where we employ the following normalisation

$$[T^a, T^b] = i\sqrt{2}f^{abc}T^c, \quad \text{Tr}[T^a T^b] = \delta^{ab}. \quad (2.1.2)$$

According to the Feynman rules, we shall have a factor of $(T^a)_i^{\bar{j}}$ for each gluon-quark-antiquark vertex, a structure constant f^{abc} for each pure gluon three-vertex and contracted products of structure constants $f^{abe}f^{cde}$ for each pure gluon four-vertex. Clearly, replacing all the structure constants f^{abc} by means of (2.1.1) produces a long string of trace factors of the form $\text{Tr}(\dots T^a \dots) \text{Tr}(\dots T^a \dots) \dots (\dots)$ if we consider only external gluonic states. If we include external quarks, then there will also be some strings of trace factors terminating with (anti) fundamental indices of the form $\text{Tr}(T^a \dots T^b)_i^{\bar{j}}$. Let us now introduce the Fierz identity

$$(T^a)_i^{\bar{j}}(T^a)_k^{\bar{l}} = \delta_i^{\bar{l}}\delta_k^{\bar{j}} - \frac{1}{N_c}\delta_i^{\bar{j}}\delta_k^{\bar{l}}, \quad (2.1.3)$$

where summation over repeated indices is understood. At tree level, by means of (2.1.3), we are able to cast all the structure constants in terms of sums of single traces of generators. As we are mostly concerned with gluon scattering, we may write a general amplitude as

$$A_n^{\text{tree}} = g^{n-2} \sum_{\sigma_i \in S_n/Z_n} \text{Tr}[T^{a_{\sigma_1}} T^{a_{\sigma_2}} \dots T^{a_{\sigma_n}}] \mathcal{A}_n^{\text{tree}}(\sigma_1, \sigma_2, \dots, \sigma_n), \quad (2.1.4)$$

where g is the gauge coupling, S_n is the set of permutations of n objects and Z_n is the subset of cyclic permutations so that the sum in (2.1.4) is taken over the set of inequivalent traces. The $\mathcal{A}_n^{\text{tree}}(\sigma_1, \sigma_2, \dots, \sigma_n)$ quantities are the *partial amplitudes*, which contain all the kinematic information. These *colour ordered* sub-amplitudes are simpler to deal with because they correspond to only one specific colour ordering and thus they depend on less kinematic variables¹. For example, the simplest of such sub-amplitudes, will be

$$A_3^{\text{tree}} = g (\text{Tr}[T^{a_1} T^{a_2} T^{a_3}] \mathcal{A}_3^{\text{tree}}(1, 2, 3) + \text{Tr}[T^{a_1} T^{a_3} T^{a_2}] \mathcal{A}_3^{\text{tree}}(1, 3, 2)). \quad (2.1.5)$$

¹Specifically, they will depend on only adjacent momenta.

The usefulness of partial amplitudes really becomes manifest as the number of external legs increases. For example, computing the five-gluon amplitude would require only ten colour-ordered diagrams as opposed to forty if we use all the Feynman diagrams. Had we to include matter in the fundamental representation, the strings of matrices appearing in (2.1.4) would carry (anti)-fundamental indices i, \bar{j} ; however, the matrices will not be traced as the i, \bar{j} indices of the fundamental representation run freely. Equation (2.1.3) is a mathematical statement about the tracelessness of the T^a generators of $SU(N_c)$: the $1/N_c$ term subtracts the trace of $U(N_c)$ group in which $SU(N_c)$ is embedded. If we consider a theory with gauge group $U(N_c) = SU(N_c) \times U(1)$, then the $U(1)$ generator will be given by

$$(T_{U(1)}^a)_i^{\bar{j}} = \frac{1}{\sqrt{N_c}} \delta_i^{\bar{j}}, \quad (2.1.6)$$

which, once added to (2.1.3), will cancel the term proportional to $\frac{1}{N_c}$. Thus, from a physical point of view, (2.1.3) instructs us to subtract at each vertex the contribution coming from a $U(1)$ gauge boson, generally called the photon as it is colourless and it does not couple to gluons. At loop level, additional colour structures, such as double traces in the one-loop n -gluon amplitude, appear. In the large- N_c limit ($N_c \rightarrow \infty$) [9], the single-trace terms would give rise to planar leading-colour contributions while multi-trace terms would give rise to non-planar subleading-colour contributions. For example, the one-loop five-gluon amplitude takes the following colour decomposition

$$\begin{aligned} A_5^{1\text{-loop}} = g^5 & \left[\sum_{\sigma \in S_5/Z_5} N_c \text{Tr}(T^{a_{\sigma_1}}, \dots, T^{a_{\sigma_5}}) \mathcal{A}_5^{1\text{-loop}}(\sigma_1, \dots, \sigma_5) \right. \\ & \left. + \sum_{\sigma \in S_5/(S_2 \times S_3)} \text{Tr}(T^{a_{\sigma_1}} T^{a_{\sigma_2}}) \text{Tr}(T^{a_{\sigma_3}} T^{a_{\sigma_4}} T^{a_{\sigma_5}}) \mathcal{A}_{5,\text{non-planar}}^{1\text{-loop}}(\sigma_1, \dots, \sigma_5) \right]. \end{aligned} \quad (2.1.7)$$

Nevertheless, one may utilise formulæ which relate double-traces terms to permutations of colour-ordered quantities [17, 58, 59].

We conclude this section by mentioning that it was 't Hooft [9] who realised that for gauge theories with gauge group $SU(N_c)$, apart from the coupling g_{YM} there exists a dimensionless parameter, $1/N_c$, which can be employed in an expansion. The 't Hooft limit $N_c \rightarrow \infty$ with $\lambda = g^2 N_c = \text{constant}$ and N_c the number of colours, has been at the core in the studies of the AdS/CFT correspondence [8]. Succinctly, without entering this vast topic and referring the reader to the original work, the correspondence conjectures an equivalence between conformal four dimensional gauge theories and string theories in $AdS \times X$. The most studied and used version of this correspondence involves $\mathcal{N} = 4$ supersymmetric gauge theory with gauge group $SU(N_c)$ on one side and Type IIB string theory on $AdS_5 \times S^5$ on the other. The correspondence is also conjectured to hold for M-theory and non-conformal gauge theories although it is much less understood for the last two cases.

2.2 Spinor Helicity Notation

We can now turn to the second important ingredient for calculating scattering amplitudes. Introduced back in the early eighties to represent polarisation vectors [60–64], spinors of massless particles have brought about a major simplification in the calculation of scattering amplitudes. Spinors of lightlike particles are solutions of the massless Dirac equation

$$p_\mu \gamma^\mu u(p) = \not{p}u(p) = 0, \quad (2.2.1)$$

where $u(p)$ is a four component spinor and γ^μ , $\mu = 0, \dots, 3$, in the chiral representation of Dirac γ -matrices, are

$$\gamma^0 = \begin{pmatrix} 0 & 1 \\ -1 & 0 \end{pmatrix}, \quad \gamma^i = \begin{pmatrix} 0 & \sigma^i \\ \sigma^i & 0 \end{pmatrix}, \quad \gamma_5 = \begin{pmatrix} 0 & 1 \\ 1 & 0 \end{pmatrix} \quad (2.2.2)$$

where σ^i are the standard Pauli matrices. We write a generic negative-chirality spinor λ_α with $\alpha = 1, 2$ and, similarly, a generic positive-chirality spinor $\tilde{\lambda}_{\dot{\alpha}}$ with $\dot{\alpha} = 1, 2$, where all indices are raised and lowered with the antisymmetric tensors ϵ_{ab} , $\epsilon_{\dot{\alpha}\dot{\beta}}$ and so on. We define antisymmetric Lorentz-invariant scalar products between spinors as

$$\langle \lambda \eta \rangle = \epsilon_{\alpha\beta} \lambda^\alpha \eta^\beta = \epsilon^{\alpha\beta} \lambda_\alpha \eta_\beta = \lambda^\alpha \eta_\alpha, \quad (2.2.3)$$

$$[\tilde{\lambda} \tilde{\eta}] = \epsilon_{\dot{\beta}\dot{\alpha}} \tilde{\lambda}^{\dot{\alpha}} \tilde{\eta}^{\dot{\beta}} = \epsilon^{\dot{\beta}\dot{\alpha}} \tilde{\lambda}_{\dot{\alpha}} \tilde{\eta}_{\dot{\beta}} = \tilde{\lambda}_{\dot{\alpha}} \tilde{\eta}^{\dot{\alpha}}. \quad (2.2.4)$$

It follows that for negative-chirality spinors we have $\langle \lambda \eta \rangle = -\langle \eta \lambda \rangle$ and similarly for positive-chirality spinors. The Dirac spinors can be written as two two-component spinors

$$u(p) = \begin{pmatrix} u_\alpha(p) \\ \tilde{u}^{\dot{\alpha}}(p) \end{pmatrix}. \quad (2.2.5)$$

By writing a momentum vector p^μ as a bi-spinor $p_{\alpha\dot{\alpha}}$ with one spinor index a and \dot{a} of each chirality, we then have

$$p_{\alpha\dot{\alpha}} = p_\mu \sigma_{\alpha\dot{\alpha}}^\mu = p_0 \mathbb{1} + \vec{p} \cdot \vec{\sigma} \quad (2.2.6)$$

$$= \begin{pmatrix} p_0 + p_3 & p_1 - ip_2 \\ p_1 + ip_2 & p_0 - p_3 \end{pmatrix}, \quad (2.2.7)$$

from which $p_\mu p^\mu = \det(p_{\alpha\dot{\alpha}})$ follows. Hence, p_μ is light-like ($p^2 = 0$) if $\det(p_{\alpha\dot{\alpha}}) = 0$ which entails that massless vectors are those which can be cast as

$$p_{\alpha\dot{\alpha}} = \lambda_\alpha \tilde{\lambda}_{\dot{\alpha}}, \quad (2.2.8)$$

for some Weyl spinors $(\lambda_\alpha, \tilde{\lambda}_{\dot{\alpha}})$ defined up to the scaling

$$(\lambda, \tilde{\lambda}) \rightarrow (c\lambda, c^{-1}\tilde{\lambda}) \in \mathbb{C}, \quad (2.2.9)$$

for a complex number c^2 .

It is interesting to consider spinors in different signatures. In Minkowski signature $(+ - - -)$ for real null momenta, the spinors λ_α and $\tilde{\lambda}_{\dot{\alpha}}$ have to be taken complex conjugates of each other

$$\bar{\lambda}_{\dot{\alpha}} = \pm \tilde{\lambda}_{\dot{\alpha}}, \quad (2.2.10)$$

where the \pm refers to whether p_μ has a positive (incoming particle) or negative (outgoing particle) energy. For complex momenta, the spinors λ_α and $\tilde{\lambda}_{\dot{\alpha}}$ are independent complex variables while in signature $(+ + - -)$, the spinors λ_α and $\tilde{\lambda}_{\dot{\alpha}}$ are real and independent. However, $p_\mu p^\mu = \det(p_{\alpha\dot{\alpha}})$ holds generally so that we can write the scalar product for any two light-like vectors p and q as

$$-2(p \cdot q) = \langle \lambda_p \lambda_q \rangle [\tilde{\lambda}_p \tilde{\lambda}_q], \quad (2.2.11)$$

where in (2.2.11) we use the standard sign convention found in the perturbative field theory literature which differ by a minus sign from the string literature.

To describe massless particles of helicity \pm , in addition to their momentum vector p_μ , we introduce a spinor representation for their polarisation vectors ε_μ

$$\varepsilon_\mu^+(p_i, \kappa_i) = \frac{\langle \kappa_i | \gamma_\mu | p_i \rangle}{\sqrt{2} \langle \kappa_i p_i \rangle}, \quad \varepsilon_\mu^-(p_i, \kappa_i) = \frac{\langle p_i | \gamma_\mu | \kappa_i \rangle}{\sqrt{2} [p_i q_i]}, \quad (2.2.12)$$

where κ is some massless reference momentum. In terms of bi-spinor, (2.2.12) can be written as

$$\varepsilon_{\alpha\dot{\alpha}}^+ = \frac{\lambda_{\kappa_i\alpha} \tilde{\lambda}_{p_i\dot{\alpha}}}{\sqrt{2} \langle \lambda_{\kappa_i} \lambda_{p_i} \rangle}, \quad \varepsilon_{\alpha\dot{\alpha}}^- = \frac{\lambda_{p_i\alpha} \tilde{\lambda}_{\kappa_i\dot{\alpha}}}{\sqrt{2} [\lambda_{p_i} \lambda_{\kappa_i}]}. \quad (2.2.13)$$

The polarisation vectors ε_μ are constrained by the Lorentz gauge condition $\varepsilon^\pm(p, \kappa) \cdot p = 0$ since $\langle \lambda \lambda \rangle = [\tilde{\lambda} \tilde{\lambda}] = 0$. By judiciously choosing the reference momenta κ_i of like-helicity gluons to be identical and to equal the external momentum of one of the opposite-helicity set of gluons, it is possible to greatly simplify a calculation by making

²If we were not in a complex Minkowski space, the scaling c would be a pure phase $c = e^{i\phi}$.

many terms and diagrams vanish due to the following standard properties:

$$\varepsilon_i^\pm(\kappa, p_i) \cdot \kappa = 0, \quad (2.2.14)$$

$$\varepsilon_i^+(\kappa, p_i) \cdot \varepsilon_i^+(\kappa, p_i) = \varepsilon_i^-(\kappa, p_i) \cdot \varepsilon_i^-(\kappa, p_i) = 0, \quad (2.2.15)$$

$$\varepsilon_i^+(\kappa, p_j) \cdot \varepsilon_j^-(\kappa, p_i) = \varepsilon_i^-(\kappa, p_j) \cdot \varepsilon_j^+(\kappa, p_i) = 0. \quad (2.2.16)$$

We remark how the polarisation vectors in (2.2.12) (or in (2.2.13)) are independent of the choice of κ up to a gauge transformation³.

We conclude this section by listing some of the most useful spinor identities in dealing with scattering amplitudes calculations:

$$\langle q | \gamma^\mu | q \rangle = 2q^\mu \quad (\text{Gordon identity}), \quad (2.2.17)$$

$$\langle p | \gamma^\mu | q \rangle = [q | \gamma^\mu | p] \quad (\text{Charge conjugation}), \quad (2.2.18)$$

$$\langle p | \gamma^\mu | q \rangle \langle r | \gamma^\mu | s \rangle = -2 \langle pr \rangle [qs] \quad (\text{Fierz rearrangement}), \quad (2.2.19)$$

$$\langle pq \rangle \langle rs \rangle = \langle pr \rangle \langle qs \rangle + \langle ps \rangle \langle rq \rangle \quad (\text{Schouten identity}). \quad (2.2.20)$$

for some null momenta p, q, r, s .

2.3 Tree-Level Amplitudes

In this section we deal with three-point amplitudes and describe how the use of complex momenta yields a result which would otherwise be zero had real momenta been used. In particular, we derive the first term of the series of MHV tree amplitudes for gluons as conjectured by Parke and Taylor [65] and proved by Berends and Giele [66]. The role of supersymmetry at tree level is also reviewed. Tree-level supersymmetry is a powerful constraint on tree amplitudes. Supersymmetric Ward identities (SWI) [67, 68] relate amplitudes with different external states but the same number of particles and the same amount of total helicity. We denote $\mathcal{A}_n \equiv \mathcal{A}_n^{\text{tree}}$ throughout this section. Also, a factor of g^{n-2} will be omitted in all the tree-amplitude expressions.

2.3.1 Complex Momenta and MHV Tree-Level Amplitudes

The notion of complex momenta in the realm of quantum field theories is certainly not new. Complex momenta are extremely useful in computing three-point amplitudes

³See [10] for a proof of the independence of κ .

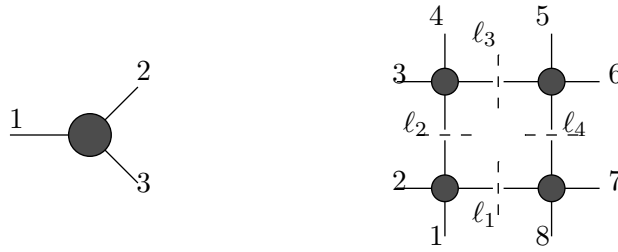


Figure 2.1: *Examples of application of complex momenta: three-point amplitude and generalised unitarity cuts.*

involving on-shell states as for any three massless legs i, j and k process with real momenta, $s_{ij} = 0$ which imposes collinearity on all three momenta. As we will see in § 2.5.3, complex momenta were essential ingredients in deriving recursion relations at tree level as well as being the building blocks for computing amplitudes by means of generalised unitarity cuts. Recall from (2.2.10) that for real null momenta, spinors λ_α and $\tilde{\lambda}_{\dot{\alpha}}$ are complex conjugate of each other so that spinor products are complex square roots of the Lorentz products

$$\langle jl \rangle = \pm \sqrt{s_{jl}} e^{i\phi_{jl}}, \quad [jl] = \pm \sqrt{s_{jl}} e^{-i\phi_{jl}}. \quad (2.3.1)$$

Hence, for vanishing s_{ij} all the spinor products follow suit. However, for complex momenta, (2.3.1) does not hold anymore. In order to explain the latter statement, let us have a look at the three-point vertex depicted in Figure 2.1. Momentum conservation dictates that

$$\lambda_1 \tilde{\lambda}_1 = \lambda_2 \tilde{\lambda}_2 + \lambda_3 \tilde{\lambda}_3. \quad (2.3.2)$$

For complex momenta, we can choose either the holomorphic or anti-holomorphic spinors to be proportional. Let us choose the antiholomorphic spinors $\tilde{\lambda}$

$$\tilde{\lambda}_1 = c_1 \tilde{\lambda}_2, \quad \tilde{\lambda}_3 = c_2 \tilde{\lambda}_2, \quad (2.3.3)$$

which entails that

$$[\tilde{\lambda}_1 \tilde{\lambda}_2] = [\tilde{\lambda}_2 \tilde{\lambda}_3] = [\tilde{\lambda}_3 \tilde{\lambda}_1] = 0, \quad (2.3.4)$$

for some complex c_1 and c_2 . With this choice of kinematics, the tree-level amplitude with two negative-helicity and one positive-helicity states does not vanish although all the momentum invariants s_{ij} do according to (2.2.11). For the case of gluons, the \mathcal{A}_3 can be computed by means of the three-gluon-vertex as provided by the colour-ordered

Feynman rules

$$\begin{aligned} \mathcal{A}_3(1^-, 2^-, 3^+) &= \frac{i}{\sqrt{2}} [\varepsilon_1^- \cdot \varepsilon_2^- \varepsilon_3^+ \cdot (p_1 - p_2) + \varepsilon_2^- \cdot \varepsilon_3^+ \varepsilon_1^- \cdot (p_2 - p_3) \\ &\quad + \varepsilon_3^+ \cdot \varepsilon_1^- \varepsilon_2^- \cdot (p_3 - p_1)]. \end{aligned} \quad (2.3.5)$$

Judiciously choosing the reference vectors as $\kappa_1 = \kappa_2$ and $\kappa_3 = p_1$ and Fierz-rearrange the expression, (2.3.5) reduces to only one term

$$\begin{aligned} \mathcal{A}_3(1^-, 2^-, 3^+) &= i\sqrt{2}\varepsilon_2^- \cdot \varepsilon_3^+ \varepsilon_1^- \cdot p_2 \\ &= i \frac{[\kappa_1 3] \langle 12 \rangle [\kappa_1 2] \langle 21 \rangle}{[\kappa_1 2] \langle 13 \rangle [\kappa_1 1]} \\ &= i \frac{[\kappa_1 3] \langle 12 \rangle^2 \langle 32 \rangle}{[\kappa_1 1] \langle 31 \rangle \langle 32 \rangle} \\ &= i \frac{\langle 12 \rangle^3}{\langle 23 \rangle \langle 31 \rangle}, \end{aligned} \quad (2.3.6)$$

which can be written as

$$\mathcal{A}_3(1^-, 2^-, 3^+) = i \frac{\langle 12 \rangle^4}{\langle 12 \rangle \langle 23 \rangle \langle 31 \rangle}. \quad (2.3.7)$$

Equation (2.3.7) is the first term of the MHV tree-level amplitude for n gluons, conjectured by Parke and Taylor [65] and proved by Berends and Giele [66]

$$\mathcal{A}_n(1^+, \dots, i^-, \dots, j^-, \dots, n^+) = i \frac{\langle 14 \rangle^4}{\langle 12 \rangle \langle 23 \rangle \dots \langle n1 \rangle}. \quad (2.3.8)$$

There exists a similar expression for two positive-helicity and the rest all negative-helicity states obtained by taking the complex conjugate of (2.3.8)

$$\mathcal{A}_n(1^-, \dots, i^+, \dots, j^+, \dots, n^-) = -i \frac{[14]^4}{[12][23] \dots [n1]}, \quad (2.3.9)$$

called the *googly* MHV amplitude. We notice that both (2.3.8) and (2.3.9) hold for $n \geq 4$ for real momenta. Other useful tree-level amplitudes results are

$$\begin{aligned} \mathcal{A}_n(1^+, \dots, n^+) &= 0, \\ \mathcal{A}_n(1^+, \dots, i^-, \dots, n^+) &= 0, \\ \mathcal{A}_n(1_f^-, 2_f^+, 3^+, \dots, n^+) &= 0, \end{aligned} \quad (2.3.10)$$

where ... are any number of positive-helicity gluons. We prove (2.3.10) in the next section within the context of supersymmetry. While these relations hold for any loop in SUSY theories, they cease to hold at loop-level in QCD.

2.3.2 Supersymmetry at Tree Level

At tree level, gluon scattering amplitudes are the same in pure YM as they are in $\mathcal{N} = 4$ so that we can regard tree-level QCD as effectively supersymmetric. The reason behind this interesting observation goes as follows. If we consider an n -gluon tree amplitude, there are no fermions anywhere in any Feynman diagrams. As such, we could regard the fermions as living in the adjoint representation, which amounts to saying that the pure YM theory could be regarded as supersymmetric [69]. This statement holds for any number of supersymmetries and it leads to the more general result

$$\mathcal{A}_{\text{QCD}}^{\text{tree}} = \mathcal{A}_{\mathcal{N}=1}^{\text{tree}} = \mathcal{A}_{\mathcal{N}=2}^{\text{tree}} = \mathcal{A}_{\mathcal{N}=4}^{\text{tree}}. \quad (2.3.11)$$

The way gluon tree-level amplitudes in pure YM relate to supersymmetric amplitudes with fermions and scalars is mathematically implemented by SWI⁴, which were first considered in [67–70]. At one loop, (2.3.11) ceases to hold; nevertheless, we can still make use of the useful supersymmetric decomposition for gluon amplitudes which we review in § 2.4.

To obtain the SWI, let us consider an amplitude written in terms of fields Φ_i acting on the vacuum

$$\langle 0 | \Phi_1 \Phi_2 \cdots \Phi_n | 0 \rangle. \quad (2.3.12)$$

In an $\mathcal{N} = 1$ supersymmetric theory we introduce a supercharge $Q(\eta)$, with η the fermionic parameter of the supersymmetry. $Q(\eta)$ annihilates the vacuum, for we consider unbroken supersymmetric theories. Thus, we can write

$$0 = \langle 0 | [Q(\eta), \Phi_1 \Phi_2 \cdots \Phi_n] | 0 \rangle = \sum_{i=1}^n \langle 0 | \Phi_1 \cdots [Q(\eta), \Phi_i] \cdots \Phi_n | 0 \rangle. \quad (2.3.13)$$

In order to prove the vanishing of the tree-level amplitudes (2.3.10), we need the expressions of the commutators of the supercharge $Q(\eta)$ with the gluons $g^\pm(k)$ and the fermions $\Lambda^\pm(k)$

$$[Q(\eta), g^\pm(k)] = \Gamma^\pm(k, \eta) \Lambda^\pm(k), \quad [Q(\eta), \Lambda^\pm(k)] = \Gamma^\mp(k, \eta) g^\pm(k), \quad (2.3.14)$$

where

$$\Gamma^+(k, \eta) = \theta[qk], \quad \Gamma^-(k, \eta) = \theta\langle qk \rangle. \quad (2.3.15)$$

⁴The following is also nicely reviewed in a number of places including [71, 72].

In (2.3.15) θ is a Grassmann parameter and q a null vector with Weyl polarisation spinors $\phi(q)$ and $\bar{\phi}(q)$ such that

$$\eta_\alpha(q) = \frac{\theta\phi_\alpha(q)}{\sqrt{2}}, \quad \bar{\eta}^{\dot{\alpha}}(q) = \frac{\theta\bar{\phi}^{\dot{\alpha}}(q)}{\sqrt{2}}. \quad (2.3.16)$$

We begin with the first formula of (2.3.10), the amplitude with all-plus helicity gluons. We act on

$$\langle 0 | \Lambda_1^+ g_2^+ \cdots g_n^+ | 0 \rangle$$

$$\begin{aligned} 0 &= \langle 0 | [Q(\eta), \Lambda_1^+ g_2^+ \cdots g_n^+] | 0 \rangle \\ &= \langle qk_1 \rangle \mathcal{A}_n(g_1^+, g_2^+, \dots, g_n^+) + \langle qk_2 \rangle \mathcal{A}_n(\Lambda_1^+, \Lambda_2^+, \dots, g_n^+) \\ &\quad + \cdots + \langle qk_n \rangle \mathcal{A}_n(\Lambda_1^+, g_2^+, \dots, \Lambda_n^+). \end{aligned} \quad (2.3.17)$$

In (2.3.17), only the first amplitude does not vanish for gluinos, like quarks, must satisfy helicity conservation at each interaction. Thus, we proved that the all-plus amplitude of (2.3.10) vanishes as well. The one negative-helicity case follows a similar pattern. We begin by acting on $\langle 0 | \Lambda_1^+ g_2^- \cdots g_n^+ | 0 \rangle$

$$\begin{aligned} 0 &= \langle 0 | [Q(\eta), \Lambda_1^+ g_2^- \cdots g_n^+] | 0 \rangle \\ &= \langle qk_1 \rangle \mathcal{A}_n(g_1^+, g_2^-, \dots, g_n^+) + \langle qk_2 \rangle \mathcal{A}_n(\Lambda_1^+, \Lambda_2^-, \dots, g_n^+), \end{aligned} \quad (2.3.18)$$

where we have omitted all the amplitudes violating helicity conservation. By choosing the reference vector in the same manner as we did to derive (2.3.6), we retrieve the second and third formula of (2.3.10). Setting $q = k_1$ and $q = k_2$ yields the answer. The first non-zero amplitudes appear with two negative-helicity gluons. We act on $\langle 0 | g_1^-, \dots, g_i^-, \dots, \Lambda_j^+, \dots, g_n^+ | 0 \rangle$

$$\begin{aligned} 0 &= \langle 0 | [Q(\eta), g_1^- \cdots g_i^- \cdots \Lambda_j^+ \cdots g_n^+] | 0 \rangle \\ &= \langle qk_1 \rangle \mathcal{A}_n(\Lambda_1^-, \dots, g_i^-, \dots, \Lambda_j^+, \dots, g_n^+) + \langle qk_i \rangle \mathcal{A}_n(g_1^-, \dots, \Lambda_i^-, \dots, \Lambda_j^+, \dots, g_n^+) \\ &\quad + \langle qk_j \rangle \mathcal{A}_n(g_1^-, \dots, g_i^-, \dots, g_j^+, \dots, g_n^+). \end{aligned} \quad (2.3.19)$$

Setting $q = k_1$, we find an expression relating gluon amplitudes to an amplitudes with two fermions of opposite helicity

$$\mathcal{A}_n(g_1^-, \dots, \Lambda_i^-, \dots, \Lambda_j^+, \dots, g_n^+) = \frac{\langle 1k_j \rangle}{\langle 1k_i \rangle} \mathcal{A}_n(g_1^-, \dots, g_i^-, \dots, g_j^+, \dots, g_n^+). \quad (2.3.20)$$

Extending the supersymmetry to $\mathcal{N} = 4$, allows one to enlarge (2.3.20) as to include scalar particles. We can summarise all the previous SWI identities relating non-zero

amplitudes as

$$\mathcal{A}_n(g_1^-, \dots, \Pi_i^-, \dots, \Pi_j^+, \dots, g_n^+) = \left(\frac{\langle 1k_j \rangle}{\langle 1k_i \rangle} \right)^{2(1-|h_\Pi|)} \mathcal{A}_n(g_1^-, \dots, g_i^-, \dots, g_j^+, \dots, g_n^+), \quad (2.3.21)$$

where Π is either a scalar or a fermion and $h_\Pi = 0, \frac{1}{2}$ the corresponding helicity⁵. For scalar particles helicity \pm refers to particle or antiparticle. We conclude by mentioning that the derivation of (2.3.21) made no use of perturbative approximations. Thus, (2.3.21) is valid to any order in the loop expansion of supersymmetric theories as well as for QCD at tree-level.

2.4 Supersymmetric Decomposition

Supersymmetric field theories play a fundamental role in the understanding of the gauge theories of the Standard Model (SM). For instance, we have seen in the previous section how computing a tree-level gluon amplitude in \mathcal{A}_{QCD} is equivalent to computing the same amplitude in $\mathcal{N} = 4$ SYM although the complexity of the calculation in the latter theory is notably less than in the former one. In general, at tree level, we could use any SYM theory with an adjoint multiplet to find the corresponding amplitude in QCD. At one loop we can still make use of supersymmetric theories to compute a purely gluonic amplitude in QCD.

$\mathcal{N} = 4$ SYM, which has the maximum amount of supersymmetry for theories containing particles with spin less or equal to 1, comes with an adjoint multiplet consisting of 1 gluon A_μ with 2 degrees of freedom (d.o.f), 6 real scalars ϕ^I with 6 d.o.f and 4 Weyl fermions χ_α with 8 d.o.f. In the literature the multiplet is usually written as (1, 4, 6, 4, 1). Theories with a reduced amount of supersymmetry are also phenomenologically important. The $\mathcal{N} = 1$ chiral multiplet (0, 1, 2, 1, 0) comprises 1 Weyl fermion and 2 real scalars (1 complex). By merely counting the number of particles in the adjoint representation of the above multiplets, it turns out that it is possible to write down the following supersymmetric decomposition for one-loop amplitudes of gluons in QCD

$$\mathcal{A}_{\text{QCD}}^{\text{one-loop}} = \mathcal{A}_{\mathcal{N}=4}^{\text{one-loop}} - 4\mathcal{A}_{\mathcal{N}=1, \text{chiral}}^{\text{one-loop}} + \mathcal{A}_{\mathcal{N}=0}^{\text{one-loop}}, \quad (2.4.1)$$

where $\mathcal{N} = 0$ refers to a complex scalar running in the loop.

At one loop, computation of amplitudes in supersymmetric theories is far less troublesome than it is in QCD. This is primarily due to the fact that there are diagram-by-

⁵We recall that in a n -point MHV amplitude $h_{tot} = \sum h_i = n - 2 - 2 = n - 4$.

diagram cancellations which remove four powers of loop momentum in the numerator for $\mathcal{N} = 4$ and two powers for $\mathcal{N} = 1$. These cancellations in turn allow only box integrals to appear in $\mathcal{N} = 4$ and box, triangle and bubble integrals in $\mathcal{N} = 1$ [17, 21]. Thus, the main hurdle in computing the RHS of (2.4.1) comes from the non-supersymmetric part of it which is nevertheless still easier to compute than the LHS as a scalar cannot propagate spin information around the loop. We conclude this section by mentioning other multiplets found in supersymmetric theories, the $\mathcal{N} = 2$ vector multiplet $(1, 2, 2, 2, 1)$, the $\mathcal{N} = 2$ hyper multiplet $(0, 2, 4, 2, 0)$ and the $\mathcal{N} = 1$ vector multiplet $(1, 1, 0, 1, 1)$.

2.5 Modern Methods

In an era in which loop calculations are vital to distinguish new physics from the known background, tree-level scattering amplitudes ought to be a relatively feasible calculation to perform. The usual approach is to follow the recipe as given by the Feynman rules. This set of rules, although mechanical, become rather inefficient as the number of particles increase, for the number of diagrams increase factorially as the table below shows. Furthermore, individual diagrams are rich in complicated tensor structures and

n	2	3	4	5	6	7	8
# of diagrams	4	25	220	2485	34300	559405	10525900

Table 2.1: *The number of Feynman diagrams contributing to the scattering process $gg \rightarrow n g$. Extracted from [71].*

are not independently gauge invariant due to their being off-shell: proliferation of terms throughout the calculation becomes exceedingly cumbersome as Figure 2.2 shows. Although scarcely distinguishable, the black scribbles are actually dot products of on-shell gluons momenta k_μ with the gluon polarization vectors ε_μ .

An alternative and more efficient approach, based on Feynman rules, are Berends-Giele recursion relations [66], which make use of recursive methods that connect together off-shell currents. The simplification, in particular in massless theories, arises from employing colour ordering and spinor helicity formalism which we described earlier in this chapter. Although the use of gauge invariance and on-shell conditions keep off-shell quantities to a minimum, the calculation still suffers from rather long expressions which render inputting numerical quantities a quite strenuous task. In recent times⁶, two related methods to perform tree-level calculation appeared. We describe them below.

⁶We mean geologically speaking.

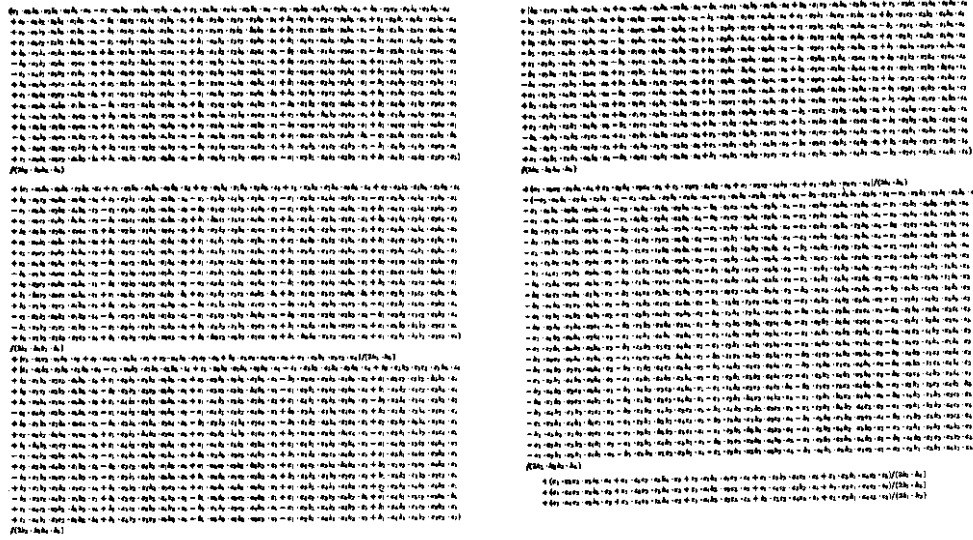


Figure 2.2: The five-gluon tree level amplitude computed in a Feynman fashion.

2.5.1 The CSW construction

In an influential paper, [12], a novel diagrammatic approach stemmed from an insight which relates the perturbative expansion of $\mathcal{N} = 4$ super Yang-Mills theory to D-instanton expansion in the topological B model in super twistor space⁷ $CP^{3|4}$ [10]. A experimental investigation of YM amplitudes in twistor space yielded the interesting fact that MHV amplitudes localise on complex lines in twistor space. In turn, lines in twistor space map to points in space-time. This suggested to use MHV vertices as building blocks in the following manner

1. Draw all possible MHV diagrams using MHV amplitudes as vertices.
2. Connect all the MHV vertices, helicities $-$ to $+$, by off-shell scalar propagators $\frac{i}{P^2}$ assuming conservation of momentum P flowing between the vertices (opposite helicities are connected by the propagator).
3. Assign a holomorphic spinor $|P_i^{\flat}\rangle = |P_i^{\flat}\rangle\kappa$ to each legs attached to a propagator, where κ is an arbitrary spinor fixed for all diagrams. A similar off-shell continuation is viable also for anti-holomorphic spinor variables.
4. Sum all the contributions of all MHV diagrams⁸.

⁷For the interested reader, a light introduction to twistor space and the fundamental relation between MHV amplitudes and lines in twistor space are given in Appendix E. For a thorough introduction we refer to the original work referenced above.

⁸The κ -dependence disappear after summing over all the possible MHV diagrams.

A remarkable simplification happens, for if we wish to compute a scattering amplitude with q negative-helicity gluons for example, then we will have $v = q - 1$ vertices and $d = q - 2$ propagators. For n external legs the number of diagrams grows at most as n^2 . To gain a feeling on how to use the above rules, let us consider a simple example, the five-point NMHV amplitude $\mathcal{A}_5(1^-, 2^-, 3^-, 4^+, 5^+)$ which has three negative-helicity gluons. We will study NMHV amplitudes in § 4.3.

We know from our discussion in § 2.3.1 that this amplitude is given by the Parke-Taylor formula (2.3.8)

$$\mathcal{A}_5(1^-, 2^-, 3^-, 4^+, 5^+) = \frac{[45]^3}{[12][23][34][51]}, \quad (2.5.1)$$

where we have used the anti-holomorphic spinors. We now recompute (2.5.1) by utilising the above rules.

First, we draw all the diagrams contributing to the amplitude which can be seen in Figure 2.3. We then consider the first diagram (the top-left one). We have

$$\begin{aligned} & \frac{\langle 1(-P_{51}^b) \rangle^3}{\langle (-P_{51}^b)5 \rangle \langle 51 \rangle} \frac{1}{P_{51}^2} \frac{\langle 23 \rangle^3}{\langle 34 \rangle \langle 4P_{51}^b \rangle \langle P_{51}^b 2 \rangle} \\ = & \frac{\langle 1|P_{51}|\kappa \rangle^3}{\langle 5|P_{51}|\kappa \rangle \langle 51 \rangle} \frac{1}{[15]\langle 51 \rangle} \frac{\langle 23 \rangle^3}{\langle 34 \rangle \langle 4|P_{51}|\kappa \rangle \langle 2|P_{51}|\kappa \rangle} \\ = & \frac{[5\kappa]^3 \langle 23 \rangle^3}{[1\kappa][51]\langle 34 \rangle \langle 4|(5+1)|\kappa \rangle \langle 2|(5+1)|\kappa \rangle}. \end{aligned} \quad (2.5.2)$$

Setting $|\kappa] = |5]$ makes (2.5.2) vanish so that only the three remaining diagrams will contribute to the tree-amplitude. From the top-right diagram in Figure 2.3, the contributions are (rotating clockwise)

$$-\frac{\langle 34 \rangle^2 [45]^3}{[12][51]\langle 45 \rangle [52]\langle 15 \rangle [53]}, \quad (2.5.3)$$

$$-\frac{\langle 12 \rangle^2 [45]^3}{[34][51]\langle 15 \rangle [53]\langle 5P_{34} \rangle}, \quad (2.5.4)$$

$$-\frac{\langle 14 \rangle^2 [45]^3}{[23][51]\langle 45 \rangle [52]\langle 15 \rangle [53]}. \quad (2.5.5)$$

Summing all the above contributions gives the expected (2.5.1).

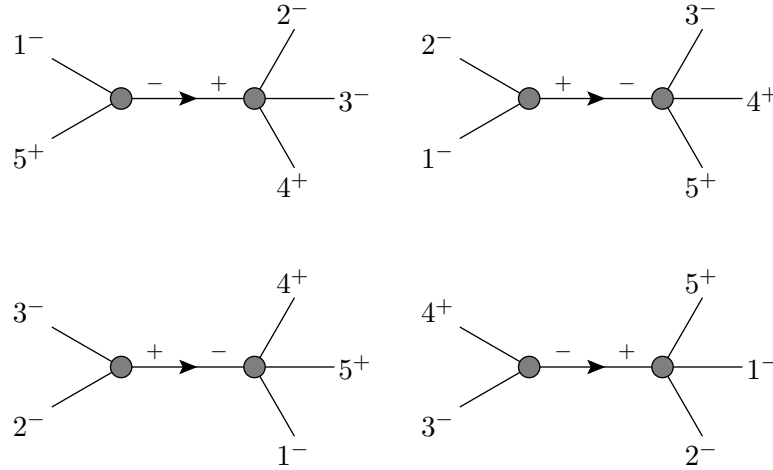


Figure 2.3: The four allowed diagrams contributing to $\mathcal{A}_5(1^-, 2^-, 3^-, 4^+, 5^+)$. Observe how all vertices are MHV.

2.5.2 CSW Extended: Fermions and Massless Scalars

We have seen above how the CSW rules allow for a relatively hassle-free computation of gluonic tree-level amplitudes. A natural extension of the CSW rules would be to include massless scalars and fermions in the adjoint or fundamental representation of YM theory. In § 2.3.2, SWI were introduced to relate gluonic amplitudes to amplitudes containing scalars or fermions in the adjoint (see (2.3.21)). On the other side, particles in the fundamental representation are obliged to be adjacent. Thus, there is no *a priori* justification not to extend the CSW rules to theories with particles other than gluons. For example, to compute the five-point NMHV amplitude $\mathcal{A}_5(1_q^-, 2^-, 3^-, 4^+, 5_q^+)$ we would have to replace some external and internal gluon lines with fermion dotted lines in such a way as to keep the fermions adjacent. The MHV diagrams contributing to the amplitude can be seen in Figure 2.4.

It would be ideal to extend the CSW procedure to include quantum corrections to the overall result. Although initially the picture emerging from twistor string theory was not encouraging, in a remarkable paper [16] the CSW rules were applied to the calculation of the one-loop n -point MHV amplitude in $\mathcal{N} = 4$ SYM, confirming earlier results at n -point [17]. Furthermore, in [18] and [20] the CSW procedure was employed to compute the one-loop n -point MHV amplitude in $\mathcal{N} = 1$ SYM and in pure Yang-Mills respectively, thus providing all the cut-constructible contributions to the n -point MHV gluon amplitude in QCD⁹. In § 4, we recalculate the n -point MHV amplitude in pure

⁹Recall the supersymmetric decomposition (2.4.1)

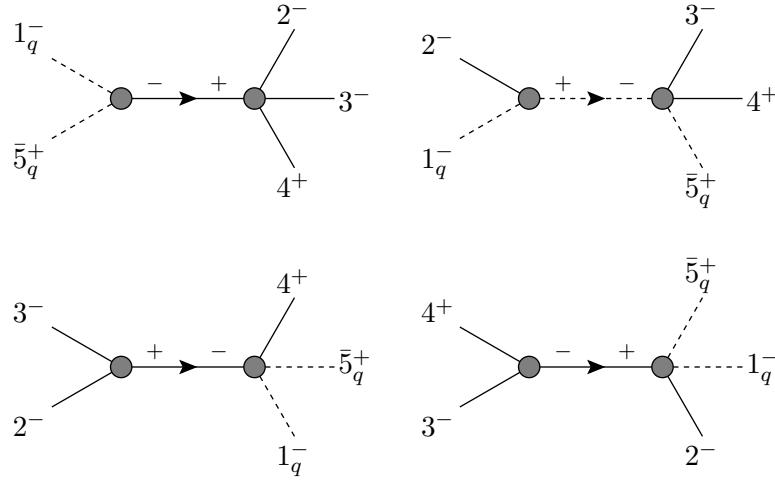


Figure 2.4: The four allowed diagrams contributing to $\mathcal{A}_5(1_q^-, 2^-, 3^-, 4^+, 5_q^+)$. We point to the fact that helicity conservation is respected and all the vertices are still MHV.

Yang-Mills by means of generalised unitarity.

2.5.3 The BCFW Recursion Relations

As mentioned in § 2.3.1, a major novelty in computing scattering amplitudes came with the introduction of complex spinors $\lambda, \tilde{\lambda} \in \mathbb{C}^4$. In a rather influential paper [23], it was shown how the use of complex analysis, in particular the Cauchy's theorem, permitted the construction of n -point tree-level amplitudes in terms of $n - 1$ -point amplitudes and lower point amplitudes¹⁰. It is this recursive structure of tree-level amplitudes which we explain below.

The main idea behind the BCFW recursion relations is to shift the null momenta p_k and p_l of two external particles in an amplitude by shifting their spinors

$$\lambda_l \rightarrow \lambda_l - z\lambda_k \quad \tilde{\lambda}_k \rightarrow \tilde{\lambda}_k + z\tilde{\lambda}_l, \quad (2.5.6)$$

where z is a complex number. Thus we make the amplitude a rational function of z , which we denote by $\mathcal{A}(z)$. The shift (2.5.6) satisfies conservation of momentum, only possible for complex momenta; also, the particles k and l may have any helicity.

Having an amplitude defined in \mathbb{C}^4 allows us to use Cauchy's Theorem and, assuming

¹⁰Ultimately, the calculation can be reduced to three-point amplitudes which are the only amplitudes derived from Feynman rules (see Appendix B).

for now that $\hat{\mathcal{A}}(z) \rightarrow 0$ as $z \rightarrow \infty$, we write

$$0 = \frac{1}{2\pi i} \oint_{\mathcal{C}_\infty} \frac{dz}{z} \hat{\mathcal{A}}(z) = \hat{\mathcal{A}}(0) + \sum_{\text{poles } p} \frac{\text{Res}_p \mathcal{A}(z)}{z_p}. \quad (2.5.7)$$

Since $\mathcal{A}(z)$ will have poles whenever a Feynman propagator goes on-shell, this in turn implies that the residue is given by

$$\lim_{P_{ij}^2 \rightarrow 0} [P_{ij}^2 \mathcal{A}] \sum_{h=\pm} \mathcal{A}(P_{ij}^h, i, \dots, j) \mathcal{A}(-P_{ij}^{-h}, j+1, \dots, i-1), \quad (2.5.8)$$

where the sum is taken over all the possible internal helicities.

If we choose $l: l \in \{i, \dots, j\}$, then the propagator P_{ij} will be shifted and there will be a pole in z because

$$\hat{P}_{ij}(z)^2 = (P_{ij} + z\lambda_k \tilde{\lambda}_l)^2 = P_{ij}^2 - z\langle k|P_{ij}|l\rangle, \quad (2.5.9)$$

yielding

$$z \equiv z_{ij} = \frac{P_{ij}^2}{\langle k|P_{ij}|l\rangle}. \quad (2.5.10)$$

Thus, combining the residue of this pole with (2.5.7) we arrive at

$$\mathcal{A}(1, \dots, n) = \sum_{\substack{i,j \in \mathcal{P} \\ h=\pm 1}} \mathcal{A}_L(z_{ij}) \frac{1}{P_{ij}^2} \mathcal{A}_R(z_{ij}), \quad (2.5.11)$$

where

$$\begin{aligned} \mathcal{A}_L(z_{ij}) &= \mathcal{A}(\hat{P}_{ij}^h, i, \dots, j), \\ \mathcal{A}_R(z_{ij}) &= \mathcal{A}(j+1, \dots, i-1, -\hat{P}_{ij}^{-h}), \end{aligned} \quad (2.5.12)$$

and \mathcal{P} is the set of all partitions into two ranges of external lines that include line l . A diagrammatic representation of (2.5.11) is shown in Figure 2.5.

We conclude this section by sketching the proof that for Yang-Mills theory

$$\lim_{z \rightarrow \infty} \mathcal{A}(z) = 0, \quad (2.5.13)$$

and we refer the interested reader to [24] for a more detailed analysis of the proof.

We choose gluon k to have negative helicity; the case where l has positive helicity follows the same reasoning with $\overline{\text{MHV}}$ replaced by MHV vertices. According to the CSW

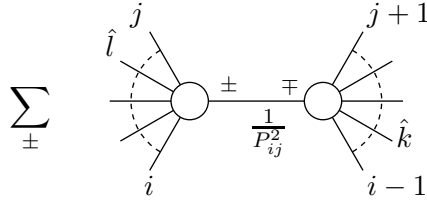


Figure 2.5: A diagrammatic representation of (2.5.11).

rules set above, the basic CSW construction consists of a number of MHV vertices continued off-shell connected by some propagators. In view of the shifts (2.5.6), the anti-holomorphic spinor of the propagator's momentum becomes $(\tilde{\lambda}_P)_{\dot{\alpha}} = (\hat{P}_{ij})_{\alpha\dot{\alpha}}\kappa^{\alpha}$ with κ an arbitrary spinor. Since $\hat{P}_{ij} = P_{ij} + z\lambda_k\tilde{\lambda}_l$, choosing $\kappa = \lambda_k$ will render $\tilde{\lambda}_P$ independent of z and so will be all the $\overline{\text{MHV}}$ vertices connected to it. The only vertex remaining dependent on z is precisely the one containing the negative-helicity gluon k . In a *googly* MHV amplitude, the shifted spinor $\tilde{\lambda}_k + z\tilde{\lambda}_l$ will appear in the denominator thus vanishing as $z \rightarrow \infty$.

2.5.4 The MHV Amplitude as a Solution of the BCF Recursion Relation

Following [23], in this section we show how the simple MHV tree-level amplitude which we recall is of the form

$$\mathcal{A}_n(1^-, 2^+, \dots, m^-, \dots, n^+) = ig^{n-2} \frac{\langle 1m \rangle^4}{\langle 12 \rangle \cdots \langle (n-1)n \rangle \langle n1 \rangle}, \quad (2.5.14)$$

satisfies (2.5.11).

Following the shift (2.5.6), we choose to shift gluons 1 and 2

$$\tilde{\lambda}_1 \rightarrow \tilde{\lambda}_1 - z\tilde{\lambda}_2, \quad \lambda_2 \rightarrow \lambda_2 + z\lambda_1. \quad (2.5.15)$$

If we take $m > 3$ there is only one non-vanishing contribution to (2.5.11), namely $i = 2$ and $j = 3$, a pictorial representation of which is provided in Figure 2.6. For $m \leq 3$ the analysis is similar although with a different partition of momenta.

The shifted momentum flowing through our partition becomes $\hat{P}_{23} \equiv \hat{P}$ so that, according to (2.5.9), $\hat{P}_{23}^2(z)$ vanishes when $z = P_{23}^2/\langle 1|P|2 \rangle$. Assuming that the Parke-

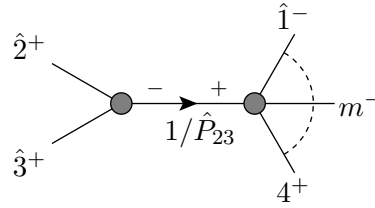


Figure 2.6: *The only diagram contributing to $\mathcal{A}_n(1^-, 2^+, \dots, m^-, \dots, n^+)$ for $m > 3$. Notice that the vertex on the left is a googly MHV amplitude.*

Taylor formula is valid for $n - 1$ gluons, the BCF recursion relations yields

$$\frac{\langle \hat{1}m \rangle^4}{\langle 45 \rangle \cdots \langle n\hat{1} \rangle \langle \hat{1}\hat{P} \rangle \langle \hat{P}4 \rangle} \frac{1}{P_{23}^2} \frac{[\hat{2}3]^3}{[3\hat{P}][\hat{P}2]}, \quad (2.5.16)$$

where $P_{23}^2 = \langle 23 \rangle [32]$ and hatted quantities are the shifted momenta. Since we shifted only the anti-holomorphic component of p_1 we can omit the hats in (2.5.16) everywhere they appear in $\langle \rangle$ brackets (similarly for the holomorphic component of p_2 in $[\]$ brackets).

Since $\hat{P}_{ij}(z) = P_{ij} + z\lambda_k \tilde{\lambda}_l$, we have that

$$\langle x\hat{P}_{ij}(z) \rangle [\hat{P}_{ij}(z)l] = \langle x|\hat{P}_{ij}(z)|l \rangle = \langle x|P_{ij}(z)|l \rangle, \quad (2.5.17)$$

$$\langle k\hat{P}_{ij}(z) \rangle [\hat{P}_{ij}(z)y] = \langle k|\hat{P}_{ij}(z)|y \rangle = \langle k|P_{ij}(z)|y \rangle, \quad (2.5.18)$$

for any generic spinor x and y . Thus, we can recast $\langle 1\hat{P} \rangle$ as

$$\langle 1\hat{P} \rangle = \frac{\langle 1|2+3|2 \rangle}{[\hat{P}2]} = \frac{\langle 13 \rangle [32]}{[\hat{P}2]}, \quad (2.5.19)$$

and similarly

$$\langle \hat{P}4 \rangle = -\frac{\langle 43 \rangle [32]}{[\hat{P}2]}, \quad [3\hat{P}] = \frac{\langle 12 \rangle [32]}{\langle 1\hat{P} \rangle}, \quad [\hat{P}2] = -\frac{\langle 13 \rangle [32]}{\langle 1\hat{P} \rangle}. \quad (2.5.20)$$

Inserting (2.5.19) and (2.5.20) into (2.5.16) we retrieve the Parke-Taylor formula (2.5.14) for MHV tree-level amplitudes.

Chapter 3

Unitarity

The concept of the unitarity of the scattering matrix S lies at the heart of any consistent quantum field theory. Without it, we would have to forsake conservation of probability, clearly an unquestionable requirement. In this chapter, by recurring to the analytic properties of Feynman integrals, we formulate the Cutkosky rules [73–76], which allow to compute the discontinuity of a scattering amplitude, *i.e.* its absorptive part, by replacing propagators connecting external states by delta functions, a procedure which goes under the name of *cutting* the amplitude. The main idea is that, given the discontinuity of the amplitude in some channel, it is possible in principle to reconstruct the full amplitude by means of dispersion integrals. We will see how this can be accomplished by employing only on-shell information, a rather desirable feature.

A modern approach to unitarity as pioneered in [17], reverses the cutting by *sewing* tree-level amplitudes to form one-loop amplitudes. Rather than computing dispersion integrals, it relies on the existence of a basis of known scalar integrals reducing the computation of amplitudes to purely algebraic exercises in some cases. This knowledge of the set of integral functions comes from the underlying QFT, which was not an accepted tool in the times of the old S-matrix approach of the sixties. Unitarity is well described in many textbooks (see [178] for example) on quantum field theory and, for our purpose, we revise the details of the most salient aspects of it, referring more to concrete examples as we go along and to later sections.

3.1 The Optical Theorem

By recalling that a scattering amplitude is given by the non-forward part of S , $T = -i(S - 1)$, unitarity $S^\dagger S = 1$ implies

$$-i(T - T^\dagger) = T^\dagger T, \quad (3.1.1)$$

so that in terms of initial p_{in} and final p_{fin} states, we can write the LHS of (3.1.1) as

$$\begin{aligned} -i(\langle p_{\text{fin}}|T|p_{\text{in}}\rangle - \langle p_{\text{fin}}|T^\dagger|p_{\text{in}}\rangle) &= -i\left(\langle p_{\text{fin}}|T|p_{\text{in}}\rangle - \overline{\langle p_{\text{in}}|T|p_{\text{fin}}\rangle}\right) \\ &= -i(2\pi)^4\delta^{(4)}\left(\sum(p_{f\text{in}} - p_{\text{in}})\right) \\ &\quad \times (\mathcal{S}(p_{\text{in}} \rightarrow p_{\text{fin}}) - \bar{\mathcal{S}}(p_{\text{fin}} \rightarrow p_{\text{in}})) \\ &= -i(2\pi)^4\delta^{(4)}\left(\sum(p_{\text{fin}} + p_{\text{in}})\right)\text{Disc } \mathcal{S}(p_{\text{fin}}; p_{\text{in}}), \end{aligned} \quad (3.1.2)$$

where we have taken p_{in} states as incoming and p_{fin} states as outgoing and

$$\langle a_{\text{fin}}|T|b_{\text{in}}\rangle = (2\pi)^4\delta^{(4)}\left(\sum(a_{\text{fin}} - b_{\text{in}})\right)\mathcal{S}(b_{\text{in}} \rightarrow a_{\text{fin}}). \quad (3.1.3)$$

Hence, the LHS of (3.1.1) corresponds to a discontinuity in the scattering amplitude, that is a branch cut in complex momenta. This discontinuity gives the absorptive part of an amplitude. In order to obtain the RHS of (3.1.1) one could insert a complete set of intermediate states $\{q_i\}$

$$1 = \sum_i \int \frac{d^4 q_i}{(2\pi)^4} \delta^{(+)}(q_i^2 - m_i^2) |q_i\rangle \langle q_i|, \quad (3.1.4)$$

so that

$$\begin{aligned} \langle p_{\text{fin}}|T^\dagger T|p_{\text{in}}\rangle &= \sum_n \left(\prod_{i=1}^n \int \frac{d^4 q_i}{(2\pi)^4} \delta^{(+)}(q_i^2 - m_i^2) \right) \langle p_{\text{fin}}|T^\dagger|q_i\rangle \langle q_i|T|p_{\text{in}}\rangle \\ &= (2\pi)^4\delta^{(4)}\left(\sum(p_{\text{fin}} + p_{\text{in}})\right) \sum_n \int d\text{LIPS}(n) \bar{\mathcal{S}}(p_{\text{fin}} \rightarrow q_i) \mathcal{S}(p_{\text{in}} \rightarrow q_i), \end{aligned} \quad (3.1.5)$$

where $d\text{LIPS}$ is the multiparticle Lorentz-invariant phase space measure.

$$d\text{LIPS} = \prod_i d^4 q_i \delta^{(+)}(q_i^2 - m_i^2) \delta^{(4)}\left(p_{\text{fin}} + p_{\text{in}} - \sum_i q_i\right). \quad (3.1.6)$$

$$2\text{Im} \left(\text{Diagram} \right) = \sum_{q_i} \int d \Pi_{q_i} \left(\text{Diagram}_1 \right) \left(\text{Diagram}_2 \right) \quad (3.1.8)$$

Figure 3.1: *The optical theorem (3.1.7): the imaginary part of the forward scattering amplitude given as a sum of intermediate states.*

Combining the LHS and RHS of (3.1.1) we arrive at the Optical Theorem

$$-i \text{Disc } \mathcal{S}(p_{\text{fin}}; p_{\text{in}}) = \sum_n \int d\text{LIPS}(n) \bar{\mathcal{S}}(p_{\text{fin}} \rightarrow q_i) \mathcal{S}(p_{\text{in}} \rightarrow q_i), \quad (3.1.7)$$

a pictorial representation of which is given in Figure 3.1.

3.2 Cutkosky Rules

At loop level, the discontinuity of the amplitude may be computed by “cutting” it. It was shown in [73–76] how, by applying a series of steps, the discontinuity of any Feynman diagram could be retrieved. At one loop the rules are as follows:

1. Cut, in a given kinematic invariant, the two propagators separating the external states carrying that kinematic invariant from the rest of the diagram.
2. Replace each cut propagator by a delta function,

$$\frac{i}{p^2 \pm i\varepsilon} = P\left(\frac{i}{p^2}\right) \mp \pi\delta(p^2) \rightarrow \mp \pi\delta(p^2), \quad (3.2.1)$$

where P stands for the principal value prescription.

3. Perform the integration over the two-particle $d\text{LIPS}$

$$d\text{LIPS}(\ell_2, -\ell_1; P_\ell) = d^4\ell_1 \delta^{(+)}(\ell_1^2) d^4\ell_2 \delta^{(+)}(\ell_2^2) \delta^{(4)}(\ell_2 - \ell_1 + P_\ell), \quad (3.2.2)$$

to obtain the discontinuity in the branch cut of a kinematic invariant in a particular channel. P_ℓ is the momentum flowing outside the loop.

3.2.1 One Step Backward, Two forward

At this point, performing the dispersion integrals would in principle provide the full amplitude. However, it would be rather favourable to avoid carrying out cumbersome integrations and, to this end, we depart from the Cutkosky rules and we go one step backward: we replace the delta functions associated with cuts with propagators thus generating Feynman integrals, that is we promote the cut to a full loop integral. The result can then be written in terms of a basis of integral functions. By repeating this in all kinematic channels, we can reconstruct the full amplitude. It was in [17] that this alternative route was successfully applied for the first time by computing the one-loop MHV amplitudes in $\mathcal{N} = 4$ SYM. We are going to discuss this alternative procedure below.

At one loop, any colour-ordered amplitude to $\mathcal{O}(\epsilon^0)$ can be expressed in terms of a linear combination of known scalar integrals

$$A_n^{1\text{-loop}} = \sum_{i \in \mathcal{B}} c_i \mathcal{I}_i + \text{rational terms}, \quad (3.2.3)$$

where \mathcal{B} is a basis of integrals which comprises scalar bubble, triangle and box integral functions and the coefficients c_i are rational functions of momenta and polarisation vectors. For the moment we put the so-called rational terms appearing in (3.2.3) aside. The way to proceed is to evaluate the cuts in each channel and express them as linear combinations of cuts of integrals \mathcal{I}_i times some coefficients c_i in that channel. To elucidate the procedure, let us take the simplest case known, namely a one-loop MHV amplitude in $\mathcal{N} = 4$ SYM. In § 4, we will offer a more intricate case which needs considerable more effort to be disentangled.

It was shown in [17] that MHV amplitudes in $\mathcal{N} = 4$ SYM can be expressed in terms of only integral box functions I_i

$$\mathcal{A}_n^{1\text{-loop}} = \sum_{i | I_i \in \mathcal{B}} c_i I_i. \quad (3.2.4)$$

Let us consider a cut in a particular channel with momentum K , where

$$s = (k_1 + \dots + k_2)^2 = K^2. \quad (3.2.5)$$

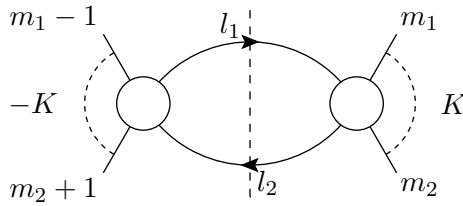


Figure 3.2: A pictorial representation of (3.2.6).

We obtain from the LHS of (3.2.4)

$$\begin{aligned}
 -i \text{Disc } \mathcal{A}_n^{1\text{-loop}} &= \sum_{\text{helicity}} \int \frac{d^{4-2\epsilon} \ell_1}{(2\pi)^{4-2\epsilon}} \frac{d^{4-2\epsilon} \ell_2}{(2\pi)^{4-2\epsilon}} \pi \delta^{(+)}(\ell_1^2) \mathcal{A}_{\text{tree}}(\ell_1, m_1, \dots, m_2, -\ell_2) \\
 &\quad \times \pi \delta^{(-)}(\ell_2^2) \mathcal{A}_{\text{tree}}(\ell_2, m_2 + 1, \dots, m_1 - 1, -\ell_1) \quad (3.2.6) \\
 &\rightarrow \sum_{\text{helicity}} \int \frac{d^{4-2\epsilon} \ell_1}{(2\pi)^{4-2\epsilon}} \frac{d^{4-2\epsilon} \ell_2}{(2\pi)^{4-2\epsilon}} \frac{i}{\ell_1^2} \mathcal{A}_{\text{tree}}(\ell_1, m_1, \dots, m_2, -\ell_2) \\
 &\quad \times \frac{i}{\ell_2^2} \mathcal{A}_{\text{tree}}(\ell_2, m_2 + 1, \dots, m_1 - 1, -\ell_1),
 \end{aligned}$$

a pictorial representation of which can be found in Figure 3.2. Dimensional regularisation is employed in (3.2.6) to regulate both IR and UV divergences.

In light of the tree-level amplitudes results given in 2.3.10, the two tree amplitudes appearing in (3.2.6) must be MHV in order not to be zero. Moreover, the negative-helicity states i and j can reside either both in the same tree amplitude or in opposite ones. The two planar cut diagrams that contribute to the channel in consideration are depicted in Figure 3.3.

Summing over the $\mathcal{N} = 4$ multiplet¹ gives rise to the same integrand for both cases as a few lines of algebra show

$$-\mathcal{A}_n^{\text{MHV,tree}} \frac{\langle (m_1 - 1) m_1 \rangle \langle \ell_1 \ell_2 \rangle^2 \langle m_2 (m_2 + 1) \rangle}{\langle (m_1 - 1) \ell_1 \rangle \langle \ell_1 m_1 \rangle \langle m_2 \ell_2 \rangle \langle \ell_2 (m_2 + 1) \rangle}. \quad (3.2.7)$$

The way to proceed is to transform the denominator to scalar propagators by rewriting

$$\frac{1}{\langle \ell_1 m_1 \rangle} = \frac{[m_1 \ell_1]}{2\ell_1 \cdot m_1} = \frac{[m_1 \ell_1]}{(\ell_1 - m_1)^2}, \quad (3.2.8)$$

and similarly for any other spinor product involving loop momentum². By doing so,

¹Here we only sum over internal helicity states for the cut diagram on the right of Figure 3.3.

²We wish to stress that (3.2.8) is only true when on-shell, *i.e.* this way of manipulating the denom-

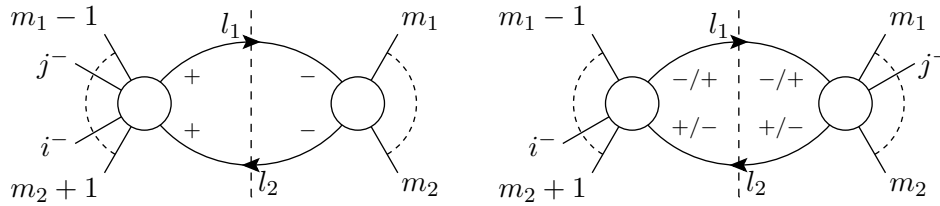


Figure 3.3: *The two possibilities: either i and j on the same side of the cut or on opposite sides.*

an hexagon integral with the numerator written as a function of the loop momentum is obtained. Notice that in Yang-Mills theory, a computation of a generic n -point amplitude gives up to n loop propagators and up to rank n tensors integrals

$$I_n[P(\ell^\mu)] = -i(4\pi)^2 \int \frac{d^{4-2\epsilon}\ell}{(2\pi)^{4-2\epsilon}} \frac{P(\ell^\mu)}{\ell^2(\ell - K_1)^2(\ell - K_1 - K_2)^2 \cdots (\ell + K_n)^2}. \quad (3.2.9)$$

Let us stress once more that in arriving at (3.2.6) we have replaced the delta functions with Feynman propagators. Had we not done so, we would have had to integrate over the two-particle LIPS of the internal particles rather than integrating over full momenta.

A way to perform tensor integrals of the form (3.2.9) is to use some sort of integral reduction such as the Passarino-Veltman (PV) reduction [77]. In practice, by knowing which tensors the integral can depend on, the PV reduction breaks the integrand into a sum of integrals with a lower number of propagators. Iterating this procedure, we are left with a sum of scalar integrals, each of which corresponds to an integral of the basis. Matching the various integrals to the basis then allows one to read off the various coefficients. However, in a general amplitude, it is not sufficient to look in a single channel. Eq. (3.2.6) only gives the discontinuity of the Feynman integrals which share a branch cut in that particular channel: several integrals contributing to the amplitude may appear only in this channel, others may share different channels and must be taken only once. Combining the several cuts into a single function yields the full amplitude, up to some rational terms which we have hitherto neglected and we are now going to discuss.

On general grounds, a loop amplitude will have some additional rational functions of kinematic variables which in general elude the cut-construction method. Indeed, while it was shown in [17] that one-loop amplitudes in SYM are free of rational terms, such rational terms do make their appearance in QCD amplitudes. Theories whose rational inator into scalar propagators must be done before promoting the delta functions to full off-shell loop integrals.

terms are uniquely linked to cuts are called *cut-constructible*³. Amplitudes in SYM belong to this category and are thus completely determined by the study of their cuts. In light of the supersymmetric decomposition 2.4.1 of QCD amplitudes, one is then left to find only those rational terms coming from the pure Yang-Mills contribution, *i.e.* a scalar running in the loop. A way to compute these missing rational terms requires continuing the cut momenta to $4 - 2\epsilon$ dimensions. We will return to $4 - 2\epsilon$ -dimensional unitarity in § 3.4 where we will rederive the $++++$ amplitude in pure Yang-Mills. This amplitude, which vanishes in SYM theory, consists of purely rational terms.

3.3 Generalised Unitarity in $D = 4$

We have seen in the previous section how the discontinuity across a cut in the amplitude can be computed by a unitarity cut where the two cut propagators are put on-shell. In (3.2.6), we considered a cut in a given channel's kinematic invariant and we emphasised the fact that (3.2.6) is only sensitive to integrals which share the same cut in the same channel. Sewing together two tree amplitudes to form the cut in a given channel selects only those integrals which have both propagators cut thereby yielding the coefficients only for those integrals. Thus, a careful consideration of cuts in all the other channels is required to obtain the full amplitude. If one were allowed to cut more propagators at once fewer terms would survive and it would greatly simplify the calculation by cutting loop amplitudes into smaller tree amplitudes. This observation goes under the name of *generalised unitarity*. Although known since [76], generalised unitarity was put into practice only in [78] to compute amplitudes in $\mathcal{N} = 4$ SYM, specifically targeting coefficients of box integrals. Ideally, we would like to have just the right number of cuts to isolate a single integral and a single coefficient. This is only possible for box integrals and, following the reasoning offered in [79], we move on to show it below.

3.3.1 The Box Example

Cutting four propagators fixes the coefficient of a box integral as a product of four tree amplitudes. In four dimensions the four delta functions completely freeze the loop momentum. Hence, obtaining the coefficient becomes an algebraic exercise of purely multiplying tree amplitudes. Since we will go through a more complicated n -point box integral in a later section, we give here a simpler example which embodies all

³In [17, 21] a power-counting criterion which cut-constructible theories obey was found. It was shown that SYM theory satisfies this power-counting criterion. Namely, the criterion states that the degree n of the polynomial numerator in a n -point loop integral is reduced to $n - 4$ and $n - 2$ for $\mathcal{N} = 4$ and $\mathcal{N} = 1$ SYM respectively.

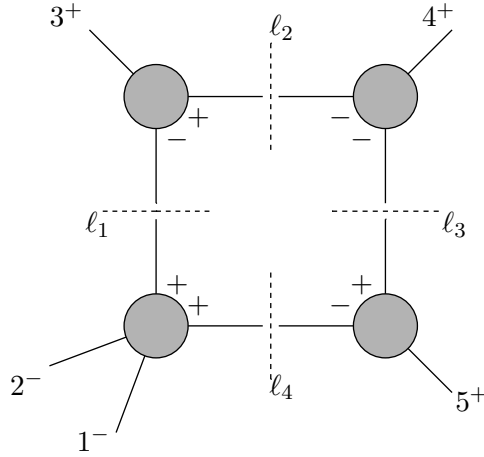


Figure 3.4: A possible quadruple-cut contributing to the $1^-2^-3^+4^+5^+$ amplitude. The remaining quadruple-cuts are obtained by a colour-ordered cyclic permutations of the external states.

the characteristics of the general example. Let us try to compute the coefficient of a box integral for a MHV five-point amplitude, $\mathcal{A}_5^{1\text{-loop}}(1^-, 2^-, 3^+, 4^+, 5^+)$. For such an amplitude there are five possible one-mass box integrals each with a different massive corner, $K_{12} = (k_1 + k_2)$, K_{23} , K_{34} , K_{45} or K_{51} . The quadruple-cut associated with the one-mass box integral $\mathcal{I}_{K_{12}}$ is depicted in Figure 3.4, where

$$\mathcal{I}(K_{12}) = \int \frac{d^{4-2\epsilon} \ell}{(2\pi)^{4-2\epsilon}} \frac{1}{\ell^2 (\ell - K_{12})^2 (\ell - K_{123})^2 (\ell + k_5)^2}. \quad (3.3.1)$$

However, we do not have to compute all the coefficients. The coefficients of $\mathcal{I}(K_{51})$ and $\mathcal{I}(K_{45})$ are related to the coefficients of $\mathcal{I}(K_{23})$ and $\mathcal{I}(K_{34})$ respectively since the amplitude $\mathcal{A}_5^{1\text{-loop}}(1^-, 2^-, 3^+, 4^+, 5^+)$ is antisymmetric under the reflection $(12345) \leftrightarrow (21543)$.

Applying generalised cuts leads us to a product of four tree-amplitudes. According to the discussion of § 2.3.1, if we restrict to four dimensions, the three three-point amplitudes would vanish unless we take the momenta to be complex. Let us examine the momentum ℓ_2 which is connecting two three-point vertices. As momenta are complex the holomorphic λ and anti-holomorphic $\tilde{\lambda}$ spinor components of the momenta k_3 and k_4 are independent and their kinematics goes as follows

$$\begin{aligned} \lambda_{\ell_2} &\sim \lambda_3 & \vee & & \tilde{\lambda}_{\ell_2} &\sim \tilde{\lambda}_3, \\ \lambda_{\ell_2} &\sim \lambda_4 & \vee & & \tilde{\lambda}_{\ell_2} &\sim \tilde{\lambda}_4. \end{aligned} \quad (3.3.2)$$

In general $s_{34} \neq 0$ which entails that $\lambda_3 \approx \lambda_4$ and $\tilde{\lambda}_3 \approx \tilde{\lambda}_4$. Thus the only allowed

solutions are

$$(\lambda_{\ell_2} \sim \lambda_3 \quad \wedge \quad \tilde{\lambda}_{\ell_2} \sim \tilde{\lambda}_4) \quad \vee \quad (\lambda_{\ell_2} \sim \lambda_4 \quad \wedge \quad \tilde{\lambda}_{\ell_2} \sim \tilde{\lambda}_3). \quad (3.3.3)$$

Eq. (3.3.3) implies that two adjacent three-vertices must have opposite helicity configurations in order not to vanish. Moreover, the four-point amplitude with all-like helicities or all-like helicities but one vanish according to (2.3.10). This further constrains the helicity configurations, forcing the internal legs associated to momenta ℓ_1 and ℓ_4 to have both positive helicities thus fixing the helicity configuration of each vertex. Hence, the only possible solution is the first set of conditions in (3.3.3). The coefficient of the one-mass box integral is then the product of four tree-amplitudes

$$\begin{aligned} c_{12} &= \mathcal{A}_4^{\text{tree}}(-\ell_4, 1^-, 2^-, \ell_1) \mathcal{A}_3^{\text{tree}}(-\ell_1, 3^+, \ell_2) \mathcal{A}_3^{\text{tree}}(-\ell_2, 4^+, \ell_3) \mathcal{A}_3^{\text{tree}}(-\ell_3, 5^+, \ell_4) \\ &= \frac{\langle 12 \rangle^3 [3\ell_2]^3 \langle \ell_2 \ell_3 \rangle^3 [\ell_3 5]^3}{\langle \ell_4 1 \rangle \langle 2 \ell_1 \rangle \langle \ell_1 \ell_4 \rangle [\ell_1 3] [\ell_2 \ell_1] \langle \ell_2 4 \rangle \langle 4 \ell_3 \rangle [5 \ell_4] [\ell_4 \ell_3]} \\ &= -\frac{\langle 12 \rangle^3 [3|\ell_2 \ell_3|5]^3}{\langle 2|\ell_1|3 \rangle \langle 4|\ell_2 \ell_1 \ell_4|5 \rangle \langle 1|\ell_4 \ell_3|4 \rangle}, \end{aligned} \quad (3.3.4)$$

which can be simplified to a function of only one loop momentum

$$\begin{aligned} c_{12} &= \frac{\langle 12 \rangle^3 \langle 4|\ell_2|3 \rangle^2 [45]^3}{\langle 2|\ell_2|3 \rangle \langle 34 \rangle \langle 15 \rangle \langle 45 \rangle \langle 4|\ell_2|5 \rangle} \\ &= -\frac{\langle 12 \rangle^3 s_{34} s_{45}}{\langle 23 \rangle \langle 34 \rangle \langle 45 \rangle \langle 51 \rangle} \\ &= i s_{34} s_{45} \mathcal{A}_5^{\text{tree}}(1^-, 2^-, 3^+, 4^+, 5^+). \end{aligned} \quad (3.3.5)$$

Substituting the appropriate invariants, the one-mass box integral $\mathcal{I}(K_{12})$ is given by

$$\begin{aligned} \mathcal{I}(K_{12}) &= -i \frac{2r_\Gamma}{s_{34} s_{45}} \left\{ -\frac{1}{\epsilon^2} \left[\left((-s_{34})^{-\epsilon} + (-s_{45})^{-\epsilon} + (-s_{12})^{-\epsilon} \right) \right] \right. \\ &\quad \left. + \text{Li}_2 \left(1 - \frac{s_{12}}{s_{34}} \right) + \text{Li}_2 \left(1 - \frac{s_{12}}{s_{45}} \right) + \frac{1}{2} \ln^2 \left(\frac{s_{34}}{s_{45}} \right) + \frac{\pi^2}{6} \right\}. \end{aligned} \quad (3.3.6)$$

The two remaining $\mathcal{I}(K_{23})$ and $\mathcal{I}(K_{34})$ boxes with their helicity assignment of the quadruple cuts are shown in Figure 3.5. A similar calculation to the one above shows that the coefficients for $\mathcal{I}(K_{23})$ and $\mathcal{I}(K_{34})$ are similar to (3.3.5) with different kinematic invariants multiplying the tree amplitude. Hence, we can write down the full box

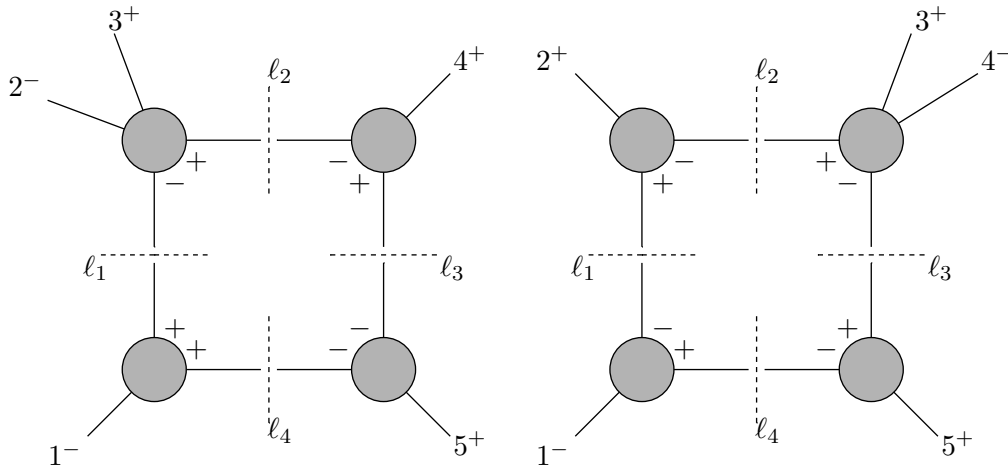


Figure 3.5: *The remaining quadruple-cuts contributing to the one-loop $1^-2^-3^+4^+5^+$ amplitude.*

contribution to the one-loop amplitude as

$$\begin{aligned}
 \mathcal{A}_5^{1\text{-loop}}(1^-, 2^-, 3^+, 4^+, 5^+) &= r_{\Gamma} \mathcal{A}_5^{\text{tree}}(1^-, 2^-, 3^+, 4^+, 5^+) & (3.3.7) \\
 &\left\{ -\frac{1}{\epsilon^2} \left[\left((-s_{34})^{-\epsilon} + (-s_{45})^{-\epsilon} + (-s_{12})^{-\epsilon} \right) \right] \right. \\
 &+ \text{Li}_2\left(1 - \frac{s_{12}}{s_{34}}\right) + \text{Li}_2\left(1 - \frac{s_{12}}{s_{45}}\right) + \frac{1}{2} \ln^2\left(\frac{s_{34}}{s_{45}}\right) \\
 &\left. + \frac{\pi^2}{6} + \text{cyclic permutations} \right\}.
 \end{aligned}$$

If we were to compute this amplitude in $\mathcal{N} = 4$ SYM, (3.3.7) would be the end of the story. The quadruple cut calculates the contribution to the amplitude coming only from the box functions. In $\mathcal{N} = 1$ SYM, the same calculation would yield the box contributions to the amplitude in that theory although, due to conservation of helicity⁴, such quadruple cuts as the one appearing on the left of Figure 3.5 would not appear as we could only have fermions and scalar running in the loop (at least in the chiral $\mathcal{N} = 1$). However, we would need to compute triangle and bubble functions as well which do appear in $\mathcal{N} = 1$ SYM. In non-supersymmetric theories a further twist appears, for rational terms which contribute to the amplitude cannot be detected by four-dimensional cuts. An ingenious implementation of generalised unitarity allows for non-supersymmetric amplitudes to be fully reconstructed from their cuts at the cost of working in $4 - 2\epsilon$ dimensions. In the next section we introduce the concept of generalised unitarity in $D = 4 - 2\epsilon$ dimensions. In § 4 we show how to carry out quadruple and

⁴The bottom vertices of the left quadruple cut appearing in Figure 3.5 do not satisfy helicity conservation, thus vanishing in $\mathcal{N} = 1$ SYM.

triple cuts in order to compute the cut-constructible part of an n -point MHV amplitude in scalar Yang-Mills theory.

3.4 Generalised Unitarity in $D = 4 - 2\epsilon$

As mentioned above, one-loop amplitudes in supersymmetric theories are somewhat special⁵. Their form is completely reconstructed by their cuts in four dimensions in the sense that each term of the amplitude is intimately linked to cuts. In non-supersymmetric theories amplitudes contain additional rational terms which are not linked to discontinuities. Hence, the usual approach to reproduce the amplitude from its cuts seems to fail. However, the latter observation is only true if we work in $D = 4$, that is if we keep in the amplitude terms only up to $\mathcal{O}(\epsilon^0)$. In fact, if we extend the cut-momenta states to $D = 4 - 2\epsilon$ and keep higher orders in ϵ , rational terms R will develop discontinuities of the form $R(-s)^{-\epsilon} = R - \epsilon \log(-s)R + \mathcal{O}(\epsilon^2)$ which in turn can be detected by cuts. In virtue of the supersymmetric decomposition (2.4.1), we have to resort to D -dimensional unitarity only for a scalar running in the loop. The usual manner to approach such a calculation is to think of the massless scalar in D dimensions as a massive scalar in four dimension and decompose the massless scalar with D -dimensional momentum $\ell_{(4-2\epsilon)}$ into a four-dimensional part with momentum $\ell_{(4)}$ and a -2ϵ -dimensional part with momentum $\ell_{(-2\epsilon)}$ such that

$$\ell_{(4-2\epsilon)}^2 = \ell_{(4)}^2 + \ell_{(-2\epsilon)}^2 = \ell_{(4)}^2 - \mu^2, \quad (3.4.1)$$

where the -2ϵ -dimensional and four-dimensional subspaces are taken to be orthogonal and $\ell_{(-2\epsilon)}^2 = \mu^2$. We emphasise that the “mass” μ^2 has to be integrated over.

The idea of using unitarity in $D = 4 - 2\epsilon$ dimensions was first outlined and put into practice in [80–82]. A more recent example is given in [83] where the $++++$, $-++++$ and $+++++$ one-loop amplitudes in pure Yang-Mills, which vanish in SYM, together with the MHV amplitudes $--++$ and $-+-+$ are recomputed by means of generalised unitarity in $D = 4 - 2\epsilon$, showing agreements with the results obtained in previous calculations [81, 84]. In order to elucidate how generalised unitarity in higher dimensions works, hereafter we reproduce the calculation carried in [83] for the simple case of $++++$ one-loop gluon amplitude with a complex scalar running in the loop.

⁵It is conjectured that all-loop amplitudes in $\mathcal{N} = 4$ can be arrived at by a study of their cuts.

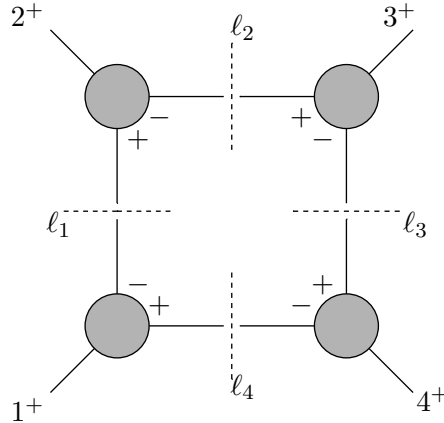


Figure 3.6: One of the two possible quadruple cuts contributing to the $1^+2^+3^+4^+$ amplitude. The other diagram, which is identical to the one depicted here, is obtained by flipping the internal helicities so that the final result is achieved by doubling the contribution coming from the diagram in this Figure.

This amplitude⁶ is given to all-orders in ϵ by [81]

$$\mathcal{A}_4^{\text{scalar}}(1^+, 2^+, 3^+, 4^+) = \frac{2i}{(4\pi)^{2-\epsilon}} \frac{[12][34]}{\langle 12 \rangle \langle 34 \rangle} K_4, \quad (3.4.2)$$

where⁷

$$K_4 \equiv I_4[\mu^4] = -\epsilon(1-\epsilon)I_4^{8-2\epsilon} = -\frac{1}{6} + \mathcal{O}(\epsilon). \quad (3.4.3)$$

Let us consider the quadruple-cut diagram illustrated in Figure 3.6. Following the rules described in § 3.2, it is obtained by sewing four three-point scattering amplitudes with one massless gluon and two massive scalars of mass μ^2 . The three-point amplitudes for any two massive internal scalar particles and a gluon with positive helicity is given by [85]

$$\mathcal{A}(\ell_1^+, k^+, \ell_2^-) = \frac{\langle \kappa | \ell_1 | k \rangle}{\langle \kappa k \rangle}, \quad (3.4.4)$$

where κ is an arbitrary reference spinor, and momentum conservation guarantees that $\ell_1 + \ell_2 + k = 0$.

Thus, the D -dimensional quadruple cut of Figure 3.6 is given by

$$\frac{\langle \kappa_1 | \ell_1 | 1 \rangle \langle \kappa_2 | \ell_2 | 2 \rangle \langle \kappa_3 | \ell_3 | 3 \rangle \langle \kappa_4 | \ell_4 | 4 \rangle}{\langle \kappa_1 1 \rangle \langle \kappa_2 2 \rangle \langle \kappa_3 3 \rangle \langle \kappa_4 4 \rangle}. \quad (3.4.5)$$

⁶It was first computed in [86] using a string-inspired formalism.

⁷Integrals with μ^{2m} as integrand are related to $4 + 2m - 2\epsilon$ -dimensional integrals.

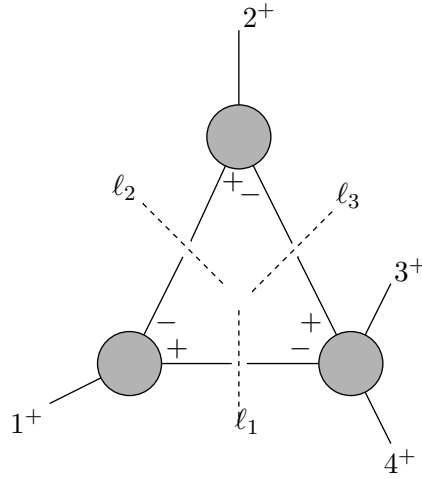


Figure 3.7: *The triple-cut diagram contributing to the $1^+2^+3^+4^+$ amplitude. There are four such diagrams obtained by cyclic permutations of the external particles.*

Choosing $\kappa_1 = 2$ and $\kappa_2 = 1$ and the fact that the internal on-shell momenta square to μ^2 , the first two terms of (3.4.5) reduce to

$$\frac{\langle \kappa_1 | \ell_1 | 1 \rangle \langle \kappa_2 | \ell_2 | 2 \rangle}{\langle \kappa_1 1 \rangle \langle \kappa_2 2 \rangle} = -\mu^2 \frac{[12]}{\langle 12 \rangle}. \quad (3.4.6)$$

Similarly, taking $\kappa_3 = 4$ and $\kappa_4 = 3$, the remaining two terms of (3.4.5) are

$$\frac{\langle \kappa_3 | \ell_3 | 3 \rangle \langle \kappa_4 | \ell_4 | 4 \rangle}{\langle \kappa_3 3 \rangle \langle \kappa_4 4 \rangle} = -\mu^2 \frac{[34]}{\langle 34 \rangle}, \quad (3.4.7)$$

so that (3.4.5) becomes

$$\mu^4 \frac{[12]}{\langle 12 \rangle} \frac{[34]}{\langle 34 \rangle}. \quad (3.4.8)$$

Lifting the four delta functions of the quadruple cut to Feynman propagators, we arrive at the scalar box integral as given in (3.4.3). Including a factor of two coming from the fact that a complex scalar runs in the loop, the final result of (3.4.2) is reproduced.

In the triple-cut depicted in Figure 3.7, we see that one of the tree-amplitudes is an amplitude with two helicity-positive gluons and two massive scalars⁸, the form of which was given in [82]

$$\mathcal{A}(\ell_3^+, 3^+, 4^+, \ell_1^-) = \mu^2 \frac{[34]}{\langle 34 \rangle [(\ell_3 - k_3)^2 - \mu^2]}, \quad (3.4.9)$$

while the remaining two tree-level amplitudes are as before. Thus, the triple cut in

⁸Recall that this tree amplitude vanishes in four dimensions (as $\mu^2 \rightarrow 0$).

Figure 3.7 gives rise to the following integrand

$$-\mu^4 \frac{[12][34]}{\langle 12 \rangle \langle 34 \rangle} \frac{1}{[(\ell_3 - k_3)^2 - \mu^2]}, \quad (3.4.10)$$

which, after uplifting the three delta functions to Feynman propagators yields again (3.4.2), thus showing that there are no new contributions coming from triple cuts.

Having exhausted our introductory chapter on (generalised) unitarity, we move to the next chapter where we recalculate by means of generalised unitarity the cut-constructible part of the n -gluon MHV amplitude in pure Yang-Mills.

Chapter 4

Scalar One-Loop Amplitudes

It is common knowledge that the unitarity method, introduced in [17, 21] and further developed in [88], proved itself to be a powerful as well as elegant tool for computing loop scattering amplitudes (see [79] and references therein for a comprehensive review). In fact, recent years have witnessed impressive achievements in the calculation of two- and higher-loop scattering amplitudes with much of the effort mostly focused on the maximally supersymmetric $\mathcal{N} = 4$ Yang-Mills theory (MSYM) [38, 39, 89, 90]. This is primarily due to the simplicity of the perturbative expansion in the 't Hooft (planar) limit of MYSM suggested by an intriguing duality that relates MSYM at strong coupling to weakly-coupled gravity on $AdS_5 \times S^5$ [8]. A short while ago, this duality was exploited as a different manner to compute amplitudes in MSYM [41] and in the case of four-gluon amplitudes agreement was found with an all-loop order *ansatz* put forward in [39].

In this chapter, following the original work [49] of the author of this thesis, we focus on one-loop MHV amplitudes in pure Yang-Mills theory. These amplitudes are of particular interest as they constitute an example of one-loop n -point scattering amplitudes in QCD, where both external and internal particles are gluons. In pure Yang-Mills the n -gluon one-loop amplitudes may be decomposed as

$$\mathcal{A}_{\text{gluon}}^n = \mathcal{A}_{\mathcal{N}=4}^n - 4\mathcal{A}_{\mathcal{N}=1,\text{chiral}}^n + \mathcal{A}_{\text{scalar}}^n. \quad (4.0.1)$$

Although each contribution of (4.0.1) has been computed for the case of MHV amplitudes using the unitarity method [17, 21], the MHV diagram approach [16, 18–20] and, to some extent, generalised unitarity [78, 91], an explicit double-check of the last term of (4.0.1), namely the contribution arising from a complex scalar particle running in the loop, is still lacking for the case of MHV amplitudes with non-adjacent negative-

helicity gluons¹. As we felt obliged to do so, we aim to rederive the cut-constructible scalar contribution to the n -gluon MHV amplitude by means of the generalised unitarity method [75, 76, 78, 88].

At one loop, generalised unitarity instructs us to cut the amplitude into a product of up to four on-shell tree amplitudes and to replace the propagators connecting the sub-amplitudes by on-shell delta functions², which put the internal particles on shell. When four propagators are cut (quadruple cut) the momentum integral is completely frozen and the resulting product of four tree-amplitudes³ can be identified directly with coefficients of scalar box functions [78]. One route to obtain the coefficients for the remaining scalar triangle and bubble functions is to use triple cuts and conventional two-particle cuts. An efficient method to extract directly, individual coefficients of specific scalar integral functions using a convenient parametrisation for the cut momenta was presented recently in [92].

For the extraction of triangle and bubble coefficients we want to follow a slightly different approach [83, 91]. Here one considers the triple cut of a one-loop amplitude, which in general has contributions from triangle and box functions. One can in principle subtract off the box contributions using quadruple cuts but strictly speaking this is not needed. The three delta functions do not completely freeze the loop integration, hence we simplify the integrand as much as possible using the three loop momentum constraints where the loop momenta are allowed to take complex values. In the final step the cut integral is lifted back up to a loop integral by replacing the on-shell delta functions by the corresponding propagators. The result contains terms that have the correct cuts in the channel under consideration, and possibly terms with cuts in other channels; the latter terms can be dropped. Considering all possible cuts should then give the complete amplitude. An important comment is in order here. The procedure outlined above also produces linear triangle integral functions (triangle integrals with one loop momentum in the numerator), which, as is well known, can be written as linear combinations of scalar triangle and bubble integrals. Therefore, this method can also produce bubble functions which a priori would require the use of additional two-particle cuts. At this point we do not have a proof that two-particle cuts can be avoided for general amplitudes but, for the examples considered in [83, 91] and in our calculation, this method produces the correct answers. The examples include NMHV one-loop amplitudes with adjacent negative-helicity gluons considered in [91], all four-

¹So far that term has only been calculated using MHV diagrams in [20], while the special case of adjacent negative-helicity gluons was first found in [21].

²Since the solutions of the momentum constraints can be complex in general we replace a cut propagator by $\delta(l_i^2)$ and not by $\delta^{(+)}(l_i^2)$. Also in the subsequent manipulations of the integrands we allow the loop momenta to be complex.

³To be more precise, in general the result is a weighted sum over the two complex solutions of the momentum constraints.

point one-loop amplitudes in pure Yang-Mills considered in [83] and the MHV one-loop amplitudes considered in this chapter. Obviously, it would be interesting to study this observation in more detail.

In this chapter we focus on the rederivation of the cut-constructible parts of MHV one-loop amplitudes by considering a complex scalar running in the loop. In the case that both negative-helicity gluons are adjacent all quadruple cuts vanish and, hence, the answer does not contain box functions. In the case that the negative-helicity gluons are not adjacent box functions do contribute and can be determined either directly using quadruple cuts (see [91]) or with the triple cut method outlined above. As a consistency check we have also considered the quadruple cuts in section § 4.2. Therefore, in the following discussion we will concentrate on the triple cuts, which in the case at hand allow us to determine the full cut-constructible part of this class of amplitudes. Explicitly, the non-vanishing triple cuts of the scalar loop contribution to the n -gluon MHV amplitude (see Figure 4.1 and Figure 4.2) take the form:

$$\begin{aligned} \mathcal{A}_{\text{scalar}}^n \Big|_{\text{cut}} = & \sum_{\pm} \int d^4 \ell_1 d^4 \ell_2 d^4 \ell_3 \delta(\ell_1^2) \delta(\ell_2^2) \delta(\ell_3^2) \delta^4(\ell_3 - \ell_1 - Q) \delta^4(\ell_1 - \ell_2 - P) \\ & \times \mathcal{A}_{\text{tree}}(\ell_1, (m_2 + 1), \dots, j^-, \dots, -\ell_2) \mathcal{A}_{\text{tree}}(\ell_2, m_1, -\ell_3) \mathcal{A}_{\text{tree}}(\ell_3, \dots, i^-, \dots, m_2, -\ell_1), \end{aligned} \quad (4.0.2)$$

where the allowed values of m_1 and m_2 are

$$j + 1 \leq m_1 \leq i - 1, \quad i + 1 \leq m_2 \leq j - 1. \quad (4.0.3)$$

The tree amplitudes entering the integrand involve two MHV amplitudes with two scalars and one anti-MHV three-point amplitude with two scalars. The \pm in (4.0.2) refers to the fact that we have a complex scalar running in the loop. Thus, there are two possible helicity configurations, each of which gives rise to the same integrand.

On general grounds, four-dimensional cuts alone suffice to reconstruct the full amplitudes in supersymmetric theories at one loop [17, 21]. However, in theories not protected by supersymmetry, there are additional rational terms which cannot be detected by cuts, unless one decides to work in $D = 4 - 2\epsilon$ dimensions and keep higher orders in ϵ , so that even rational terms develop discontinuities which can be detected by the unitarity method. An example of such an amplitude is the one-loop four-gluon $++++$ amplitude⁴ with a complex scalar running in the loop. This amplitude consists of purely rational terms and it was first computed in [86] using a technique based on the technology of four-dimensional heterotic string theory. It was subsequently confirmed and extended to the case of an arbitrary number of positive helicity gluons in

⁴We have shown the calculation of this amplitude in $D = 4 - 2\epsilon$ dimensions in § 3.4.

[93, 94] and to the case when one of the gluons has opposite helicity from the others [93]. Furthermore, the $++++$ one-loop amplitude was recalculated in [81] by means of two-particle cuts in $D = 4 - 2\epsilon$ dimensions, in [82] where a relationship between one-loop MHV gluon amplitudes of QCD and those of $\mathcal{N} = 4$ SYM was put forward and in [83] using the generalised unitarity method in $D = 4 - 2\epsilon$ dimensions. More recently, there has been a proposal [95] in which it was argued that in a particular regularisation scheme certain Lorentz-violating counterterms provide these missing rational terms.

We wish to make it clear that we shall in this chapter only work with unitarity cuts in $D = 4$ dimensions, thus considering only the cut-constructible part of the n -gluon MHV amplitude. Hence, all the (cut) loop momenta in this chapter are kept in four dimensions until the amplitude has been expressed as a linear combination of integral functions. Only at this stage the dimensional regularisation parameter ϵ is introduced to regularise the divergences of the integral functions.

The cut-constructible part of the MHV one-loop amplitudes in pure Yang-Mills for the special case of adjacent negative-helicity gluons has already been calculated in [21] using unitarity whereas the general helicity configuration was dealt with in [20] by means of the MHV diagram method. The rational parts of these amplitudes have been computed analytically in [22, 35] using the powerful method of on-shell recursion relations, thus providing the full n -gluon one-loop MHV amplitude in QCD. The purpose of the following calculation is to show how generalised unitarity correctly reproduces the cut-constructible parts of the n -gluon amplitudes with less effort than conventional two-particle cuts or the MHV diagram method. We discuss the adjacent negative-helicity case in the next section and the general case in section § 4.2

4.1 The MHV Scalar Amplitude: The Adjacent Case

In this section we show how generalised unitarity may be used to compute the n -point MHV one-loop amplitude in pure Yang-Mills for the case of adjacent negative-helicity gluons.

Let us consider the triple-cut diagram depicted in Figure 4.1, where we choose all momenta to be outgoing. There are two such diagrams, which are obtained by flipping all the internal helicities of the scalar particles running in the loop. Without loss of generality we set $i = 1$ and $j = 2$ throughout this section. Observe that in this case the range of m is $3 \leq m \leq n$. Furthermore, in the adjacent case all quadruple cuts vanish and, hence, no box functions appear in the amplitude.

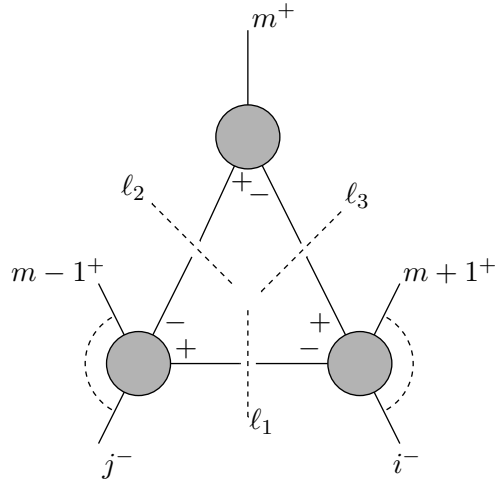


Figure 4.1: *The three-particle cut diagram contributing to the n -gluon amplitude in the case of adjacent negative-helicity gluons*

The triple cut of an n -point amplitude is obtained by sewing three tree-level amplitudes. Ignoring factors of i and 2π , the product of the tree amplitudes appearing in the triple cut (4.0.2) is

$$\frac{[m\ell_2][m\ell_3]}{[\ell_2\ell_3]} \times \frac{\langle 1\ell_1 \rangle^2 \langle 1\ell_3 \rangle^2}{\langle (m+1)(m+2) \rangle \dots \langle n1 \rangle \langle 1\ell_1 \rangle \langle \ell_1\ell_3 \rangle \langle \ell_3(m+1) \rangle} \times \frac{\langle 2\ell_1 \rangle^2 \langle 2\ell_2 \rangle^2}{\langle 23 \rangle \dots \langle (m-2)(m-1) \rangle \langle (m-1)\ell_2 \rangle \langle \ell_2\ell_1 \rangle \langle \ell_12 \rangle} . \quad (4.1.1)$$

Thus (4.0.2) together with (4.1.1) gives

$$\begin{aligned} \mathcal{A}_{\text{scalar}}^n \Big|_{\text{cut}} &= 2i A_{\text{tree}} \int \frac{d^4\ell_2 \prod_{i=1}^3 \delta(\ell_i^2)}{(2\pi)^4} \frac{\langle 2\ell_2 \rangle^2 \langle \ell_1 2 \rangle \langle 1\ell_1 \rangle \langle 1\ell_3 \rangle^2}{\langle 1 2 \rangle^3 \langle \ell_2\ell_1 \rangle \langle \ell_1\ell_3 \rangle [\ell_2\ell_3]} \\ &\times \frac{\langle (m-1)m \rangle \langle m(m+1) \rangle [m\ell_2] [\ell_3 m]}{\langle (m-1)\ell_2 \rangle} \\ &= 2i A_{\text{tree}} \int \frac{d^4\ell_2}{(2\pi)^4} \frac{\langle 2|\ell_2|m \rangle \langle 1m \rangle \langle 1|P\ell_2|2 \rangle \langle 2|P\ell_2|1 \rangle [1 2]^3}{2^5 (1 \cdot 2)^3 (\ell_1 \cdot \ell_2)^2 \ell_1^2 \ell_2^2 \ell_3^2} \Big|_{\text{cut}} , \end{aligned} \quad (4.1.2)$$

where we have factored out the MHV tree level amplitude and cancelled certain spinor brackets in the numerator and denominator of (4.1.1). In order to arrive at the last line of (4.1.2) we have used the fact that the holomorphic spinors of the momenta appearing in the anti-MHV three-point amplitude are proportional to each other, *i.e.* $\lambda_m \propto \lambda_{\ell_2} \propto \lambda_{\ell_3}$. The factor of two accounts for the fact that we have already summed over the two possible internal helicities. Finally, the delta functions have been replaced by full propagators and the three-particle phase-space integral has been promoted to an unrestricted loop integral. The symbol $|_{\text{cut}}$ indicates that this replacement is only valid in the channel defined by a given triple-cut.

Let us clarify some notations. We define the general external momenta k_p as $k_p := p$. Also, we define

$$P := q_{j,m-1}, \quad Q := q_{m+1,i}, \quad (4.1.3)$$

where $q_{p_i,p_j} := \sum_{l=p_i}^{p_j} k_l$. We set $i = 1$ and $j = 2$ for the adjacent case.

Converting (4.1.2) into Dirac traces yields the following integrand:

$$\frac{\text{tr}_+(\not{X}\not{Z}\not{P}\not{\ell}_2)\text{tr}_+(\not{X}\not{Z}\not{\ell}_2\not{m})\text{tr}_+(\not{Z}\not{X}\not{\ell}_2\not{P})}{2^5(1\cdot 2)^3(\ell_1\cdot\ell_2)^2}. \quad (4.1.4)$$

Thus, the task reduces to computing the three-index tensor integral

$$\mathcal{I}^{\mu\nu\rho}(m, P, Q) = \int \frac{d^4\ell_2}{(2\pi)^4} \frac{\ell_2^\mu \ell_2^\nu \ell_2^\rho}{\ell_1^2 \ell_2^2 \ell_3^2}, \quad (4.1.5)$$

which may be done by standard PV integral reduction [77]. Details of the calculation can be found in Appendix D.

The result of the PV reduction has to be inserted into (4.1.4). Doing so yields a series of terms of which, after some manipulations, only the following two remain:

$$A_1 = -\frac{A_{tree}}{(t_1^{[2]})^2} \frac{1}{6} \frac{[I_2(P^2) - I_2(Q^2)]}{(Q^2 - P^2)^2} (1\ 2\ Q\ m)^2, \quad (4.1.6)$$

$$A_2 = \frac{A_{tree}}{(t_1^{[3]})^3} \frac{1}{3} \frac{[I_2(P^2) - I_2(Q^2)]}{(Q^2 - P^2)^3} (1\ 2\ Q\ m)^2 (1\ 2\ m\ Q), \quad (4.1.7)$$

where $t_i^{[k]} := (p_i + p_{i+1} + \dots + p_{i+k-1})^2$ are sums of colour-adjacent momenta and the I_2 functions are the scalar bubble functions as defined in Appendix C. In obtaining (4.1.6) and (4.1.7), we made use of the fact that momentum conservation dictates that on the triple-cut $(\ell_1 \cdot \ell_2)^2 = 4/P^4$ and $(m \cdot Q) = -(m \cdot P) = -(1/2)(Q^2 - P^2)$. Also, in order to make the formulæ more compact, we introduced the notation $(a_1 a_2 a_3 a_4) := \text{tr}_+(\not{a}_1 \not{a}_2 \not{a}_3 \not{a}_4)$, which we will use throughout the rest of the paper.

In (4.1.6) and (4.1.7) the combinations $[I_2(P^2) - I_2(Q^2)] / ((Q^2 - P^2)^r)$ appear, which are ϵ -dependent triangle functions expressed as differences of two bubble functions. For convenience we choose to write them as

$$T_\epsilon^{(r)}(m, P, Q) := \frac{1}{\epsilon} \frac{(-P^2)^{-\epsilon} - (-Q^2)^{-\epsilon}}{(Q^2 - P^2)^r}, \quad (4.1.8)$$

where r is a positive integer and the momenta on which $T^{(r)}$ depends satisfy $m + P + Q = 0$.

As mentioned in the introduction to this chapter, we are working in $D = 4$ dimensions so that we really should take the $\epsilon \rightarrow 0$ limit of (4.1.8). For $P^2 \neq 0$ and $Q^2 \neq 0$ we define the finite, ϵ -independent triangle function,

$$T^{(r)}(m, P, Q) := \frac{\log(Q^2/P^2)}{(Q^2 - P^2)^r}. \quad (4.1.9)$$

In the event of the vanishing of either of the kinematic invariants, (4.1.8) gives rise to infrared-divergent terms since one of the numerator terms in (4.1.8) vanishes. There are two possibilities:

- $P = k_2$ with $P^2 = 0$,
- $Q = k_1$ with $Q^2 = 0$.

Finally, the amplitude takes the following form:

$$\mathcal{A}_n^{\text{scalar}} = \mathcal{A}_{\text{poles}} + \mathcal{A}_1 + \mathcal{A}_2, \quad (4.1.10)$$

where

$$\begin{aligned} \mathcal{A}_{\text{poles}} &= -\frac{i}{6} \mathcal{A}_{\text{tree}} \frac{1}{\epsilon} \left[(-t_2^{[2]})^{-\epsilon} + (-t_n^{[2]})^{-\epsilon} \right], \\ \mathcal{A}_1 &= -\frac{2i}{6} \mathcal{A}_{\text{tree}} \frac{1}{(t_1^{[2]})^2} \sum_{m=4}^{n-1} [(1\ 2\ P\ m)^2] T^{(2)}(m, P, Q), \\ \mathcal{A}_2 &= -\frac{2i}{3} \mathcal{A}_{\text{tree}} \frac{1}{(t_1^{[2]})^3} \sum_{m=4}^{n-1} [(1\ 2\ P\ m)^2 (1\ 2\ m\ P)] T^{(3)}(m, P, Q), \end{aligned} \quad (4.1.11)$$

where we used $t_i^{[k]} := (p_i + p_{i+1} + \dots + p_{i+k-1})^2$ and the triangle functions introduced in (4.1.9).

Equation (4.1.11)⁵, which gives the cut-constructible part of the n -point one-loop scattering amplitudes with two adjacent gluons of negative helicity, agrees with the amplitudes found in [21] using conventional unitarity and with the amplitude found in [20] using MHV diagrams.

⁵We point that in the notation of [20, 21] $q_{m,1} = -P$. Also, we dropped an overall, ϵ -dependent factor c_{Γ} [21] and did not make the symmetry properties of the amplitude under the exchange of the gluons $1 \leftrightarrow 2$ manifest in writing our result, thus explaining a factor of two compared to [20, 21].

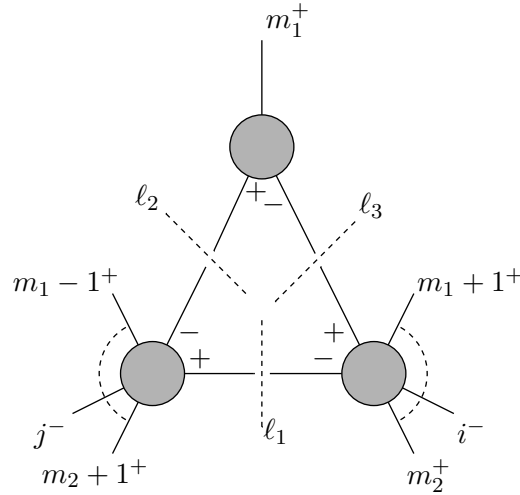


Figure 4.2: One of the two possible triple cut diagrams contributing to the n -gluon amplitude in the general case. The other triple cut diagram is obtained by swapping i and j through the replacements $m_1 - 1 \rightarrow m_1$ and $m_2 \leftrightarrow m_1$.

4.2 The MHV Scalar Amplitude: The General Case

The case in which the two negative-helicity gluons are non-adjacent is more involved. Fortunately, the calculation turns out to be more straightforward than expected, since some of the algebraic manipulations involved can be related to manipulations appearing in the MHV diagram calculation of the same amplitudes [20].

As in the adjacent case, our starting expression is (4.0.2). A direct, brute force calculation yields rather unpleasant four-tensor box integrals. However, we do not follow this approach as it would spoil our goal to show the simplicity of the generalised unitarity method. Instead, by using momentum conservation arguments to eliminate ℓ_3 from (4.0.2), we arrive at a more elegant and manageable expression for the amplitude given by

$$\mathcal{A}_{\text{scalar}}^n \Big|_{\text{cut}} = -\frac{2i A_{\text{tree}}}{\langle ij \rangle^4} \sum_{m_1, m_2} \int \frac{d^4 \ell_2}{(2\pi)^4} \frac{\langle j \ell_1 \rangle^2 \langle j \ell_2 \rangle^2 \langle i \ell_1 \rangle^2 \langle i \ell_2 \rangle^2}{\ell_1^2 \ell_2^2 \ell_3^2 \langle \ell_1 \ell_2 \rangle^2} \times \frac{\langle m_2 (m_2 + 1) \rangle \langle (m_1 - 1) m_1 \rangle \langle \ell_2 m_1 \rangle}{\langle \ell_1 (m_2 + 1) \rangle \langle (m_1 - 1) \ell_2 \rangle \langle m_2 \ell_1 \rangle} \Big|_{\text{cut}}, \quad (4.2.1)$$

where in deriving (4.2.1) we made use of the fact that

$$\begin{aligned} \lambda_{\ell_2} &= \alpha \lambda_{m_1}, \\ \lambda_{\ell_3} &= \beta \lambda_{m_1}, \\ \tilde{\lambda}_{\ell_2} &= \frac{1}{\alpha} \tilde{\lambda}_{m_1} + \frac{\beta}{\alpha} \tilde{\lambda}_{\ell_3}, \end{aligned} \quad (4.2.2)$$

for some complex α and β with λ and $\tilde{\lambda}$ holomorphic and anti-holomorphic spinors of negative and positive helicity respectively.

In order to reduce the hexagon integral (4.2.1) to a linear combination of box and triangle integrals, we notice that multiplying and dividing (4.2.1) by $\langle \ell_2 m_1 \rangle$ allows us to write the integrands⁶, after applying the Schouten identity twice, as a sum of four terms

$$\mathcal{C}(m_2+1, m_1) - \mathcal{C}(m_2+1, m_1-1) - \mathcal{C}(m_2, m_1) + \mathcal{C}(m_2, m_1-1), \quad (4.2.3)$$

where

$$\mathcal{C}(a, b) := \frac{\langle j \ell_1 \rangle^2 \langle j \ell_2 \rangle \langle i \ell_1 \rangle \langle i \ell_2 \rangle^2}{\langle \ell_1 \ell_2 \rangle^2 \langle i j \rangle^4} \cdot \frac{\langle i a \rangle \langle j b \rangle}{\langle \ell_1 a \rangle \langle \ell_2 b \rangle}. \quad (4.2.4)$$

Therefore, we find

$$\mathcal{A}_{\text{scalar}}^n \Big|_{\text{cut}} = 2i A_{\text{tree}} \left[\int \frac{d^4 \ell_2}{(2\pi)^4} \frac{1}{\ell_1^2 \ell_2^2} - \int \frac{d^4 \ell_2}{(2\pi)^4} \frac{1}{\ell_1^2 \ell_3^2} \right] \sum_{a,b} \mathcal{C}(a, b) \Big|_{\text{cut}}, \quad (4.2.5)$$

where the sum stands for the sum of four terms (with signs) in (4.2.3).

One of the triple cuts contributing to the amplitude may be seen in Figure 4.2 where we defined $P := q_{m_2+1, m_1-1}$ and $Q := q_{m_1+1, m_2}$. Our choice for the momentum flow explains why we find the \mathcal{C} coefficients with $a \leftrightarrow b$ compared to [20].

Although the calculation carried out in [20] is conceptually different from the one we are performing here, we can nevertheless make use of formula (B.16) in that paper, which gives a rather convenient expression for \mathcal{C} :

$$\begin{aligned} -\mathcal{C}(a, b) &= \frac{(i j \ell_1 \ell_2)(i j \ell_2 \ell_1)(i j \ell_1 a)(i j b \ell_2)}{2^8 (i \cdot j)^4 (\ell_1 \cdot \ell_2)^2 (\ell_1 \cdot a)(\ell_2 \cdot b)} \\ &= \frac{1}{2^8 (i \cdot j)^4} (\mathcal{H}_1 + \dots + \mathcal{H}_4), \end{aligned} \quad (4.2.6)$$

where the \mathcal{H}_i are given by

$$\begin{aligned} \mathcal{H}_1 &:= \frac{(i j b a)(i j \ell_1 P)(i j P \ell_1)(i j \ell_1 a)}{(\ell_1 \cdot \ell_2)^2 (a \cdot b)(\ell_1 \cdot a)} \\ &\quad - \frac{(i j b a)(i j P \ell_2)(i j \ell_2 P)(i j \ell_2 b)}{(\ell_1 \cdot \ell_2)^2 (a \cdot b)(\ell_2 \cdot b)}, \end{aligned} \quad (4.2.7)$$

⁶The reader might argue, in view of (4.2.2), that $\langle \ell_2 m_1 \rangle$ is zero which entails that we are effectively multiplying (4.2.1) by $\frac{0}{0}$. However, at this point we are off-shell as we have *uplifted* the cut integral to a Feynman integral by replacing on-shell delta functions by full Feynman propagators.

and

$$\mathcal{H}_2 := -\frac{(i j a b)(i j b a)(i j P \ell_1)(i j \ell_1 a)}{(\ell_1 \cdot \ell_2)(a \cdot b)^2(\ell_1 \cdot a)} - \frac{(i j a b)(i j b a)(i j \ell_2 P)(i j \ell_2 b)}{(\ell_1 \cdot \ell_2)(a \cdot b)^2(\ell_2 \cdot b)}, \quad (4.2.8)$$

$$\mathcal{H}_3 := -\frac{(i j a b)^2(i j b a)(i j \ell_1 a)}{(a \cdot b)^3(\ell_1 \cdot a)} + \frac{(i j a b)^2(i j b a)(i j \ell_2 b)}{(a \cdot b)^3(\ell_2 \cdot b)}, \quad (4.2.9)$$

$$\mathcal{H}_4 := -\frac{(i j a b)^2(i j b a)^2(b P \ell_1 a)}{4(a \cdot b)^4(\ell_1 \cdot a)(\ell_2 \cdot b)}. \quad (4.2.10)$$

Thus, we produce, in ascending order from \mathcal{H}_4 to \mathcal{H}_1 , linear box integrals and linear, two-tensor and three-tensor triangle integrals. We focus first on the triangle integral contributions.

Substituting for a and b in the expressions for \mathcal{H} and keeping only those terms that actually contribute to the particular triple cut depicted in Figure 4.2 yields combinations of differences of traces. In order to express our result in a more compact fashion, we find it useful to define the following quantities:

$$\begin{aligned} A_{m_1 m_2}^{ij} &:= \frac{(i j m_1 m_2 + 1)}{(m_1 \cdot (m_2 + 1))} - \frac{(i j m_1 m_2)}{(m_1 \cdot m_2)}, \\ S_{m_1 m_2}^{ij} &:= \frac{(i j m_1 m_2 + 1)(i j m_2 + 1 m_1)}{(m_1 \cdot (m_2 + 1))^2} - \frac{(i j m_1 m_2)(i j m_2 m_1)}{(m_1 \cdot m_2)}, \\ I_{m_1 m_2}^{ij} &:= \frac{(i j m_1 m_2 + 1)(i j m_2 + 1 m_1)^2}{(m_1 \cdot (m_2 + 1))^3} - \frac{(i j m_1 m_2)(i j m_2 m_1)^2}{(m_1 \cdot m_2)^3}, \end{aligned} \quad (4.2.11)$$

which exhibit the following symmetry properties

$$A_{m_1 m_2}^{ij} = -A_{m_1 m_2}^{ji}, \quad S_{m_1 m_2}^{ij} = S_{m_1 m_2}^{ji}. \quad (4.2.12)$$

The only integrals that survive from (4.2.5) are the ones with the correct triple cut, *i.e.* those integrals that have all three propagators that are cut in Figure 4.2. Hence, many of the triangle integrals can be neglected⁷ and after the dust has settled we are

⁷One consequence of these considerations is that the first integral on the right hand side of (4.2.5) can be ignored altogether.

left with:

$$\mathcal{H}_1 = A_{m_1 m_2}^{ij} \frac{(i j P \ell_2)(i j \ell_2 P)(i j \ell_2 m_1)}{2^8 (i \cdot j)^4 (\ell_1 \cdot \ell_2)^2 (\ell_2 \cdot m_1)}, \quad (4.2.13)$$

$$\mathcal{H}_2 = S_{m_1 m_2}^{ij} \frac{(i j \ell_2 P)(i j \ell_2 m_1)}{2^8 (i \cdot j)^4 (\ell_1 \cdot \ell_2) (\ell_2 \cdot m_1)}, \quad (4.2.14)$$

$$\mathcal{H}_3 = I_{m_1 m_2}^{ij} \frac{(i j \ell_2 m_1)}{2^8 (i \cdot j)^4 (\ell_2 \cdot m_1)}. \quad (4.2.15)$$

Before we present the complete amplitude, we wish to inspect the coefficient of the box function depicted in Figure 4.3 and compare it with the results found in [20] using MHV diagrams and in [91] using quadruple cuts. The crucial term in the function $\mathcal{C}(a, b)$ that enters the triple cut (4.2.5) of the amplitude and gives rise to a triple cut of a box function is:

$$-\frac{1}{2^8 (i \cdot j)^4} \mathcal{H}_4 = \left[\frac{(i j m_2 m_1)^2 (i j m_1 m_2)^2}{2^8 (i \cdot j)^4 (m_2 \cdot m_1)^4} \right] \frac{(m_1 P \ell_1 m_2)}{4 (l_1 \cdot m_2) (\ell_2 \cdot m_1)}, \quad (4.2.16)$$

which may be written more compactly as

$$-\frac{1}{2^8 (i \cdot j)^4} \mathcal{H}_4 = \frac{1}{4} [b_{m_1 m_2}^{ij}]^2 \frac{(m_1 P \ell_1 m_2)}{(l_1 \cdot m_2) (\ell_2 \cdot m_1)}, \quad (4.2.17)$$

in terms of the coefficient of the box integral function appearing in the one-loop $\mathcal{N} = 1$ MHV amplitude with the same helicity configuration computed in [21]

$$b_{m_1 m_2}^{ij} := -\frac{1}{8} \frac{(i j m_2 m_1)(i j m_1 m_2)}{(i \cdot j)^2 (m_1 \cdot m_2)^2}. \quad (4.2.18)$$

for which we find the following:

$$\mathcal{H}_4 = \left[\frac{(i j m_2 m_1)^2 (i j m_1 m_2)^2}{2^8 (i \cdot j)^4 (m_2 \cdot m_1)^4} \right] \frac{(m_1 P \ell_1 m_2)}{4 (l_1 \cdot m_2) (\ell_2 \cdot m_1)}, \quad (4.2.19)$$

Let us observe that (4.2.17) gives rise to a linear two-mass easy box integral whose PV reduction is given in Appendix C. Inserting the result of the PV reduction into (4.2.17) reproduces the correct coefficient of the box function. A brief comment is in order here. In the final result [20] only the finite part $B(s, t, P^2, Q^2)$ of the two-mass easy box function appears (as defined e.g. in eq. (4.7) of [20]). We have checked that this is indeed the case and is due to the presence of scalar triangle functions in the PV reduction of Appendix D which precisely cancel the IR divergences of the scalar box function $I_4[1]$ once all triple-cut channels are taken into account.

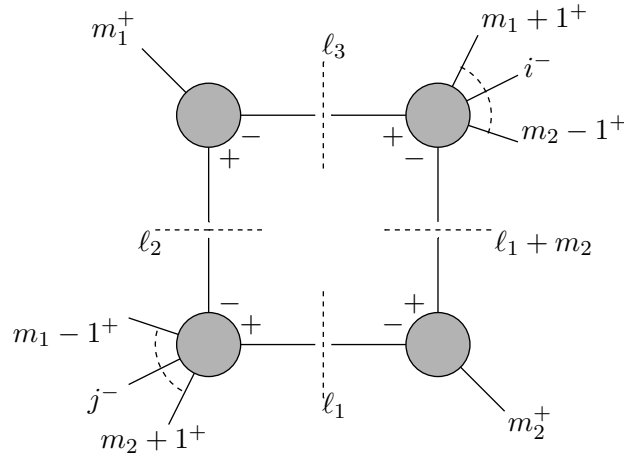


Figure 4.3: A quadruple cut diagram contributing to the n -gluon amplitude in the general case.

We can now present the complete result⁸ for the one-loop n -gluon MHV amplitude (4.0.2) reconstructed using the generalised unitarity method:

$$\begin{aligned}
\mathcal{A}_{\text{scalar}}^n &= 2i \mathcal{A}_{\text{tree}} \left\{ \sum_{m_1=j+1}^{i-1} \sum_{m_2=i}^{j-1} \frac{1}{2} [b_{m_1 m_2}^{ij}]^2 F \left(t_{m_1}^{[m_2-m_1]}, t_{m_1+1}^{[m_2-m_1-1]}, P, Q \right) \right. \\
&\quad + \left(\frac{8}{3} \sum_{m_1=j+1}^{i-1} \sum_{m_2=i}^{j-1} \left[\mathcal{A}_{m_1 m_2}^{ij} T^{(3)}(m_1, P, Q) + (i \cdot j) \tilde{\mathcal{A}}_{m_1 m_2}^{ij} T^{(2)}(m_1, P, Q) \right] \right. \\
&\quad + 2 \sum_{m_1=j+1}^{i-1} \sum_{m_2=i}^{j-1} \left[\mathcal{S}_{m_1 m_2}^{ij} T^{(2)}(m_1, P, Q) - \mathcal{I}_{m_1 m_2}^{ij} T(m_1, P, Q) \right] \\
&\quad \left. \left. + (i \leftrightarrow j) \right) \right\}, \tag{4.2.20}
\end{aligned}$$

where we have introduced for convenience the following quantities:

$$\mathcal{A}_{m_1 m_2}^{ij} := -2^{-8} (i \cdot j)^{-4} A_{m_1 m_2}^{ij} [(i j m_1 Q)(i j Q m_1)^2], \tag{4.2.21}$$

$$\tilde{\mathcal{A}}_{m_1 m_2}^{ij} := -2^{-8} (i \cdot j)^{-4} A_{m_1 m_2}^{ij} [(i j Q m_1)^2], \tag{4.2.22}$$

$$\mathcal{S}_{m_1 m_2}^{ij} := 2^{-8} (i \cdot j)^{-4} S_{m_1 m_2}^{ij} [(i j Q m_1)^2], \tag{4.2.23}$$

⁸We have already multiplied by a factor of 2 due to the two scalar helicity configurations running in the loop.

and

$$\mathcal{I}_{m_1 m_2}^{ij} := 2^{-8} (i \cdot j)^{-4} I_{m_1 m_2}^{ij} [(i j Q m_1)]. \quad (4.2.24)$$

The amplitude (4.2.20) agrees precisely with the result found in [20]. Once again, in deriving (4.2.20) we did not make use of the symmetry properties of the amplitude under exchange of the i -th and j -th gluon.

Similarly to the adjacent case, the infrared divergent terms may be extracted from the cases when either P^2 or Q^2 vanishes (see Figure 4.2). The case $Q^2 = 0$ corresponds to $m_1 = i-1$ and $m_2 = i$, while $P^2 = 0$ corresponds to $m_1 = j+1$ and $m_2 = j-1$. Hence,

$$T^{(r)}(p, P, Q) \rightarrow (-)^r \frac{1}{\epsilon} \frac{(-t_{i-1}^{[2]})^{-\epsilon}}{(t_{i-1}^{[2]})^r}, \quad Q^2 \rightarrow 0, \quad (4.2.25)$$

$$T^{(r)}(p, P, Q) \rightarrow -\frac{1}{\epsilon} \frac{(-t_j^{[2]})^{-\epsilon}}{(t_j^{[2]})^r}, \quad P^2 \rightarrow 0. \quad (4.2.26)$$

Thus, we find the following infrared-divergent terms for $Q^2 = 0$:

$$\begin{aligned} & -\frac{1}{2\epsilon} \cdot (-t_{i-1}^{[2]})^{-\epsilon} 4(i \cdot j) \frac{(i j i-1 i+1)}{((i+1) \cdot (i-1))} \\ & \cdot \left[\frac{8}{3} (i \cdot j)^2 - 2 \frac{(i j i+1 i-1)}{((i+1) \cdot (i-1))(i \cdot j)} + \frac{(i j i+1 i-1)(i j i-1 i+1)}{((i+1) \cdot (i-1))^2} \right]. \end{aligned} \quad (4.2.27)$$

Similarly, we find for $P^2 = 0$ the following:

$$\begin{aligned} & -\frac{1}{2\epsilon} \cdot (-t_j^{[2]})^{-\epsilon} 4(i \cdot j) \frac{(i j j-1 j+1)}{((j+1) \cdot (j-1))} \\ & \cdot \left[\frac{8}{3} (i \cdot j)^2 - 2 \frac{(i j j+1 j-1)}{((j+1) \cdot (j-1))(i \cdot j)} + \frac{(i j j+1 j-1)(i j j-1 j+1)}{((j+1) \cdot (j-1))^2} \right]. \end{aligned} \quad (4.2.28)$$

4.3 NMHV Scalar amplitudes

In § 4.1 and § 4.2 we have shown how triple cuts correctly reproduce the cut-constructible part of the n -gluon one-loop MHV scattering amplitudes in pure Yang-Mills, both for the adjacent and for the general case. An interesting observation of this calculation is that we did not have to make use of two particle cuts. Of course, our result is consistent with two particle cuts since it agrees with the earlier calculation of the same class of amplitudes in [21] and [20] using conventional unitarity and MHV diagram, respectively. This is in line with similar observations made in [83] and [91] where certain

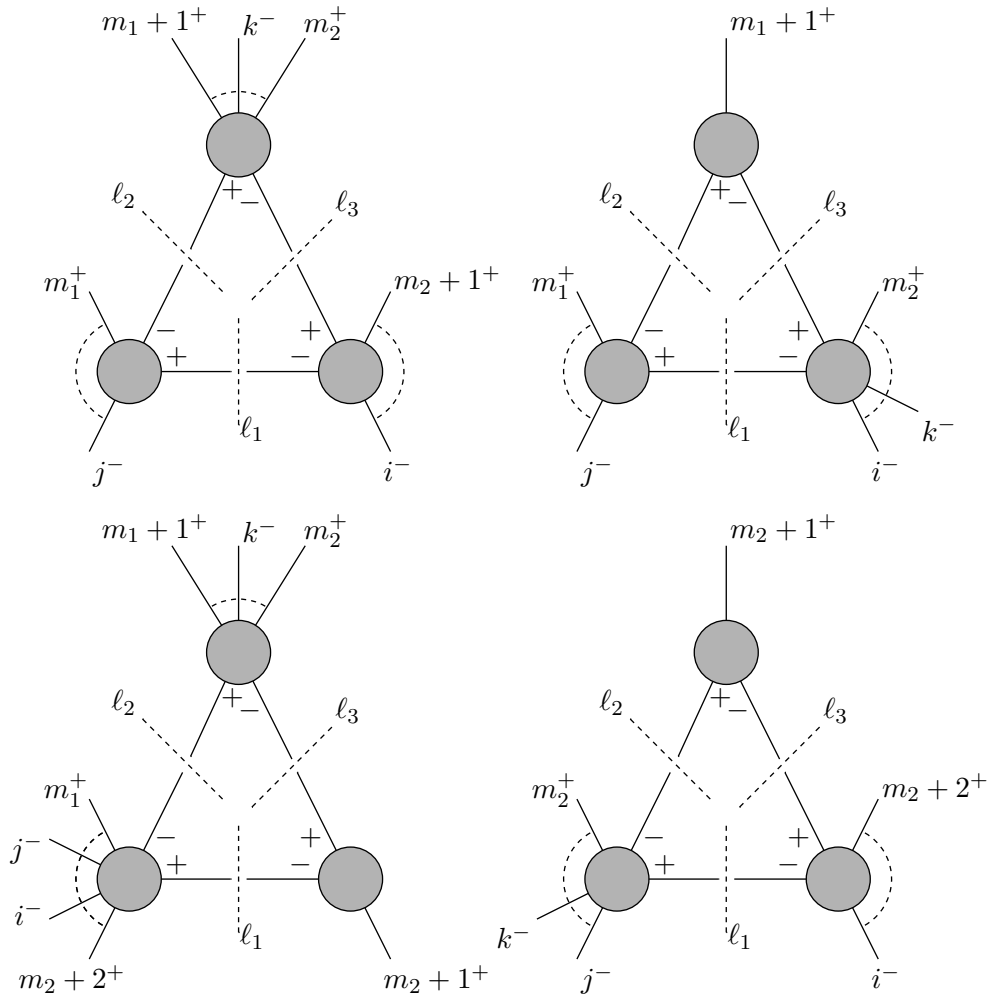


Figure 4.4: *The triple-cut diagrams contributing to the n -gluon one-loop NMHV scalar amplitude $\mathcal{A}_{\text{scalar}}^n(1^+, \dots, i^-, j^-, \dots, k^-, \dots, n^+)$.*

classes of amplitudes where obtained from triple cuts (and quadruple cuts) alone. The particular examples are NMHV one-loop amplitudes with adjacent negative-helicity gluons considered in [91] and all four-point one-loop amplitudes in pure Yang-Mills considered in [83]. Obviously, it would be interesting to investigate these observations further and understand whether this works for general amplitudes.

A first, important step would be to gain knowledge of the one-loop n -gluon NMHV, that is amplitudes with three negative helicities. While the purely gluonic 6-, 7- and n -point one-loop $\mathcal{N} = 4$ NMHV amplitudes were computed in [21, 27, 78, 96] using generalised unitarity, 6- and n -point one-loop amplitudes involving adjoint fermions and scalars in $\mathcal{N} = 4$ gauge theory were found in [97, 98]. A different approach was employed in [99] for the 7-gluon amplitudes in $\mathcal{N} = 4$ NMHV, whereby the authors managed to exploit the holomorphic anomaly of unitarity cuts to reconstruct the amplitude by

evaluating the action of a certain differential operator on the cut. Furthermore, the holomorphic anomaly was also utilised in [100] to compute the six-point one-loop $\mathcal{N} = 1$ split-helicity NMHV amplitude, while the remaining six-point one-loop $\mathcal{N} = 1$ NMHV amplitudes were calculated in [101]. Generalised unitarity provided the n -gluon one-loop $\mathcal{N} = 1$ NMHV amplitude in [91] for the case that the three negative-helicity gluons are adjacent. This latter amplitude has been calculated in pure Yang-Mills in [34] using an iterative approach. Finally, the coefficients of bubble and triangle integral functions for non-supersymmetric six-gluon amplitudes were computed in [102].

Let us conclude this section with some remarks on preliminary investigations of the NMHV case. We have investigated a particular class of non-supersymmetric NMHV amplitudes, namely $\mathcal{A}_{scalar}^n(1^+, \dots, i^-, j^-, \dots, k^-, \dots, n^+)$, *i.e.* amplitudes where the i -th and j -th negative-helicity gluons are adjacent and the k -th one is in an arbitrary position. In order to tackle the problem, we start by identifying all possible triple cuts contributing to the amplitude, which may be seen in Figure 4.4. The triple cut drawn at the top-left poses no new problems (we found structures similar to those appearing in the calculation of the MHV amplitude we investigated earlier). For the remaining triple cuts an additional difficulty arises, since the tree amplitudes appearing in the triple cut (4.0.2) may be NMHV. Thus, we cannot employ the Parke-Taylor (2.3.8) formula for the standard MHV tree amplitudes. By applying manipulations similar to those used throughout § 4.1 and § 4.2, we mostly obtain three-tensor triangle integrals although some more complicated three-tensor pentagon integrals still appear⁹. In a straightforward application of the CSW rules spurious poles arise and it is necessary to use improved formulæ for the NMHV tree amplitudes [104] that have only physical poles.

4.3.1 An Example: Coefficient of Three-Mass Triangle

We recall again that one-loop amplitudes in pure Yang-Mills can be decomposed in terms of a basis of scalar bubble, triangle and box integral functions together with additional rational pieces. Whilst rational pieces can be retrieved from the unitarity approach by imposing the cut loop momentum to live in $D = 4 - 2\epsilon$ dimensions [80], knowledge of the integral basis reduces to the task of finding the coefficients of this basis. Particularly straightforward is the computation of the coefficients of the box integral functions as shown in [78] where a combination of generalised unitarity together with complex momenta allowed for a purely algebraic computation of the sought-after coefficients¹⁰.

⁹In dealing with the NMHV tree amplitudes, we heavily used the results of [103–105].

¹⁰Basically, the four delta functions completely freeze the loop integration.

Conversely, coefficients of triangle and bubble integral functions are more challenging to compute, for cutting all the propagators in a given integral topology does not isolate a unique integral coefficient as for the box case and integrations or integral reduction techniques are needed. In [106], a way of finding these coefficients at the *integrand level* was proposed, which requires minimal information about the form of the amplitude and only involves solving some sets of equations. The solutions of these equations are the coefficients of the integral functions together with some spurious terms which vanish upon integration over loop momenta. A different approach was proposed in the very interesting [92] where coefficients for bubble and triangle integral functions were given. There, the use of double and triple cuts together with a complex parametrisation of the loop momenta allowed to determine the scalar integral coefficients via the study of their boundary conditions. It was realised in [107] that the cut-integrations reduce to contour integrals over a complex variable which allows the integrals to be analytically computed.

Below, we are interested in the computation of the coefficients of the three-mass triangle integral function $I_3^{3m}(K_1^2, K_2^2, K_3^2)$ with the momentum invariants $K_i^2 \neq 0$. This class of integral functions appears in the calculation of n -point NMHV amplitudes and was first computed in [108, 109]

$$I_3^{3m} = \frac{i}{\sqrt{\Delta_3}} \sum_{j=1}^3 \left[\text{Li}_2 \left(- \left(\frac{1+i\delta_j}{1-i\delta_j} \right) \right) - \text{Li}_2 \left(- \left(\frac{1-i\delta_j}{1+i\delta_j} \right) \right) \right] + \mathcal{O}(\epsilon), \quad (4.3.1)$$

where

$$\begin{aligned} \delta_1 &= \frac{K_1^2 - K_2^2 - K_3^2}{\sqrt{\Delta_3}}, \\ \delta_2 &= \frac{K_2^2 - K_1^2 - K_3^2}{\sqrt{\Delta_3}}, \\ \delta_3 &= \frac{K_3^2 - K_1^2 - K_2^2}{\sqrt{\Delta_3}}, \end{aligned} \quad (4.3.2)$$

with the Gram determinant of the three-mass integral function I_3^{3m} given by

$$\Delta_3 \equiv -(K_1^2)^2 - (K_2^2)^2 - (K_3^2)^2 + 2K_1^2 K_2^2 + 2K_1^2 K_3^2 + 2K_2^2 K_3^2. \quad (4.3.3)$$

By using generalised unitarity and the results of the study on the analytic structure of the cut integrals given in [107], we present the coefficients of the three-mass triangle integral functions I_3^{3m} for the n -point $\mathcal{N} = 0$ NMHV scalar amplitude.

In order to evaluate the three-mass triangle coefficients, we make use of generalised unitarity and consider the triple cut depicted in Figure 4.5 with the three negative-

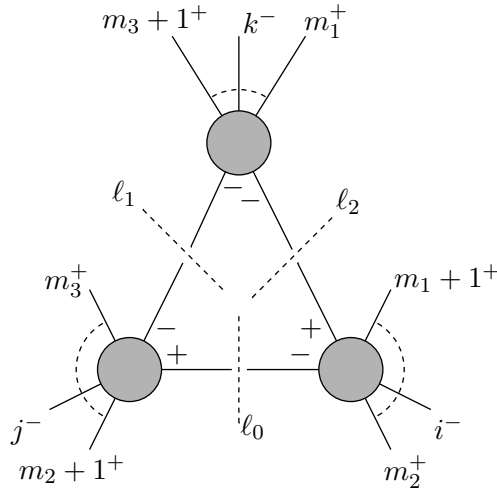


Figure 4.5: *The triple-cut diagram contributing to the n -gluon scalar NMHV amplitude $\mathcal{A}_n(1^+, \dots, i^-, \dots, j^-, \dots, k^-, \dots, n^+)$.*

helicity gluons each sitting at one of the three massive corners

$$C_3 = \sum_{i,j,k,\pm} \int d^4 \ell_1 \delta(\ell_0^2) \delta(\ell_1^2) \delta(\ell_2^2) \mathcal{A}_{\text{tree}}(\ell_0, \dots, j^-, \dots, -\ell_1) \\ \times \mathcal{A}_{\text{tree}}(\ell_1, \dots, k^-, \dots, -\ell_2) \mathcal{A}_{\text{tree}}(\ell_2, \dots, i^-, \dots, -\ell_0), \quad (4.3.4)$$

where K_i are sum of external colour-adjacent momenta k_i taken to be outgoing. Our starting point is the triple cut (4.3.4) obtained by sewing three MHV tree-level amplitudes

$$\mathcal{A}_{\text{scalar}}^n \Big|_{\text{cut}} = 2i \sum_{i,j,k} \int \frac{d^4 l_0}{(2\pi)^4} \frac{\langle j l_1 \rangle^2 \langle j l_0 \rangle^2}{\langle l_0 (m_2 + 1) \rangle \langle m_3 l_1 \rangle \langle l_1 l_0 \rangle} \frac{\langle k l_2 \rangle^2 \langle k l_1 \rangle^2}{\langle l_1 (m_3 + 1) \rangle \langle m_1 l_2 \rangle \langle l_2 l_1 \rangle} \\ \times \frac{\langle i l_0 \rangle^2 \langle i l_2 \rangle^2}{\langle l_2 (m_1 + 1) \rangle \langle m_2 l_0 \rangle \langle l_0 l_2 \rangle} \frac{\langle m_2 (m_2 + 1) \rangle \langle m_3 (m_3 + 1) \rangle \langle m_1 (m_1 + 1) \rangle}{l_0^2 l_1^2 l_2^2 \prod_{\alpha \neq m_1, m_2, m_3} \langle \alpha (\alpha + 1) \rangle} \Big|_{\text{cut}}, \quad (4.3.5)$$

where the ranges of summation of m_1, m_2 and m_3 are

$$k + 1 \leq m_1 \leq i - 1, \quad i + 1 \leq m_2 \leq j - 1, \quad j + 1 \leq m_3 \leq k - 1, \dots \quad (4.3.6)$$

In (4.3.5) we sum over the two possible helicity configurations and the delta functions have been replaced by unrestricted loop momenta.

Following the same strategy as in § 4.2, we multiply numerator and denominator of (4.3.5) by $[l_1 l_2]^2$ and we observe that

$$\langle l_0 l_1 \rangle [l_1 l_2] \langle l_2 l_0 \rangle = -\langle l_0 | K_1 \cdot K_2 | l_0 \rangle, \quad (4.3.7)$$

$$\langle l_2 l_1 \rangle [l_1 l_2] = -K_3^2. \quad (4.3.8)$$

Thus, (4.3.5) yields

$$\begin{aligned}
\mathcal{A}_n^{\mathcal{N}=0} &= 4i \sum_{m_1, m_2, m_3} \int \frac{d^4 l_0}{(2\pi)^4} \frac{\langle j l_1 \rangle^2 \langle j l_0 \rangle^2}{\langle l_0 (m_2 + 1) \rangle \langle m_3 l_1 \rangle} \frac{\langle k l_2 \rangle^2 \langle k l_1 \rangle^2}{\langle l_1 (m_3 + 1) \rangle \langle m_1 l_2 \rangle} \\
&\times \frac{\langle i l_0 \rangle^2 \langle i l_2 \rangle^2}{\langle l_2 (m_1 + 1) \rangle \langle m_2 l_0 \rangle} \frac{[l_1 l_2]^2}{\prod_{\alpha \neq m_1, m_2, m_3} \langle \alpha (\alpha + 1) \rangle} \\
&\times \frac{\langle m_2 (m_2 + 1) \rangle \langle m_3 (m_3 + 1) \rangle \langle m_1 (m_1 + 1) \rangle}{K_3^2 l_0^2 l_1^2 l_2^2 \langle l_0 | K_1 \cdot K_2 | l_0 \rangle}. \tag{4.3.9}
\end{aligned}$$

By making use of the Schouten identity on $\langle i l_0 \rangle \langle m_2 (m_2 + 1) \rangle$, $\langle k l_2 \rangle \langle m_1 (m_1 + 1) \rangle$ and $\langle j l_1 \rangle \langle m_3 (m_3 + 1) \rangle$ we obtain a sum of eight terms; however, each term will have three propagators less than (4.3.5). The first such a term would take the following form

$$\frac{\langle j l_1 \rangle \langle k l_2 \rangle \langle i l_0 \rangle \langle j l_0 \rangle^2}{\langle l_0 | K_1 \cdot K_2 | l_0 \rangle} \frac{\langle i m_2 \rangle \langle k m_1 \rangle \langle j m_3 \rangle}{\langle m_3 l_1 \rangle \langle m_1 l_2 \rangle \langle m_2 l_0 \rangle}. \tag{4.3.10}$$

We wish to make (4.3.9) a function of a single loop momentum, say l_0 . We do so by transforming spinor products in the following manner

$$\frac{\langle j l_1 \rangle}{\langle s l_1 \rangle} = \frac{\langle l_0 l_2 \rangle [l_2 l_1] \langle l_1 j \rangle}{\langle l_0 l_2 \rangle [l_2 l_1] \langle l_1 s \rangle} = \frac{\langle l_0 | K_2 \cdot K_3 | j \rangle}{\langle l_0 | K_2 \cdot K_3 | s \rangle} \equiv \frac{\langle l_0 j^{32} \rangle}{\langle l_0 s^{32} \rangle}, \tag{4.3.11}$$

$$\frac{\langle k l_2 \rangle}{\langle m_1 l_2 \rangle} = \frac{\langle l_0 l_1 \rangle [l_1 l_2] \langle l_2 k \rangle}{\langle l_0 l_1 \rangle [l_1 l_2] \langle l_2 t \rangle} \equiv \frac{\langle l_0 k^{32} \rangle}{\langle l_0 m_1^{32} \rangle}, \tag{4.3.12}$$

where $|a^{ij}\rangle \equiv K_j K_i |a\rangle$ in the notation of [107]. Thus, (4.3.9) can be recast in the more elegant following form

$$\langle i m_2 \rangle \langle k m_1 \rangle \langle j m_3 \rangle \frac{\langle l_0 j^{32} \rangle \langle l_0 k^{32} \rangle \langle l_0 i \rangle}{\prod_{y \in Y_3} \langle y l_0 \rangle} \frac{\langle j l_0 \rangle^2}{\langle l_0 | K_1 \cdot K_2 | l_0 \rangle}, \tag{4.3.13}$$

where $Y_3 = \{m_2, m_3^{32}, m_1^{32}\}$.

By repeatedly applying a generalised version of the Schouten identity

$$\frac{\langle \lambda a \rangle}{\langle \lambda b \rangle \langle \lambda c \rangle} = \frac{\langle b a \rangle}{\langle b c \rangle \langle \lambda b \rangle} + \frac{\langle c a \rangle}{\langle c b \rangle \langle \lambda c \rangle}, \tag{4.3.14}$$

we can rewrite (4.3.13) as

$$\langle i m_2 \rangle \langle k m_1 \rangle \langle j m_3 \rangle \sum_{y \in Y_3} \frac{\langle y j^{32} \rangle \langle y k^{32} \rangle}{\prod_{z \neq y \in Y_3} \langle z y \rangle} \frac{\langle l_0 i \rangle \langle j l_0 \rangle^2}{\langle l_0 y \rangle \langle l_0 | K_1 \cdot K_2 | l_0 \rangle}. \tag{4.3.15}$$

The sums in (4.3.15) are nothing but sums of canonical forms of the kind found in [107]. For the triangle integral function they take the following form

$$\frac{\langle l_0 a \rangle \langle l_0 b \rangle \langle l_0 c \rangle}{\langle l_0 | K_1 \cdot K_2 | l_0 \rangle \langle l_0 d \rangle} \longrightarrow \frac{\langle b | [K_1, K_2] | d \rangle \langle c | [K_1, K_2] | a \rangle - \Delta_3 \langle b d \rangle \langle c a \rangle}{2\Delta_3 \langle b | K_1 \cdot K_2 | d \rangle} + \frac{\langle d b \rangle \langle d c \rangle \langle a | [K_1, K_2] | d \rangle}{2\langle b | K_1 \cdot K_2 | d \rangle^2}, \quad (4.3.16)$$

where Δ_3 is the Gram determinant (4.3.3) of the three-mass integral function I_3^{3m} . Thus, we can recast (4.3.15) as

$$\langle i m_2 \rangle \langle k m_1 \rangle \langle j m_3 \rangle \sum_{y \in Y_3} \frac{\langle y j^{32} \rangle \langle y k^{32} \rangle}{\prod_{z \neq y \in Y_3} \langle z y \rangle} \times \left\{ \frac{\langle i | [K_1, K_2] | y \rangle \langle j | [K_1, K_2] | j \rangle}{2\Delta_3 \langle y | K_1 \cdot K_2 | y \rangle} + \frac{\langle y i \rangle \langle y j \rangle \langle j | [K_1, K_2] | y \rangle}{2\langle y | K_1 \cdot K_2 | y \rangle^2} \right\}. \quad (4.3.17)$$

We wish to introduce the shorthand notation

$$\langle i m_2 \rangle \langle k m_1 \rangle \langle j m_3 \rangle \sum [z \neq y \in Y_3 = m_2, m_3^{32}, m_1^{32}], \quad (4.3.18)$$

to denote the coefficient (4.3.17).

In a manner similar to the above, we compute the remaining seven terms and we present the coefficient for the three-mass triangle integral function contributing to the general n -point $\mathcal{N} = 0$ NMHV amplitude

$$C_3 = 4i \frac{\langle k | K_2 \cdot K_3 | i \rangle^2}{K_3^2 \prod_{\alpha \neq m_1, m_2, m_3} \langle \alpha (\alpha + 1) \rangle} \times \left\{ \begin{aligned} & \langle i m_2 \rangle \langle k m_1 \rangle \langle j m_3 \rangle \sum [z \neq y \in Y_3 = m_2, m_3^{32}, m_1^{32}] \\ & - \langle i m_2 \rangle \langle k m_1 \rangle \langle j m_{3,1} \rangle \sum [z \neq y \in Y_3 = m_2, m_{3,1}^{32}, m_1^{32}] \\ & - \langle i m_2 \rangle \langle k m_{1,1} \rangle \langle j m_3 \rangle \sum [z \neq y \in Y_3 = m_2, m_3^{32}, m_{1,1}^{32}] \\ & + \langle i m_2 \rangle \langle k m_{1,1} \rangle \langle j m_{3,1} \rangle \sum [z \neq y \in Y_3 = m_2, m_{3,1}^{32}, m_1^{32}] \\ & + \langle i m_{2,1} \rangle \langle k m_1 \rangle \langle j m_3 \rangle \sum [z \neq y \in Y_3 = m_{2,1}, m_3^{32}, m_1^{32}] \\ & + \langle i m_{2,1} \rangle \langle k m_1 \rangle \langle j m_{3,1} \rangle \sum [z \neq y \in Y_3 = m_{2,1}, m_{3,1}^{32}, m_1^{32}] \\ & + \langle i m_{2,1} \rangle \langle k m_{1,1} \rangle \langle j m_3 \rangle \sum [z \neq y \in Y_3 = m_{2,1}, m_3^{32}, m_{1,1}^{32}] \\ & - \langle i m_{2,1} \rangle \langle k m_{1,1} \rangle \langle j m_{3,1} \rangle \sum [z \neq y \in Y_3 = m_{2,1}, m_{3,1}^{32}, m_{1,1}^{32}] \end{aligned} \right\}, \quad (4.3.19)$$

where, with yet another notation, we define $m_{i,1} := (m_i + 1)$ for $i = 1, 2, 3$.

In [50], a similar calculation was performed providing the coefficient of the three-mass triangle for scalar NMHV amplitudes. We emphasise that we arrived at (4.3.19) independently from [50] and few months before it was published.

Chapter 5

Hidden Structures in (S)QED

One of the important realisations of the past decades is that physical observables in quantum gauge theories are far simpler than what one would expect from Feynman diagrams. For instance, the Parke-Taylor formula [65] for the MHV scattering amplitudes in colour-ordered Yang-Mills theory at tree level resums large numbers of Feynman diagrams into a stunning one-line expression. Such intriguing simplicity persists at the quantum level, culminating perhaps in the higher-loop iterative structures discovered in the higher-loop expansion of maximally SYM in [38, 39].

The perturbative expansion of supergravity theories is also full of surprises. At tree level, there are interesting relations between amplitudes in Yang-Mills and in gravity, starting with the KLT relations [110] and continuing with the recent solution of the BCF recursion relations [23, 24] for general relativity [29, 30] found in [111], which expresses amplitudes in maximal supergravity in terms of sums of squares of $\mathcal{N} = 4$ SYM amplitudes. Both KLT formulæ and the relations of [111] have echoes in the expressions for the one-loop box coefficients [112–115]. Most importantly, there is now mounting evidence of the remarkable similarities between $\mathcal{N} = 4$ SYM and $\mathcal{N} = 8$ supergravity, leading to the conjecture that the $\mathcal{N} = 8$ theory could be ultraviolet finite, just like its non-gravitational maximally supersymmetric counterpart. This is supported both by multi-loop perturbative calculations [116–119], and string theory and M-theory considerations [120–123].

In describing the remarkable web of regularities and similarities between the perturbative expansions of gauge theory and gravity, Quantum Electrodynamics (QED) has its own place in the story. For example, multi-photon amplitudes in QED (with at least eight photons) have in common with maximally supersymmetric Yang-Mills and supergravity the no-triangle (and no-bubble) property. This is the statement that all

one-loop amplitudes can be written as sums of box functions times rational coefficients¹. This property was proved for $\mathcal{N} = 4$ SYM in [17], conjectured for $\mathcal{N} = 8$ supergravity in [112, 113, 124, 125] and subsequently proved in [126, 127]. Recently it was found in [128] that a similar statement holds for photon amplitudes in QED. We also mention the interesting connections found in [118] and [126, 128] between the unexpected cancellations in the one-loop scattering amplitudes, and the large- z behaviour of tree amplitudes observed in [29, 30, 127, 129, 130]. In unordered theories such as gravity and QED these cancellations are amplified by the summation over different orderings of the external particles.

Two more interesting facts are worth mentioning. Firstly, the one-loop MHV and four-point two-loop photon amplitudes in $\mathcal{N} = 2$ SQED have a uniform degree of transcendentality, *i.e.* at one and two loops, only terms with total polylogarithmic weight equal to 2 and 4 appear, respectively [131]. A similar fact has been recently observed in [132, 133] in the one- and two-loop graviton MHV amplitudes in maximal supergravity. Furthermore, the $\mathcal{N} = 2$ SQED result for these amplitudes can be obtained from the corresponding $\mathcal{N} = 1$ SQED result by keeping only terms with maximal transcendentality (and no ratio of kinematic scales), leading to the speculation that maximal transcendentality [134] could be a feature of *all* maximally supersymmetric theories. Moreover, slightly departing from the realm of scattering amplitudes, we would also like to recall the somewhat puzzling “simplicity” of the three-loop electron anomalous dimension [135]. Here, numerically large cancellations occur between different diagrams, a fact which is due to the breaking of gauge symmetry at the diagrammatic level, see [136] for a prescient and enjoyable discussion of this point.

It is therefore natural to ask to which extent the simplicity found in the perturbative expansion of amplitudes in supersymmetric Yang-Mills and supergravity persists in (S)QED. We are fortunate to have a large number of analytic amplitudes at our disposal to test this. The one-loop four-photon amplitudes for massless and massive fermions were first computed in [137, 138]. Corrections to light-by-light scattering at two loops were determined about fifty years later in [139] using the modern unitarity method [17, 21]. The four-point results of [139] were confirmed in [131] and extended to $\mathcal{N} = 1$ and $\mathcal{N} = 2$ SQED by analysing the tensorial structure of the amplitudes found in [137, 138]. In [140], analytic expressions for one-loop MHV photon amplitudes for an arbitrary number of photons were calculated with the help of the off-shell currents found in [141]. In [142], analytical results for all six-photon QED amplitudes were given whilst in [143], formulæ for n -point MHV amplitudes in QED, scalar QED and $\mathcal{N} = 1$ SQED

¹One-loop photon amplitudes in (S)QED are somewhat special since they are both infrared and ultraviolet finite. This implies particular relations between the box coefficients, since the infrared divergences must cancel.

were obtained, together with the analytical results for the six-point NMHV QED and $\mathcal{N} = 1$ SQED amplitudes, which confirmed earlier work of [140, 142].

At tree level, the simplest nonvanishing scattering amplitude one encounters in massless QED is the MHV amplitude with n photons and two fermions,²

$$\begin{aligned} \mathcal{A}_{\text{MHV}}(\bar{q}, q, 1^+, 2^+, \dots, i^-, \dots, n^+) &= i \frac{\langle q i \rangle^3 \langle \bar{q} i \rangle}{\langle \bar{q} q \rangle^2} \prod_{l=1}^n \frac{\langle \bar{q} q \rangle}{\langle q l \rangle \langle l \bar{q} \rangle} \\ &= i \frac{\langle q i \rangle^3 \langle \bar{q} i \rangle}{\langle \bar{q} q \rangle^2} \sum_{\mathcal{P}\{1, 2, \dots, n\}} \frac{\langle \bar{q} q \rangle}{\langle q 1 \rangle \langle 1 2 \rangle \cdots \langle n \bar{q} \rangle}, \end{aligned} \quad (5.0.1)$$

where the fermion q and the i^{th} photon have negative helicity, and all the other particles have positive helicity. Equation (5.0.1) shows two important features. Firstly, the MHV amplitude in QED is given by a compact, one-line expression, see the first line of (5.0.1). Furthermore, this amplitude can be derived by summing over permutations of colour-ordered amplitudes in Yang-Mills where the photons are replaced by gluons with the same helicities.³ This is explicitly shown in the second line of (5.0.1), where each term in the sum over permutations $\mathcal{P}\{1, 2, \dots, n\}$ is equal to a colour-ordered Yang-Mills MHV amplitude with n gluons and two fundamental fermions q and \bar{q} .

This observation leads directly to the first result [51] we present in this chapter. We will discuss how the one-loop MHV amplitude of photons in supersymmetric and in pure QED can be derived directly by summing over appropriate permutations of the corresponding result for gluon MHV amplitudes in supersymmetric or pure Yang-Mills theory. As we mentioned before, one-loop photon amplitudes in (S)QED can be written in terms of (the finite parts of) box functions for $n \geq 8$. We will therefore show that the box coefficients of the Yang-Mills amplitudes, summed over appropriate permutations of the external gluons, directly give the box coefficients of the QED amplitudes. We will also outline the proof of this interesting fact, based on a *gedanken* MHV diagram calculation [16, 18, 20, 144, 145].

The second observation we make [51] in this chapter is aimed at uncovering possible cross-order relations in the perturbative expansion of $\mathcal{N} = 2$ SQED. The first example of iterative structures was found in planar $\mathcal{N} = 4$ SYM for the four-point MHV amplitudes in [38]. In a later paper [39], Bern, Dixon and Smirnov (BDS) put forward a conjecture for the all-loop resummation of the planar n -point MHV amplitudes in $\mathcal{N} = 4$ SYM, which has been tested up to three loops in the four-point case [39] and up to two loops in the five-point case [40, 146].

²Recall that there is no tree-level photon amplitude corresponding to the gluon MHV amplitude in Yang-Mills.

³See [71] for a discussion of this important feature.

In a remarkable paper [41], Alday and Maldacena succeeded in using the AdS/CFT correspondence to calculate scattering amplitudes at strong coupling, in particular relating them to expectation values of lightlike polygonal Wilson loops, and confirming the BDS *ansatz* at strong coupling in the four-point case. In a subsequent series of papers, it was shown that the vacuum expectation value of the same Wilson loops is related to MHV amplitudes in $\mathcal{N} = 4$ SYM also at weak coupling [42, 43]. Calculations at two loops of four-sided [44] and five-sided Wilson loops [45] found agreement with the field theory amplitudes and the BDS *ansatz*. However, in [147] it was realised that the BDS *ansatz* is incomplete at least for a large number of external gluons. More concretely, a calculation of the lightlike hexagon Wilson loop [47] showed that the BDS *ansatz* breaks down, and has to be amended by adding a dual conformal invariant remainder function. In [46], a direct calculation of the two-loop six-gluon MHV amplitude in $\mathcal{N} = 4$ SYM confirmed the result of [47, 48]. The remainder function has been studied in detail numerically for $n = 6$ points in [46, 48] and more recently in [148] for $n = 6, 7, 8$.

Motivated by this, we will consider the four-photon MHV amplitude at one and two loops in maximally supersymmetric $\mathcal{N} = 2$ SQED, and test the possibility that the two-loop amplitude could be written as a polynomial in the one-loop amplitude. One important difference compared to Yang-Mills is that in QED the one- and two-loop four-photon amplitudes are finite. Thus, one lacks the guiding principle of the exponentiation of infrared divergences, which is central to the all-loop ABDK/BDS *ansatz*. Despite this, we find that, quite surprisingly, the two-loop photon MHV amplitudes in maximally supersymmetric QED is not exactly given but well approximated (in a wide kinematic region) by a polynomial in the one-loop MHV four-photon amplitude. We will also discuss the limitations of such an approximate formula.

The rest of the chapter is organised as follows. In § 5.1 we present the relationship mentioned earlier between the box coefficients of one-loop MHV (S)QED amplitudes and sums of permutations of box coefficients of the same amplitudes in (S)YM, and prove it using one-loop MHV diagrams. In § 5.2, after reviewing salient features of the BDS *ansatz*, we investigate approximate recursive structures for MHV four-photon amplitudes in $\mathcal{N} = 2$ SQED.

5.1 In Search of the (S)QED-(S)QCD Correspondence

In this section we explore a one-loop connection between massless scalar QED and pure Yang-Mills amplitudes, as well as a similar one between $\mathcal{N} = 1$ SQED and $\mathcal{N} = 1$ SYM amplitudes.

We start by considering the expressions for the scalar QED and $\mathcal{N} = 1$ SQED photon MHV amplitudes at one loop. These amplitudes were computed in [143], and are given by

$$\begin{aligned} \mathcal{A}_n^{\text{scalar}/\mathcal{N}=1}(1^-, 2^-, 3^+, \dots, n^+) &= i \frac{(e\sqrt{2})^n}{16\pi^2} \sum_{\mathcal{P}\{1,2\}} \sum_{\mathcal{P}\{3,\dots,n\}} \frac{d^{\text{scalar}/\mathcal{N}=1}}{(n-4)!} B^{1m}(s_{23}, s_{24}, s_{15\dots n}) \\ &+ i \frac{(e\sqrt{2})^n}{16\pi^2} \sum_{\mathcal{P}\{1,2\}} \sum_{\mathcal{P}\{3,\dots,n\}} \sum_{m=5}^{n-1} \frac{(-1)^m d^{\text{scalar}/\mathcal{N}=1}}{(n-m)!(m-4)!} \\ &\times B^{2me}(s_{135\dots m}, s_{145\dots m}, s_{15\dots m}, s_{2m+1\dots n}), \end{aligned} \quad (5.1.1)$$

where

$$d^{\text{scalar}} = -2 \frac{\langle 13 \rangle \langle 14 \rangle \langle 23 \rangle \langle 24 \rangle}{\langle 34 \rangle^2} \prod_{\substack{i=5 \\ i \neq 3,4}}^n \frac{\langle 34 \rangle^{n-4}}{\langle 3i \rangle \langle 4i \rangle}, \quad (5.1.2)$$

$$d^{\mathcal{N}=1} = -\langle 12 \rangle^2 \prod_{\substack{i=5 \\ i \neq 3,4}}^n \frac{\langle 34 \rangle^{n-4}}{\langle 3i \rangle \langle 4i \rangle}. \quad (5.1.3)$$

Let us explain the notation employed in (5.1.1). Firstly, the sums in (5.1.1) are over permutations \mathcal{P} of the massless states inside the curly brackets. Secondly, the functions B^{1m} and B^{2me} appearing in (5.1.1) are the finite parts of the one-mass and two-mass easy scalar box functions F respectively. These are given by [16, 108]

$$\begin{aligned} F^{1m}(s, t, P^2) &= -\frac{1}{\epsilon^2} [(-s)^{-\epsilon} + (-t)^{-\epsilon} - (-P^2)^{-\epsilon}] + B^{1m}(s, t, P), \quad (5.1.4) \\ F^{2me}(s, t, P, Q) &= -\frac{1}{\epsilon^2} [(-s)^{-\epsilon} + (-t)^{-\epsilon} - (-P^2)^{-\epsilon} - (-Q^2)^{-\epsilon}] + B^{2me}(s, t, P, Q), \end{aligned}$$

where

$$\begin{aligned} B^{1m}(s, t, P^2) &= \text{Li}_2\left(1 - \frac{P^2}{t}\right) + \text{Li}_2\left(1 - \frac{P^2}{s}\right) + \frac{1}{2} \ln^2\left(\frac{t}{s}\right) + \frac{\pi^2}{6}, \quad (5.1.5) \\ B^{2me}(s, t, P^2, Q^2) &= \text{Li}_2(1 - aP^2) + \text{Li}_2(1 - aQ^2) - \text{Li}_2(1 - as) - \text{Li}_2(1 - at), \end{aligned}$$

with

$$a := \frac{P^2 + Q^2 - s - t}{P^2 Q^2 - st}, \quad (5.1.6)$$

and $s := (P+p)^2$, $t := (P+q)^2$, with $p+q+P+Q=0$, where p and q are the massless legs (sitting at opposite corners, in the two-mass easy boxes), and P and Q the massive legs (with either $P^2=0$ or $Q^2=0$ for the one-mass box). The arguments of the box functions appearing in (5.1.1) are the kinematic invariants $s_{i\dots j} := (k_i + \dots + k_j)^2$.

In Figure 5.1 we provide a representation of the box function appearing in the second

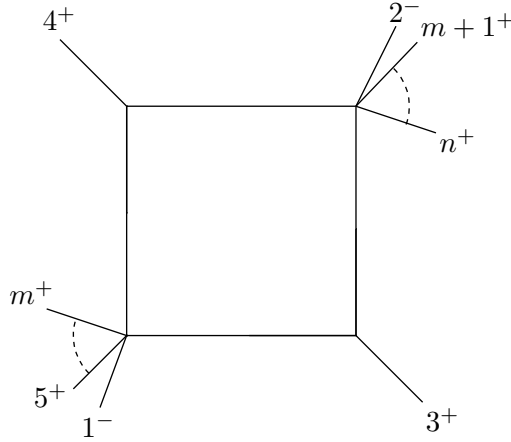


Figure 5.1: *The two-mass easy box function appearing in (5.1.1). The momenta $p = k_3$ and $q = k_4$ are null, whereas $P := k_1 + k_5 + \dots + k_m$ and $Q := k_2 + k_{m+1} + \dots + k_n$ are massive. The one-mass box function in (5.1.1) is obtained by setting $m = n$, so that the top right corner becomes massless (and contains only the momentum k_2).*

line of (5.1.1). The massless legs there correspond to the positive helicity photons 3^+ and 4^+ . The negative-helicity photons 1^- and 2^- are always part of (different) massive corners P and Q , which contain $m-3$ and $n-m+1$ legs respectively. The combinatorial coefficients appearing in (5.1.1) correspond to the number of permutations of the positive helicity photons inside P and Q (which obviously leave the box function invariant).

In (5.1.2) and (5.1.3), we have slightly departed from the expressions for these coefficients as originally given in [143]. Specifically, we have multiplied their result for d^{scalar} by a factor of 2 to account for the fact that we are working with complex scalar fields. Furthermore, we have rewritten (5.1.2) and (5.1.3) in terms of eikonal factors

$$\mathcal{S}(a, i, b) := \frac{\langle a b \rangle}{\langle a i \rangle \langle i b \rangle}, \quad (5.1.7)$$

for reasons which will become clear shortly.

Finally, let us stress that the amplitudes given in (5.1.1) are infrared and ultraviolet finite. Because of Furry's theorem, they are nonvanishing only for n even.

Having discussed the expressions of the one-loop MHV photon amplitudes in QED and SQED, we turn to the corresponding amplitudes in Yang-Mills. Here we will always be considering the coefficient of the single-trace contribution to the amplitude. The simplest amplitudes are given by the infinite sequence of MHV amplitudes in $\mathcal{N} = 4$ SYM, first derived by Bern, Dixon, Dunbar and Kosower in [17] using unitarity [21]

and collinear limits, and later confirmed in [16] using one-loop MHV diagrams. At the planar level, the result for the colour-ordered amplitudes is

$$\mathcal{A}_n^{\mathcal{N}=4} = \mathcal{A}_n^{\text{tree}} \mathcal{M}_n, \quad (5.1.8)$$

where the helicity-blind function \mathcal{M}_n is

$$\mathcal{M}_n = \sum_{p=j+1}^{i-1} \sum_{q=i+1}^{j-1} F^{2me}(p, q, P, Q), \quad (5.1.9)$$

and

$$\mathcal{A}_n^{\text{tree}}(1^+, \dots, i^-, \dots, j^-, \dots, n^+) := i \frac{\langle i j \rangle^4}{\langle 1 2 \rangle \langle 2 3 \rangle \dots \langle n 1 \rangle}, \quad (5.1.10)$$

is the tree-level amplitude, given by the Parke-Taylor formula [65]. i and j label the two negative-helicity gluons, each in one of the two opposite massive corners.

The one-loop MHV amplitude in $\mathcal{N} = 1$ SYM was presented in [21] and confirmed in [18] using MHV diagrams. The contribution to the amplitude of an $\mathcal{N} = 1$ chiral multiplet running in the loop is given by the following compact formula,

$$\mathcal{A}_n^{\mathcal{N}=1}(1^+, \dots, i^-, \dots, j^-, \dots, n^+) = \sum_{p=j+1}^{i-1} \sum_{q=i+1}^{j-1} [c^{\mathcal{N}=1}]_{pq}^{ij} B^{2me}(p, q, P, Q) + \dots, \quad (5.1.11)$$

where

$$[c^{\mathcal{N}=1}]_{pq}^{ij} = \frac{1}{2} \mathcal{A}_n^{\text{tree}} b_{pq}^{ij}, \quad (5.1.12)$$

and

$$b_{pq}^{ij} = 2 \frac{\langle i p \rangle \langle j q \rangle \langle i q \rangle \langle j p \rangle}{\langle i j \rangle^2 \langle p q \rangle^2}. \quad (5.1.13)$$

$\mathcal{A}_n^{\text{tree}}$ is the Parke-Taylor amplitude in (5.1.10). The dots stand for triangle and bubble functions, which will not be relevant for our discussion.⁴

Lastly, the one-loop n -point non-supersymmetric Yang-Mills MHV amplitudes were computed in [20, 21, 84] and confirmed in [49] using generalised unitarity [78], with the result

$$\mathcal{A}_n^{\text{scalar}}(1^+, \dots, i^-, \dots, j^-, \dots, n^+) = \sum_{p=j+1}^{i-1} \sum_{q=i+1}^{j-1} [c^{\text{scalar}}]_{pq}^{ij} B^{2me}(p, q, P, Q) + \dots, \quad (5.1.14)$$

where

$$[c^{\text{scalar}}]_{pq}^{ij} = \frac{1}{2} \mathcal{A}_n^{\text{tree}} [b_{pq}^{ij}]^2. \quad (5.1.15)$$

⁴This is because of the no-triangle property of QED amplitudes [128], which ensures that the bubble and triangle coefficients vanish.

As before, the dots in (5.1.14) stand for triangle and bubble functions, as well as for the rational terms of the amplitude (not linked to cut-constructible terms), which will not be relevant in the following discussion.

Our goal will be to find a relation between the coefficients $d^{\text{scalar}/\mathcal{N}=1}$ of the two-mass easy box functions in the expression for the MHV photon scattering amplitudes in (S)QED, given in (5.1.1), and the corresponding coefficients of the same box function, $c^{\text{scalar}/\mathcal{N}=1}$, of the MHV gluon amplitudes in $\mathcal{N} = 1$ and pure Yang-Mills in (5.1.12) and (5.1.15).

We begin by making the intuitive observation that, in order to be able to match a gluon amplitude to a target (S)QED amplitude, we need to “unorder” an otherwise colour-ordered expression. We do so by introducing appropriate sums over permutations, which we now illustrate.

To begin with a simple example, consider the six-point MHV $\mathcal{N} = 1$ SQED case. Holding the two massless legs of the box function fixed, we sum over permutations of the gluons appearing at the massive corners. This amounts to computing

$$\begin{aligned} \mathcal{P}_{2me}^{\mathcal{N}=1}(\mathcal{A}_6^{\text{tree}}) &:= \frac{1}{2} \sum_{\mathcal{P}\{1,5\}} \sum_{\mathcal{P}\{2,6\}} \mathcal{A}_6^{\text{tree}}(4, \{1, 5\}, 3, \{2, 6\}) b_{34}^{12}, & (5.1.16) \\ \mathcal{P}_{1m}^{\mathcal{N}=1}(\mathcal{A}_6^{\text{tree}}) &:= \frac{1}{2} \sum_{\mathcal{P}\{1,5,6\}} \mathcal{A}_6^{\text{tree}}(\{1, 5, 6\}, 3, 2, 4) b_{34}^{12}, \end{aligned}$$

for the two-mass easy and the one-mass part of (5.1.1) respectively. We have calculated these sums numerically and analytically using standard identities. Our result is

$$\mathcal{P}^{\mathcal{N}=1}(\mathcal{A}_6^{\text{tree}}) = \frac{\langle 12 \rangle^2}{\langle 64 \rangle \langle 36 \rangle \langle 53 \rangle \langle 45 \rangle}. \quad (5.1.17)$$

Remarkably, this expression exactly matches the result for $d^{\mathcal{N}=1}$ given in (5.1.2). Similarly, replacing b_{pq}^{ij} with $[b_{pq}^{ij}]^2$ in (5.1.16), yields

$$\mathcal{P}^{\text{scalar}}(\mathcal{A}_6^{\text{tree}}) = 2 \frac{\langle 14 \rangle \langle 13 \rangle \langle 24 \rangle \langle 23 \rangle}{\langle 64 \rangle \langle 36 \rangle \langle 53 \rangle \langle 45 \rangle \langle 34 \rangle^2}, \quad (5.1.18)$$

which is identical to the expression for d^{scalar} shown in (5.1.3).

We can extend these two simple examples to an arbitrary number of legs. An elegant

way to perform the sums in (5.1.16) is provided by the “eikonal” identity [71]

$$\sum_{\mathcal{P}\{1,2,\dots,\ell\}} \frac{\langle r s \rangle}{\langle r 1 \rangle \langle 1 2 \rangle \cdots \langle \ell s \rangle} = \prod_{\substack{i=1 \\ i \neq r,s}}^{\ell} \frac{\langle r s \rangle}{\langle r i \rangle \langle i s \rangle}, \quad (5.1.19)$$

where we take r and s to be two fixed spinors. Equation (5.1.19) relates sums of permutations of MHV-like terms to products of eikonal factors, and can be proved by iteratively using the Schouten identity.

By choosing $r = 3$ and $s = 4$ in (5.1.19) we have

$$\begin{aligned} & \sum_{\mathcal{P}_1} \sum_{\mathcal{P}_2} \frac{\langle 1 2 \rangle^4}{\langle 3 2 \rangle \langle 2(m+1) \rangle \cdots \langle (n-1)n \rangle \langle n 4 \rangle \langle 4 1 \rangle \langle 1 5 \rangle \cdots \langle m 3 \rangle} \\ &= \langle 1 2 \rangle^4 \prod_{\substack{i=1 \\ i \neq r,s}}^n \frac{\langle r s \rangle}{\langle r i \rangle \langle i s \rangle} \\ &= \langle 1 2 \rangle^4 \frac{\langle 3 4 \rangle^{n-4}}{\langle 3 1 \rangle \langle 1 4 \rangle \cdots \langle 3 n \rangle \langle n 4 \rangle}, \end{aligned} \quad (5.1.20)$$

where $\mathcal{P}_1 := \mathcal{P}\{2, m+1, \dots, n\}$ and $\mathcal{P}_2 := \mathcal{P}\{1, 5, \dots, m\}$ are permutations of the massless legs in the massive corners of the box function in Figure 1.

Multiplying (5.1.20) by b_{34}^{12} we recover the expression for $[d^{\mathcal{N}=1}]_{34}^{12}$ given in (5.1.2). A similar argument runs for the one-mass box coefficients $[d^{\text{scalar}}]_{pq}^{ij}$, with the only difference that the sum in the first line of (5.1.20) is over one set of permutations rather than two.

One can arrive at the same conclusion by performing a one-loop MHV diagram calculation akin to [16, 18, 20] with MHV rules adapted to QED as done at tree level in [145]. For a one-loop MHV photon amplitude we have to glue two tree-level MHV vertices with two internal scalar propagators, and perform an appropriate loop integration [16]. We will not give details of the calculation because we can recycle results from [16, 18, 20]. The crucial observation is that the only diagrams contributing are those where all gluons are external and the two internal legs of each MHV vertex are either scalars or fermions with opposite helicity. This also implies that the two external negative-helicity gluons must belong to different MHV vertices. The relevant MHV QED tree amplitudes can be obtained from the corresponding MHV tree amplitude in QCD with $n-1$ positive helicity gluons, one negative-helicity gluon and two fermions (scalars) of opposite helicity and summing over the $n!$ permutations of the n gluons. Writing the QED MHV vertices with two fermions and n gluons in terms of QCD tree MHV vertices, see the second line of (5.0.1), reduces the calculation to sums

of permutations of MHV one-loop diagrams for MHV amplitudes in pure Yang-Mills and $\mathcal{N} = 1$ SYM [18, 20]. It can be seen easily that this reproduces exactly the observations made earlier in this section on the box coefficients of the one-loop (S)QED MHV amplitudes. Triangle and box coefficients are guaranteed to vanish because of the no-triangle property [128].

Finally, we observe that this has implications for the twistor-space localisation properties of the coefficients, which are inherited from those of the (S)YM amplitudes, *i.e.* the coefficients localise on sets of two, possibly intersecting lines in twistor space.

In summary, we have found the intriguing result that the coefficients $d^{\text{scalar}/\mathcal{N}=1}$ of the finite boxes in the one-loop photon MHV amplitudes in massless SQED and non-supersymmetric QED can be derived by summing over appropriate permutations of coefficients of the same boxes in $\mathcal{N} = 1$ SYM and in pure Yang-Mills. It would be very interesting to study whether this remarkable structure is present in non-MHV amplitudes and at higher loops.

5.2 Approximate Iterative Structures in $\mathcal{N} = 2$ SQED

Motivated by the existence of iterative structures for amplitudes in $\mathcal{N} = 4$ SYM, we have investigated the possible existence of recursive-like structures for MHV amplitudes in the maximally supersymmetric $\mathcal{N} = 2$ SQED theory.⁵ Before discussing our results, let us briefly review the iterative relations in $\mathcal{N} = 4$ SYM [38, 39]. It was shown in [38] that the two-loop four-point MHV amplitude in $\mathcal{N} = 4$ SYM satisfies an intriguing cross-order relation,

$$\mathcal{M}_4^{(2)}(\epsilon) - \frac{1}{2}(\mathcal{M}_4^{(1)}(\epsilon))^2 = f^{(2)}(\epsilon)\mathcal{M}_4^{(1)}(2\epsilon) + C^{(2)} + \mathcal{O}(\epsilon). \quad (5.2.1)$$

Here $\mathcal{M}_n^{(L)}$ is the helicity-blind function obtained by taking the ratio between the L -loop MHV amplitude and the corresponding tree amplitude. Furthermore $f^{(2)}(\epsilon) = -(\zeta_2 + \zeta_3\epsilon + \zeta_4\epsilon^2)$, and $C^{(2)} = -(5/4)\zeta_4$.

In [39], a resummed, exponentiated expression for the scalar function \mathcal{M}_n was proposed, and checked explicitly in a three-loop calculation in the four-point case. The

⁵A similar analysis has been performed in [132, 133] for the four-point MHV amplitude in $\mathcal{N} = 8$ supergravity, and highlighted a remarkably simple structure for the two-loop term in the expansion of logarithm of the helicity-blind ratio $\mathcal{M}^{\mathcal{N}=8}/\mathcal{M}_{\text{tree}}$. The functions appearing in the ratio were also found to have uniform transcendentality.

BDS conjecture is expressed as [39]

$$\mathcal{M}_n := 1 + \sum_{L=1}^{\infty} a^L \mathcal{M}_n^{(L)}(\epsilon) = \exp \left[\sum_{L=1}^{\infty} a^L \left(f^{(L)}(\epsilon) \mathcal{M}_n^{(1)}(L\epsilon) + C^{(L)} + E_n^{(L)}(\epsilon) \right) \right], \quad (5.2.2)$$

where $a = [g^2 N / (8\pi^2)] (4\pi e^{-\gamma})^\epsilon$. Here $f^{(L)}(\epsilon)$ is a set of functions,

$$f^{(L)}(\epsilon) := f_0^{(L)} + f_1^{(L)} \epsilon + f_2^{(L)} \epsilon^2, \quad (5.2.3)$$

one at each loop order, which appear in the exponentiated all-loop expression for the infrared divergences in generic amplitudes in dimensional regularisation [149] (and generalise the function $f^{(2)}$ in (5.2.1)).

BDS also suggested a resummed expression for the appropriately defined finite part of the n -point MHV amplitude,

$$\mathcal{F}_n = e^{F_n^{\text{BDS}}}, \quad (5.2.4)$$

where

$$F_n^{\text{BDS}}(a) = \frac{1}{4} \gamma_{\text{cusp}}(a) F_n^{(1)}(0) + C(a). \quad (5.2.5)$$

Notice that the entire dependence on kinematics of the BDS *ansatz* enters through the finite part of the one-loop box function, $F_n^{(1)}(0)$.

In analogy with the BDS *ansatz*, we would like to investigate the existence of cross-order relations in the four-point amplitude $\mathcal{M}_4(1^-, 2^-, 3^+, 4^+)$ in $\mathcal{N} = 2$ SQED. To this end, we consider a decomposition of the two-loop term in the expansion of this amplitude as

$$[\mathcal{M}_4^{(2)}]_{\text{ansatz}} = b [\mathcal{M}_4^{(1)}]^2 + c \mathcal{M}_4^{(1)} + d, \quad (5.2.6)$$

where $\mathcal{M}_4^{(1)}$ is the four-point one-loop MHV amplitude, and b, c and d have to be determined.⁶

The expressions for photon-photon scattering amplitudes at one and two loops entering (5.2.6) were derived in [131]. At one loop, the light-by-light scattering amplitude can be written as

$$\mathcal{M}^{(1)} = \mathcal{M}^{(1),S} + \mathcal{M}^{(1),F}, \quad (5.2.7)$$

where the contributions on the right-hand side of (5.2.7) denote the scalar electron and electron loops respectively. In the Standard Model, only the fermion loop contributes. The one-loop MHV scattering amplitude in $\mathcal{N} = 1$ SQED is given by

$$\mathcal{M}_4^{(1)} = -4[(X - Y)^2 + \pi^2], \quad (5.2.8)$$

⁶From now on, we will denote as \mathcal{M}_n the SQED amplitudes.

where

$$X = \log\left(\frac{-t}{s}\right), \quad Y = \log\left(\frac{-u}{s}\right). \quad (5.2.9)$$

At one loop, there is no contribution from the gauge multiplet. Thus, (5.2.8) is the one-loop four-point MHV amplitude in $\mathcal{N} = 1$ and $\mathcal{N} = 2$ SQED.

A few comments are in order here. Firstly, we notice that in the physical region $s > 0$ and $t, u < 0$ the expression (5.2.8) is real. Outside this region, an analytic continuation is needed as the u - and t -channels develop a discontinuity. Secondly, we observe in (5.2.8) the absence of any dimensionless ratios of the kinematic scales t^2/s^2 . Furthermore, all the functions appearing in the expression for $\mathcal{M}_4^{(1)}$ have uniform degree of transcendentality, equal to 2.

The two-loop expression for the four-point MHV $\mathcal{N} = 2$ SQED amplitude is still rather compact and simple. It is given by [131]

$$\begin{aligned} \mathcal{M}_4^{(2)} = & -16 \operatorname{Li}_4(y) + 8Y \operatorname{Li}_3(x) + 8Y \operatorname{Li}_3(y) + \frac{16}{45}\pi^4 \\ & - \frac{2}{3}XY\pi^2 - \frac{2}{3}Y^3(Y - 4X) \\ & + i\pi\left[16 \operatorname{Li}_3(x) - \frac{4}{3}Y\pi^2 - \frac{4}{3}Y^2(Y - 3X)\right] + \{u \leftrightarrow t\}, \end{aligned} \quad (5.2.10)$$

where X and Y are defined in (5.2.9) and

$$x := -t/s, \quad y := -u/s = 1 - x. \quad (5.2.11)$$

As in (5.2.8), also in (5.2.10) there are no terms proportional to ratios of kinematic scales, and we only have functions with transcendentality equal to 4. Therefore, we expect the coefficients b , c and d to have transcendentality 0 and 2 and 4, respectively.

The real part of (5.2.10) can be recast in the following suggestive form,

$$\begin{aligned} \operatorname{Re}\left[\mathcal{M}_4^{(2)}\right] = & -16 \operatorname{Li}_4(y) - 16 \operatorname{Li}_4(x) + 8(X + Y)(\operatorname{Li}_3(x) + \operatorname{Li}_3(y)) + 4X^2Y^2 - \frac{4}{3}XY\pi^2 \\ & - \frac{1}{24}\left[\mathcal{M}_4^{(1)}\right]^2 - \frac{\pi^2}{3}\mathcal{M}_4^{(1)} + \frac{2}{45}\pi^4. \end{aligned} \quad (5.2.12)$$

In (5.2.12), we have re-written the result of [131] in a way that already incorporates the functions $\mathcal{M}_4^{(1)}$ and $[\mathcal{M}_4^{(1)}]^2$ appearing in (5.2.6), see the last line of (5.2.12).

In order to find a set of coefficients b, c and d which best fit our proposed *ansatz* (5.2.6), we build a system of three equations for some three random values of y and solve for b, c and d . We then plug the values of these coefficients in (5.2.6) and match it against the real part of (5.2.10). The result of such algebraic manipulation can be seen

in Figure 5.2, where (the real part of) (5.2.10) as well as our *ansatz* are plotted. The values of b, c and d used in the plot are given by the set of values I for y shown in Table 1 below,

Coefficients	I	II	III	IV	V	VI	VII
b	-0.0386	-0.038	-0.0387	-0.0417	-0.0412	-0.0415	-0.0412
c	-2.567	-2.571	-2.574	-2.812	-2.894	-3.009	-2.877
d	-5.784	-5.894	-5.938	-11.46	-14.689	-25.098	-14.489
$F(b, c, d)^{\mathcal{N}=2}$	97.179	187.129	88.452	49.555	1.065	25.554	0.500

Table 5.1: Values of b, c and d for different sets of values for y . The sets I - III include points away from the boundary $y = 0$ and $y = 1$, and the resulting coefficients b, c, d vary slowly from one set to another, unlike the case of the sets IV - VI , which include points near the boundary in y space. The set VII is obtained using the least square method.

where the sets I - VI are⁷ $I = \{0.3, 0.4, 0.5\}$, $II = \{0.272, 0.342, 0.482\}$, $III = \{0.25, 0.35, 0.45\}$, $IV = \{0.00001, 0.10001, 0.482\}$, $V = \{0.0006, 0.0023, 0.006\}$, $VI = \{0.0001, 0.0003, 0.0235\}$, while the values of (b, c, d) in column VII are obtained applying the least square method. We have carried out a similar analysis for the four-point MHV amplitude in $\mathcal{N} = 1$ SQED, the expression of which can also be found in [131], and we report the results in Table 2 below,

Coefficients	I	II	III	IV	V	VI	VII
b	-0.0356	-0.0356	-0.0356	-0.0277	-0.027	-0.026	-0.0278
c	-1.829	-1.828	-1.827	-1.062	-0.113	0.211	-0.719
d	-79.04	-78.99	-78.98	-60.99	18.39	32.54	-44.57
$F(b, c, d)^{\mathcal{N}=1}$	756.0	749.7	746.5	99.4	1265.9	1365.6	24.1

Table 5.2: Values of b, c and d for different sets of values for y . The sets of y used are the same as in the $\mathcal{N} = 2$ theory shown in Table 1.

Introducing

$$F(b, c, d) := \int_0^1 dy \left(\mathcal{M}_4^{(2)}(y) - [\mathcal{M}_4^{(2)}]_{\text{ansatz}}(y) \right)^2, \quad (5.2.13)$$

and minimising $F(b, c, d)$ gives the “best” values for b, c and d over all of the phase space.

Let us summarise the outcome of this analysis.

⁷Since (5.2.10) is symmetric under $x \rightarrow 1 - x$, we only choose values for y from half of the phase space.

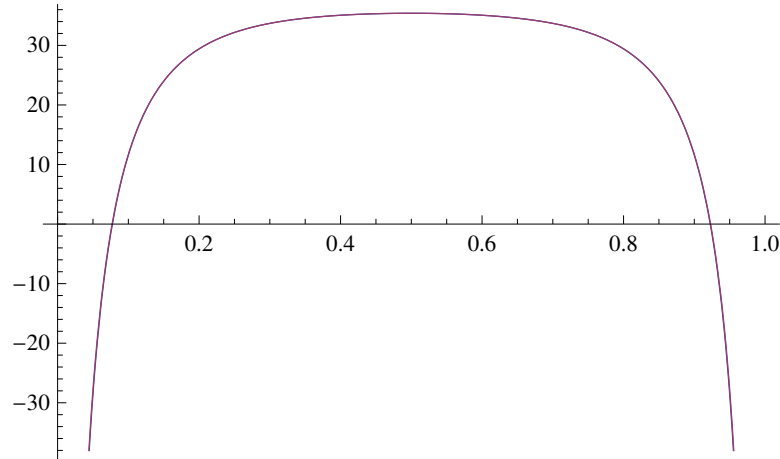


Figure 5.2: In this Figure we plot (the real part of) the right-hand side of (5.2.10), representing the four-point two-loop MHV amplitude in $\mathcal{N} = 2$ SQED, together with our ansatz (5.2.6), with $y = -u/s$ given by set I. The two overlapping functions are hardly distinguishable in this plot.

1. Unlike the case of the BDS *ansatz* for $\mathcal{N} = 4$ SYM, we find that the coefficients b , c and d are not (kinematic-independent) constants, but have different values for different kinematic points.

2. Having derived values of these three coefficients, we plot the two-loop amplitude as well as our *ansatz* as functions of the ratio y . These plots are presented in Figure 5.2, and show a very surprising overlap.

3. In order to study more closely the functional forms of the two-loop amplitude and of our *ansatz*, in Figure 3 we present a plot of the difference between (5.2.6) and (5.2.12), which we could consider as the “remainder function” for this amplitude,⁸

$$\mathcal{R}_4(y) := \mathcal{M}_4^{(2)} - \left(b [\mathcal{M}_4^{(1)}]^2 + c \mathcal{M}_4^{(1)} + d \right). \quad (5.2.14)$$

From Figure 5.3, we see that the two functions agree for a wide range of values of y , however the difference function has spikes as $y \rightarrow 0$ or $y \rightarrow 1$. In these limits the best fit would be given by the second line of (5.2.12) in which case the disagreement would be proportional to a single power of a logarithm in x or y . The presence of this divergent behaviour at the extrema of the phase space shows that our *ansatz* is certainly incomplete. However, we find it quite remarkable that large deviations only appear at the boundary of the phase space.

4. We have computed (5.2.13) for both $\mathcal{N} = 1$ and $\mathcal{N} = 2$ SQED and found the

⁸Notice that this function depends however on the choice of b , c and d we make in the *ansatz* (5.2.6).

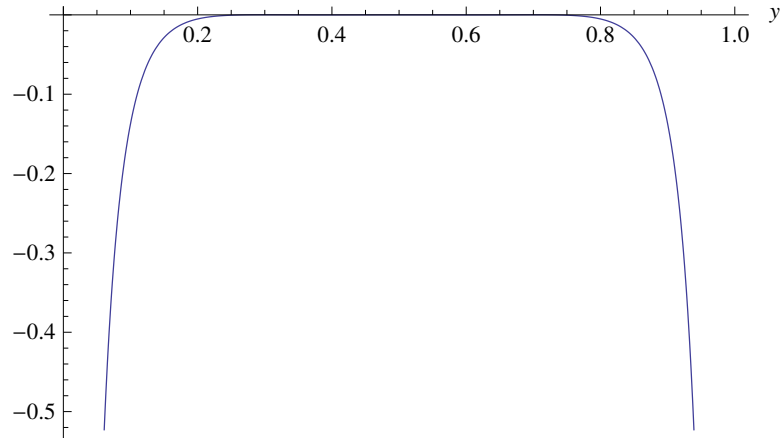


Figure 5.3: This figure shows a plot of the $\mathcal{N} = 2$ SQED remainder function, constructed as the difference between the two-loop MHV amplitude in $\mathcal{N} = 2$ SQED and (5.2.6).

values

$$F(b, c, d)^{\mathcal{N}=2} = 0.5, \quad F(b, c, d)^{\mathcal{N}=1} = 24.1. \quad (5.2.15)$$

This shows that (5.2.6) gives the most accurate approximation of the real part of the two-loop amplitude in the case of $\mathcal{N} = 2$ SQED.

5. We also observe that the four-point MHV amplitude in $\mathcal{N} = 2$ SQED can be derived from the $\mathcal{N} = 1$ SQED amplitude by keeping maximally transcendental terms and deleting contributions which multiply ratios of the kinematics invariants.

In summary, the approximate iterative structures we have explored in this section are certainly not on the same footing as those in $\mathcal{N} = 4$ SYM found in [38, 39]. Nevertheless, we find it intriguing that part of the two-loop four-photon MHV amplitude (5.2.10) is captured by a polynomial in the one-loop amplitude (5.2.8). This is surprising, given the absence of infrared divergences in these amplitudes. It would be interesting if one could find exact iterative structures, written in terms of an appropriate QED remainder function, and explain them in terms of some underlying symmetry of the theory.

It would also be interesting to find a Wilson loop interpretation of MHV scattering amplitudes in SQED, similarly to that found in $\mathcal{N} = 4$ SYM [41–43]. We give a brief introduction to the Wilson loop- $\mathcal{N} = 4$ SYM duality in the next chapter, where we show how to retrieve the collinear behaviour of $\mathcal{N} = 4$ SYM amplitudes from a Wilson loop calculation.

Chapter 6

An *Antipasto* of Wilson Loop- $\mathcal{N} = 4$ SYM Duality

Over the last few years, amplitudes in $\mathcal{N} = 4$ SYM have been extensively and successfully studied. One of the reasons for the success lies in the ultraviolet finiteness¹ of the amplitudes although they still suffers from IR divergences. Furthermore, it is opportune to remark that scattering amplitudes in $\mathcal{N} = 4$ SYM are much simpler than the same counterpart in its cousin theory, namely QCD.

To make the chapter somehow self-consistent, let us review few poignant facts about amplitudes in $\mathcal{N} = 4$ SYM. At any loop order L , a n -point MHV $\mathcal{N} = 4$ SYM amplitude [124] takes the following factorised form

$$\mathcal{A}_n^{(L)} = \mathcal{A}_n^{\text{tree}} \mathcal{M}_n^{(L)}, \quad (6.0.1)$$

where $\mathcal{M}_n^{(L)}$ is a helicity-blind function. At one loop, $\mathcal{M}_n^{(1)}$ is a sum of two-mass easy box integral functions $F^{2\text{me}}$ with coefficients equal to one

$$\mathcal{M}_n = \sum_{p=j+1}^{i-1} \sum_{q=i+1}^{j-1} F^{2\text{me}}(p, q, P, Q). \quad (6.0.2)$$

In [38], inspired by the infrared behaviour of amplitudes in gauge theory [28, 149–153, 155, 160–162], it was noticed how splitting amplitudes, which encode the limit of an amplitude as two adjacent momenta become collinear, do enjoy an iterative structure whereby a two-loop splitting amplitude could be expressed solely in terms of one-loop

¹See [170, 171] for a review on the finiteness of $\mathcal{N} = 4$.

terms. From this observation, an iteration relation for higher-loop amplitudes in the 't Hooft limit $N_c \rightarrow \infty$ was put forward and demonstrate to hold for a two-loop four-point amplitude. In a subsequent paper [39], a fascinating iteration conjecture for computing planar all-loops $\mathcal{N} = 4$ SYM amplitudes at weak coupling was put forward. The conjecture takes the alluring simple form

$$\mathcal{M}_n^{(L)} = \exp \left[\sum_{L=1}^{\infty} a^L \left(f^{(L)}(\epsilon) \mathcal{M}_n^{(1)}(L\epsilon) + C^{(L)} + E_n^{(L)}(\epsilon) \right) \right], \quad (6.0.3)$$

where $a = [g^2 N / 8\pi^2] (4\pi e^{-\gamma})^\epsilon$ and $f^{(L)}(\epsilon)$ is a set of functions

$$f^{(L)}(\epsilon) := f_0^{(L)} + f_1^{(L)} \epsilon + f_2^{(L)} \epsilon^2, \quad (6.0.4)$$

one at each loop order. It is relevant to observe that $f_0^{(L)} \sim \Gamma_{\text{cusp}}^{(L)}$, where Γ_{cusp} is the cusp anomalous dimension²

$$\Gamma_{\text{cusp}}(a) = \sum_{L=1}^{\infty} a^L \Gamma_{\text{cusp}}^{(L)}, \quad \Gamma_{\text{cusp}}^{(1)} = 4, \quad \Gamma_{\text{cusp}}^{(2)} = -4\zeta_2, \quad (6.0.5)$$

related to the anomalous dimension Γ_j of large-spin j twist-two operators [155, 156]

$$\Gamma_j = \frac{1}{2} \Gamma_{\text{cusp}}(a) \ln j + O(j^0), \quad j \rightarrow \infty, \quad (6.0.6)$$

for the case of the quark operator.

An all-orders conjecture for the cusp anomalous dimension was put forward in [157] in the context of integrability. The proposed integral equation agreed with the known values of Γ_{cusp} up to three loops and suggested a four-loop prediction of $f_0^{(4)}$. In [89], the four-gluon four-loop amplitude in $\mathcal{N} = 4$ SYM was computed and a disagreement for the value of $f_0^{(4)}$ predicted by [157] was found. However, parallel to [89], an improved integral equation [158] was formulated which found agreement with the results of [89] and later confirmed by yet another calculation [159] of $f_0^{(4)}$. Importantly, the constants $C^{(L)}$, $f_0^{(L)}$, $f_1^{(L)}$ and $f_2^{(L)}$ on the right hand side of (6.0.3) do not depend either on kinematics or on the number of particles n . On the other hand, the non-iterating contributions $E_n^{(L)}$ depend explicitly on n , but vanish as $\epsilon \rightarrow 0$.

On entirely different grounds, the conjecture of [39] was lent more plausibility in [41]. In this remarkable paper, the authors manage to exploit the AdS/CFT correspondence to compute the four-point amplitude at strong coupling. The computation of the amplitude is equal (at large N) to the computation of the area of the world-sheet of a

²The name finds its origin due to its appearance in the renormalisation group equation for a Wilson line for two semi-infinite straight lines meeting at a cusp [153, 154].

classical string in the boundary of AdS space which in turn is dual to the expectation value of a Wilson loop made out of four lightlike segments. The external momenta of the amplitude give the value at the point where these segments join. In [42] and in [43], it was shown how the one-loop four-point and n -point MHV $\mathcal{N} = 4$ amplitudes at weak-coupling may be recovered by means of a Wilson loop calculation. The IR divergent³ part of the amplitude is generated by propagators stretching between adjacent segments meeting at a cusp, whereas the finite part find its origins in propagators stretching between non-adjacent segments.

However, the elation was short-lived. While explicit calculation of up to three loops in the four-point case [39] and up to two loops in the five-point case [40, 146] have verified the conjecture, further investigation [47] of the lightlike hexagon Wilson loop found disagreement with (6.0.3), in that the proposed *ansatz* would need to be corrected by a dual conformal invariant remainder function. A direct calculation [72] of the two-loop six-gluon MHV amplitude in $\mathcal{N} = 4$ SYM purported the results of [47].

In this chapter we wish to compute one-loop splitting amplitudes by considering Wilson loops whose contour is n -sided lightlike polygons. We find perfect agreement with the splitting amplitudes previously found in [164–166]. However, a subtlety arises as the Wilson loop calculation does not provide any information about the polarisation of the particles involved in the scattering. At one loop, the standard Parke-Taylor tree-level amplitude, which appears as a prefactor in the $\mathcal{N} = 4$ amplitude, is not generated by the Wilson loop calculation. Thus, what we really find is the one-loop splitting amplitude stripped of any helicity information.

In § 6.1 we review the collinear limit of Yang-Mills at tree level and one loop. In § 6.2 we carry out the Wilson loop calculation to obtain the one-loop splitting amplitude.

6.1 Collinear Limit of Gluon Amplitudes

In the limit where two colour adjacent momenta become collinear, a n -point amplitude can be expressed in terms of a lower amplitude times an universal function, called *splitting amplitude*, which depends upon the external states going collinear and the internal states going on-shell and captures the leading divergence in the collinear limit of the amplitude. We parameterise the two massless colour-adjacent external momenta

³In the Wilson loop computation, cusps are source of its UV divergence. The UV part, in turn, is interpreted as the IR divergence of the amplitude. The relation between the infrared divergences of scattering amplitudes and ultraviolet divergences of Wilson loops is characterised by the appearance of the cusp anomalous dimension (6.0.5), first studied in QCD in [163].

p_a and p_b going collinear as

$$p_a \rightarrow z\ell, \quad p_b \rightarrow (1-z)\ell, \quad (6.1.1)$$

where $\ell^2 = (p_a + p_b)^2 \rightarrow 0$ in the collinear limit and $z \in [0, 1]$ the momentum fraction. As $\ell^2 \rightarrow 0$, the tree-level amplitude factor as

$$\mathcal{A}_n^{\text{tree}}(1, 2, \dots, a^{\lambda_a}, b^{\lambda_b}, \dots, n) \xrightarrow{a\parallel b} \sum_{\sigma=\pm} \mathcal{A}_{n-1}^{\text{tree}}(1, 2, \dots, (a+b)^\sigma, \dots, n) \text{Split}_{-\sigma}^{\text{tree}}(a^{\lambda_a}, b^{\lambda_b}). \quad (6.1.2)$$

For the case of gluons⁴ the splitting amplitudes take the form

$$\text{Split}_{-}^{\text{tree}}(a^-, b^-) = 0, \quad (6.1.3)$$

$$\text{Split}_{-}^{\text{tree}}(a^+, b^+) = \frac{1}{\sqrt{z(1-z)}\langle ab \rangle}, \quad (6.1.4)$$

$$\text{Split}_{+}^{\text{tree}}(a^+, b^-) = \frac{(1-z)^2}{\sqrt{z(1-z)}\langle ab \rangle}, \quad (6.1.5)$$

$$\text{Split}_{-}^{\text{tree}}(a^+, b^-) = -\frac{z^2}{\sqrt{z(1-z)}[ab]}. \quad (6.1.6)$$

The remaining helicity configurations can be derived from the above using parity arguments.

At one loop, we have similar structures to the ones at tree level. In the same notation as before, we have⁵

$$\begin{aligned} \mathcal{A}_n^{1\text{-loop}}(1, \dots, a^{\lambda_a}, b^{\lambda_b}, \dots, n) \xrightarrow{a\parallel b} \\ \sum_{\sigma} \left[\text{Split}_{-\sigma}^{\text{tree}}(a^{\lambda_a}, b^{\lambda_b}) \mathcal{A}_{n-1}^{1\text{-loop}}(1, \dots, (a+b)^\sigma, \dots, n) \right. \\ \left. + \text{Split}_{-\sigma}^{1\text{-loop}}(a^{\lambda_a}, b^{\lambda_b}) \mathcal{A}_{n-1}^{\text{tree}}(1, \dots, (a+b)^\sigma, \dots, n) \right], \end{aligned} \quad (6.1.7)$$

where the sum is over the two possible helicities $\sigma = \pm$ of the fused leg $p_a + p_b$. An expression to all orders in ϵ of $\text{Split}^{1\text{-loop}}$ was found both in [165] and in [166]. It takes the following form,

$$\text{Split}_{-\sigma}^{1\text{-loop}}(a^{\lambda_a}, b^{\lambda_b}) = \text{Split}_{-\sigma}^{\text{tree}}(a^{\lambda_a}, b^{\lambda_b}) r_1^{[1]}(z), \quad (6.1.8)$$

⁴Using appropriate MHV amplitudes one can find expression for splitting amplitudes for fermions and scalars.

⁵For a quick and thorough review of collinear limits see [167] and references therein.

where

$$r_1^{[1]}(z) = \frac{c_\Gamma}{\epsilon^2} \left(\frac{-s_{ab}}{\mu^2} \right)^2 \left[1 - {}_2F_1 \left(1, -\epsilon; 1 - \epsilon; \frac{z-1}{z} \right) - {}_2F_1 \left(1, -\epsilon; 1 - \epsilon; \frac{z}{z-1} \right) \right], \quad (6.1.9)$$

and

$$c_\Gamma = \frac{\Gamma(1+\epsilon)\Gamma^2(1-\epsilon)}{(4\pi)^{2-\epsilon}\Gamma(1-2\epsilon)}. \quad (6.1.10)$$

Extracting an helicity-dependent factor, which we recall cannot be found by means of a Wilson loop computation, we can rewrite (6.1.7) as

$$\begin{aligned} \mathcal{A}_n^{1\text{-loop}}(1, \dots, a^{\lambda_a}, b^{\lambda_b}, \dots, n) &\xrightarrow{a||b} \\ &\text{Split}_{-\sigma}^{\text{tree}}(a^{\lambda_a}, b^{\lambda_b}) \mathcal{A}_{n-1}^{\text{tree}} \mathcal{M}_{n-1}^{1\text{-loop}} + \text{Split}_{-\sigma}^{\text{tree}}(a^{\lambda_a}, b^{\lambda_b}) r_1^{[1]}(z) \mathcal{A}_{n-1}^{\text{tree}} \\ &= \text{Split}_{-\sigma}^{\text{tree}}(a^{\lambda_a}, b^{\lambda_b}) \mathcal{A}_{n-1}^{\text{tree}} \left(\mathcal{M}_{n-1}^{1\text{-loop}} + r_1^{[1]}(z) \right). \end{aligned} \quad (6.1.11)$$

By considering a Wilson loop around arbitrary lightlike n -sided polygon, we wish to calculate the quantity $\mathcal{M}_n^{1\text{-loop}}$ in the collinear limit, *i.e.*

$$\mathcal{M}_n^{1\text{-loop}} \rightarrow \mathcal{M}_{n-1}^{1\text{-loop}} + r_1^{[1]}(z). \quad (6.1.12)$$

6.2 One-Loop Splitting Amplitudes from Light-like Wilson Loops

In this section we compute, at order g^2 in the coupling, the Wilson loop given by

$$W_C = \frac{1}{N} \langle 0 | \text{Tr} P \exp \left(ig \int_C dx^\mu A_\mu(x) \right) | 0 \rangle, \quad (6.2.1)$$

where $A_\mu(x) = A_\mu^a T^a$ is a gauge field and T^a are the $SU(N_c)$ generators in the fundamental representation. P is the usual path ordering and \mathcal{C} is the integration contour. Following the reasoning of [43], where it was shown how n -point one-loop MHV amplitude can be derived using Wilson loops, we choose our polygon contour to be made out of n segments, joining at the points k_i^μ and such that the on-shell momenta of the gluons are given by

$$p_i = k_i - k_{i+1}, \quad (6.2.2)$$

and parameterised as $k_i(\tau_i) = k_i + \tau(k_{i+1} - k_i) = k_i - \tau_i p_i$, $\tau_i \in [0, 1]$.

There are three classes of diagrams which contribute to corrections of a Wilson loop.

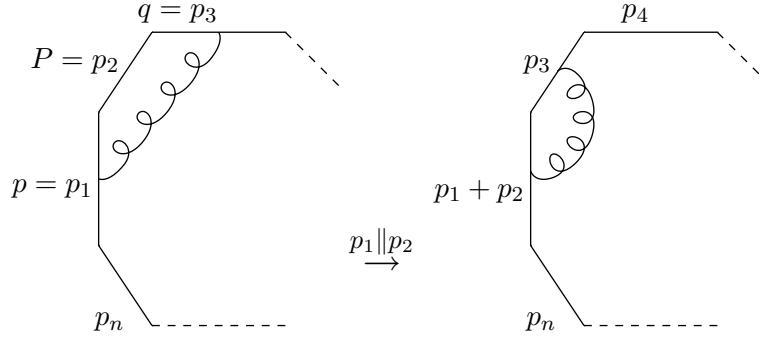


Figure 6.1: A one-loop correction to the Wilson loop, where the gluon stretches between two non-adjacent segments (left) which, in the collinear limit (right) gives rise to finite and IR contributions to $r_1^{[1]}(z)$ and IR contributions to $\mathcal{M}_{n-1}^{1\text{-loop}}$.

First, there is the class in which the propagator stretches between points of the same segment. Using the fact that we have on-shell momenta, $p_i^2 = 0$, it is straightforward to see that this kind of contributions vanish. Second, we have those diagrams in which the propagator stretches between two adjacent segments meeting at a cusp. This kind of diagrams generate infrared-divergent terms which involve only two-particle invariants and take the form

$$\mathcal{M}_n^{1\text{-loop}} \Big|_{\text{IR}} = -\frac{1}{\epsilon^2} \sum_{i=1}^n \left(\frac{-s_{ii+1}}{\mu^2} \right)^{-\epsilon}, \quad (6.2.3)$$

with $s_{ii+1} = (p_i + p_{i+1})^2$.

Thirdly, there are those Wilson loops in which the propagator connects two non-adjacent segments and contribute to the finite part of the two-mass easy box integral function $F^{2\text{me}}$. In order to evaluate (6.2.1), we make use of the gluon propagator suitably regularised in $D=4-2\epsilon$ dimensions which we can write it as

$$G_{\mu\nu}(x) = -g_{\mu\nu} \frac{\Gamma(1 - \epsilon_{\text{UV}})}{4\pi^2} (-x^2 + i\epsilon)^{-1 + \epsilon_{\text{UV}}} \pi^{\epsilon_{\text{UV}}}, \quad (6.2.4)$$

where, in light of footnote 3, we recognise

$$\epsilon_{\text{UV}} = -\epsilon_{\text{IR}} > 0. \quad (6.2.5)$$

At this point we wish to stress two important facts:

- a. the k_i variables are not the Fourier transformed coordinates in position space; they still represent momenta. In [41], the same coordinates (6.2.2) are used and they are interpreted as T-dual coordinates which determine the classical string solutions. The very same coordinates have also been used in [168, 169] to compute scattering amplitudes and in [95] in the context of MHV diagrams;
- b. the contour \mathcal{C} of (6.2.1) is defined in terms of the external gluon momenta whereas the gluon propagator (6.2.4) is defined in configuration space, not momentum space.

We begin by considering the third class of diagrams and, for now, only those which give contributions⁶ to $r_1^{[1]}(z)$, the helicity-blind component of one-loop splitting amplitudes. We choose p_1 and p_2 to be collinear. A picture of this class of diagrams may be seen in Figure 6.1. A calculation of this Wilson loop in the non-collinear limit can be followed in [43] and it yields

$$-(ig\tilde{\mu}^{\epsilon_{UV}})^2 \frac{1}{2} \frac{\Gamma(1 - \epsilon_{UV})}{4\pi^{2-\epsilon_{UV}}} \mathcal{F}_\epsilon(s, t, P, Q), \quad (6.2.6)$$

where $\mathcal{F}_\epsilon(s, t, P, Q)$ is the following integral⁷

$$\mathcal{F}_\epsilon(s, t, P, Q) = \int_0^1 d\tau_p d\tau_q \frac{P^2 + Q^2 - s - t}{[-(P^2 + (s - P^2)\tau_p + (t - P^2)\tau_q + (-s - t + P^2 + Q^2)\tau_p\tau_q)]^{1+\epsilon}}. \quad (6.2.7)$$

It is at this point that we wish take the collinear limit. Also, we stress the fact that we are working to all orders in ϵ . However, before we proceed further, some notation is imperative. We define $P = \sum_{i=p+1}^{q-1} (k_i - k_{i+1})$, with $P^2 \neq 0$ in general, the sum of momenta between two general massless legs p and q . Momentum conservation is $P + p + q = -Q$, which implies that the contour of the integration is closed. Also, $s = (P + p)^2$ and $t = (P + q)^2$ are the usual Mandelstam variables, with $p = p_1$, $q = p_3$ and $P = p_2$.

In our case limit $P^2 = 0$ in (6.2.7). Most importantly, we have $s = 2(p_1 \cdot p_2) = 2z(1 - z)\ell^2$ and $t = 2(p_2 \cdot p_3) = 2(1 - z)(\ell \cdot p_3)$ according to our parameterisation

⁶This is slightly incorrect but justified in hindsight. As we will see in the course of the chapter, different Wilson loop diagrams will give contributions to either $r_1^{[1]}(z)$ or $\mathcal{M}_{n-1}^{1\text{-loop}}$. Specifically, only those Wilson loop diagrams in which the propagator stretches between two legs $p, q \neq 1, 2$ contribute to $\mathcal{M}_{n-1}^{1\text{-loop}}$. The remaining diagrams mainly contribute to $r_1^{[1]}(z)$.

⁷From now, we set $\epsilon := -\epsilon_{UV} < 0$, where ϵ is the usual infrared regulator.

(6.1.1). This allows us to rewrite $\mathcal{F}_\epsilon(s, t, P, Q)$ as

$$\begin{aligned} \mathcal{F}_\epsilon(s, t, P, Q) &= (-s)^{-1-\epsilon} 2az\ell^2 \left(-\frac{1}{\epsilon}\right) \\ &\quad \times \int_0^1 d\tau_p \left[\frac{\left(\frac{a}{z} + \left(1 + \frac{a}{1-z}\right)\tau_p\right)^{-\epsilon}}{\frac{a}{z} + \frac{a}{1-z}\tau_p} - \frac{\tau_p^{-\epsilon}}{\frac{a}{z} + \frac{a}{1-z}\tau_p} \right], \end{aligned} \quad (6.2.8)$$

where we have performed the τ_q integration and $a = (\ell \cdot p_3)/\ell^2$. We decide to compute separately the two contributions to the integral (6.2.8).

The first one yields

$$\begin{aligned} -(-s)^{-1-\epsilon} 2az\ell^2 \frac{z-1}{a\epsilon^2} &\left\{ \left(\left(\frac{a+z-z^2}{1+a-z} \right)^\epsilon \left(\frac{a+z-z^2}{z(1-z)} \right)^{-\epsilon} {}_2F_1 \left[\epsilon, \epsilon, 1+\epsilon, \frac{(z-1)^2}{1+a-z} \right] \right) \right. \\ &\quad \left. + \left(\left(\frac{a}{1+a-z} \right)^\epsilon \left(\frac{a}{z} \right)^{-\epsilon} {}_2F_1 \left[\epsilon, \epsilon, 1+\epsilon, \frac{z-1}{z-1-a} \right] \right) \right\}, \end{aligned} \quad (6.2.9)$$

which, in turn, may be brought to the familiar form

$$-\frac{1}{\epsilon^2} (-s_{p_1+p_2, p_3})^{-\epsilon} + \frac{1}{\epsilon^2} (-s_{p_2 p_3})^{-\epsilon}, \quad (6.2.10)$$

after using one of the various identities relating hypergeometric functions

$${}_2F_1 \left[c-a, b; c; \frac{A}{A-1} \right] = (1-A)^b {}_2F_1 [a, b; c; A]. \quad (6.2.11)$$

On the other hand, the second contribution to (6.2.8) gives

$$(-s)^{-\epsilon} \frac{z}{\epsilon(1-z)(1-\epsilon)} {}_2F_1 \left[1, 1-\epsilon; 2-\epsilon; \frac{z}{z-1} \right], \quad (6.2.12)$$

where it is understood that $s \equiv s_{p_1 p_2}$.

By applying in succession two hypergeometric identities, namely

$$\begin{aligned} {}_2F_1 [a, b; c; A] &= \frac{\Gamma(c)\Gamma(b-a)}{\Gamma(b)\Gamma(c-a)} (-A)^{-a} {}_2F_1 [a, 1-c+a; 1-b+a; A^{-1}] \\ &\quad + \frac{\Gamma(c)\Gamma(b-a)}{\Gamma(b)\Gamma(c-a)} (-A)^{-b} {}_2F_1 [b, 1-c+b; 1-a+b; A^{-1}], \end{aligned} \quad (6.2.13)$$

and

$${}_2F_1 [a, b; c; A^{-1}] = 1 - {}_2F_1 [a, a-c; a-b; A] + (-A)^{-\epsilon} \Gamma(1+\epsilon)\Gamma(1-\epsilon), \quad (6.2.14)$$

we manage to bring (6.2.12) to the form

$$-\frac{1}{\epsilon^2}(-s)^{-\epsilon} \left(1 - {}_2F_1 \left[1, -\epsilon; 1 - \epsilon; \frac{z}{z-1} \right] \right), \quad (6.2.15)$$

after making use of an identity between Γ -functions, $\Gamma(x) = (x-1)\Gamma(x-1)$.

There is another Wilson loop diagram similar to Figure 6.1 coming from $3 \leftrightarrow n$, $1 \leftrightarrow 2$ and $z \leftrightarrow 1-z$ which, following a similar calculation to the above, gives

$$-\frac{1}{\epsilon^2}(-s)^{-\epsilon} \left(1 - {}_2F_1 \left[1, -\epsilon; 1 - \epsilon; \frac{z-1}{z} \right] \right) + \frac{1}{\epsilon^2}(-s_{p_1+p_2, p_n})^{-\epsilon} - \frac{1}{\epsilon^2}(-s_{p_1 p_n})^{-\epsilon}. \quad (6.2.16)$$

Thus, in the collinear limit, the two diagrams yield

$$\begin{aligned} & -\frac{1}{\epsilon^2}(-s)^{-\epsilon} \left(2 - {}_2F_1 \left[1, -\epsilon; 1 - \epsilon; \frac{z}{z-1} \right] - {}_2F_1 \left[1, -\epsilon; 1 - \epsilon; \frac{z-1}{z} \right] \right) \\ & - \frac{1}{\epsilon^2}(-s_{p_1+p_2, p_3})^{-\epsilon} + \frac{1}{\epsilon^2}(-s_{p_2 p_3})^{-\epsilon} + \frac{1}{\epsilon^2}(s_{p_1 p_n})^{-\epsilon} - \frac{1}{\epsilon^2}(-s_{p_1+p_2, p_n})^{-\epsilon}. \end{aligned} \quad (6.2.17)$$

The second class of corrections to the Wilson loop may be seen in Figure 6.2. Here, a propagator stretches between two adjacent legs, both going collinear, case a) or only one, case b). They give rise to infrared-divergent terms of the form given in (6.2.3). The contributions coming from this set of diagrams can thus be summarised as

$$\frac{1}{\epsilon^2}(-s)^{-\epsilon} - \frac{1}{\epsilon^2}(-s_{p_2 p_3})^{-\epsilon} - \frac{1}{\epsilon^2}(-s_{p_1 p_n})^{-\epsilon}. \quad (6.2.18)$$

We observe that the first term of (6.2.18) cancels a similar factor in the first line of (6.2.17) whilst the second and third term of (6.2.18) cancel respectively the second and third term in the second line of (6.2.17). The remaining terms of the second line of (6.2.17) represent infrared-divergent terms belonging to $\mathcal{M}_{n-1}^{1\text{-loop}}$, which cannot be derived from a collinear limit of a cusp of $\mathcal{M}_n^{1\text{-loop}}$.

The remaining set of Wilson loop diagrams, which are shown in Figure 6.3, give contributions to the $\mathcal{M}_{n-1}^{1\text{-loop}}$ amplitude. From the calculation in case a), since the propagator stretching between two massless legs (either adjacent or not) does not involve legs going collinear, we can factor out the $(1, 2)$ vertex, thus obtaining the usual IR and finite contributions (see (6.2.3) and (6.2.6) respectively) to the $\mathcal{M}_{n-1}^{1\text{-loop}}$. With the help of some algebraic manipulations, it can be shown that case b) gives rise to contributions in which the propagator stretches between the $1+2$ leg to the q legs, thus also contributing to the $\mathcal{M}_{n-1}^{1\text{-loop}}$.

Hence, summing all the various contributions, we have shown that the quantity

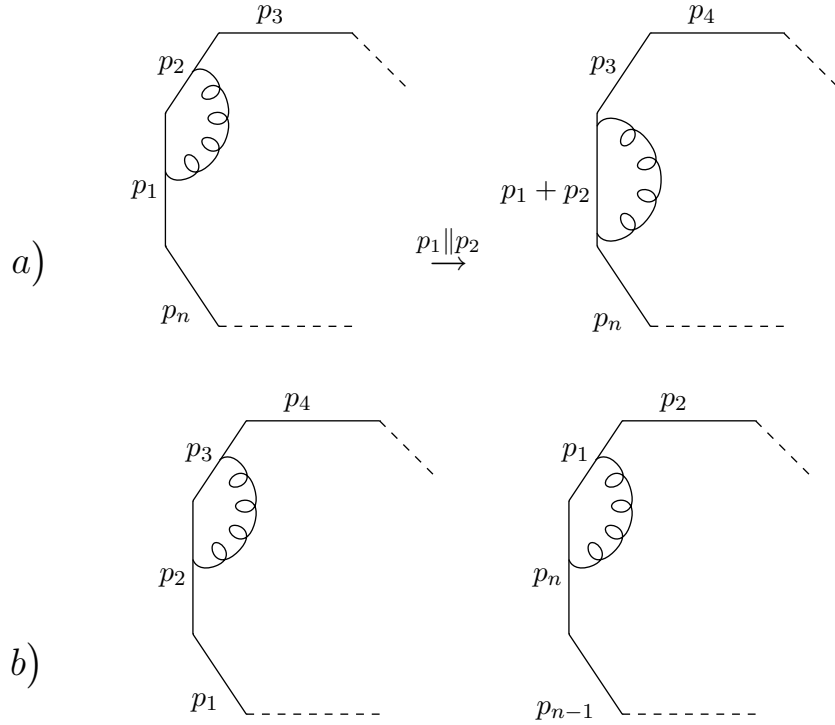


Figure 6.2: A one-loop correction to the Wilson loop, where the gluon stretches between two lightlike momenta meeting at a cusp both (case a) or only one (case b) going collinear. This kind of diagrams contributes to $r_1^{[1]}(z)$ by providing infrared-divergent terms of the form given in (6.2.3).

$\mathcal{M}_n^{1\text{-loop}}$ reduces in the collinear limit to

$$\mathcal{M}_n^{1\text{-loop}} \xrightarrow{a \parallel b} \mathcal{M}_{n-1}^{1\text{-loop}} + r_1^{[1]}(z). \quad (6.2.19)$$

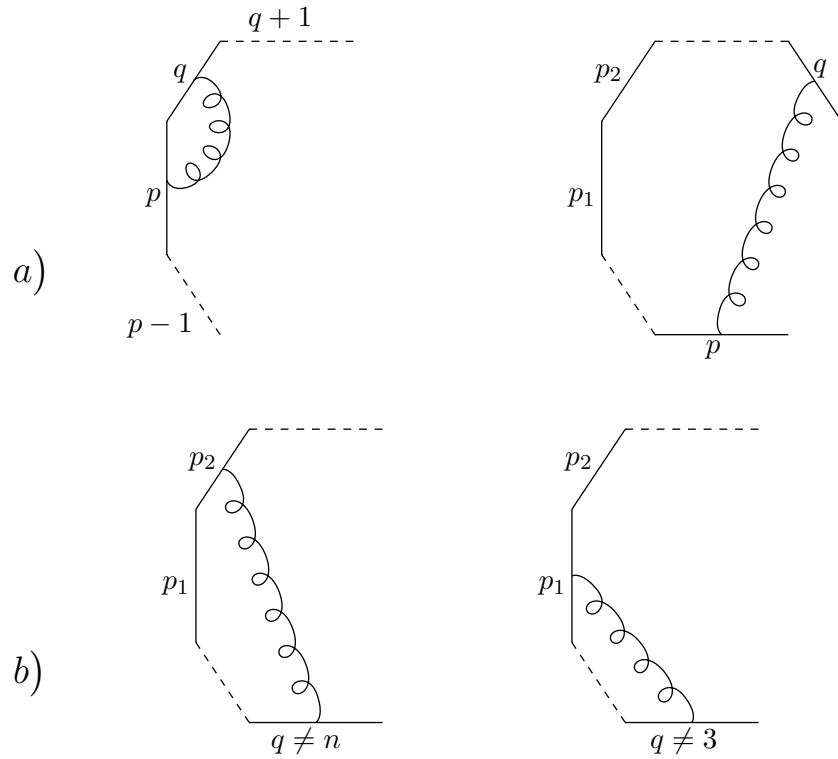


Figure 6.3: A one-loop correction to the Wilson loop, where the gluon stretches between either two adjacent lightlike momenta $p, q \neq 1, 2$ meeting at a cusp (case a) providing IR divergences to $\mathcal{M}_{n-1}^{1-loop}$ or two non-adjacent lightlike momenta with $q \neq 3, n$ (case b) contributing to the finite part of $\mathcal{M}_{n-1}^{1-loop}$.

Chapter 7

Conclusions and Outlook

In the past twenty years or so, the physics community has witnessed and enjoyed extraordinary progress in the understanding of scattering amplitudes. The simplicity of the Parke-Taylor formula (2.3.8) for MHV tree-amplitudes is indicative of the fact that gauge theories must be simpler than what one would otherwise be led to think in light of the number of Feynman diagrams needed to compute a scattering amplitude. In [10], the localisation properties of scattering amplitudes on lines in twistor space gave a justification of the simplicity of tree-level MHV amplitudes. Thriving on the seeds sown in [10], it was shown in [12] how tree-level amplitudes can be computed by gluing Parke-Taylor MHV amplitudes with scalar propagators. In [23] and proved in [24], on-shell recursion relations were found which resulted to be instrumental to the discovery of new analytic expressions for tree-amplitudes.

At NLO, developments have been just as impressive as at tree level. In [16, 18–20], despite initial skepticism, the CSW rules found in [12] were successfully employed to compute supersymmetric MHV amplitudes in SYM [16, 18, 19] together with the cut-constructible part of pure Yang-Mills amplitudes [20]. The latter result was then confirmed in [49] by means of generalised unitarity, which instructs us to cut the one-loop amplitude into a product of up to four on-shell amplitudes. An interesting outcome of [49] was the discovery that two-particle cuts, which in principle are needed to compute general amplitudes, did not appear in the calculation. The rational parts of the pure Yang-Mills amplitude was then computed in [22], closing the circle and providing the full one-loop QCD amplitude.

A short while after the computation of MHV scattering amplitudes was successfully carried out, a Lagrangian formulation of MHV diagrams was laid [13–15], whereby a non-local change of variables to the light-cone Yang-Mills Lagrangian generated a kinetic

term describing a scalar propagator connecting negative and positive helicities together with interaction terms of the infinite sequence of MHV amplitudes.

Quite recently, a deeper understanding of scattering amplitudes in maximally SYM was initiated by a remarkable and fascinating duality found between polygonal Wilson loops and MHV scattering amplitudes in $\mathcal{N} = 4$. In [41], a strong coupling calculation of scattering amplitudes in string theory was mapped to that of a polygon Wilson loop built out of light-like segments corresponding to the null momenta of the scattered particles. In [42, 43] and [44, 45, 47, 48], it was shown how the duality holds at weak coupling for one and two loops scattering amplitudes in $\mathcal{N} = 4$ SYM respectively.

It can be felt as a nuisance the fact that we have neglected gravity altogether in this thesis. This is not due to the scarcity of results in this field, rather the contrary. There has been a plethora of studies [112, 113, 119–121, 125, 172–175] which suggests that for the first time we may have a UV-finite consistent field theory of gravity.

Nevertheless, in spite of all the advancements which we hope we have conveyed in this thesis, there is still a whole host of problems waiting to be addressed. In the thesis we have been dealing almost entirely with MHV amplitudes, an already rich and diverse subject *per se*. What about NMHV amplitudes? Although a lot of progress has been done toward this front (see references in § 4.3) in spite of the challenges they offer, we still lack the knowledge of the general NMHV for QCD. Also, the study and eventual discovery of iterative structures was relegated to MHV amplitudes in planar $\mathcal{N} = 4$ SYM [38, 39] together with an approximate recursion behaviour for MHV amplitudes in the maximally supersymmetric $\mathcal{N} = 2$ SQED theory [51]. A computation of two-loop six-point NMHV amplitudes would be enough to begin testing the existence of an iteration relation for NMHV amplitudes.

Equally important, can the above Wilson loop duality and the dual superconformal symmetry [176, 177] discovered in $\mathcal{N} = 4$ SYM shed light on less supersymmetric theories? Are NMHV amplitudes also related to Wilson loop expectation values? Thinking positively and considering the pace and quality of research as it now stands, there is little room for doubt that major discoveries lie ahead of us. One thing we should always bear in mind though: if we do not try we will never know¹.

¹Prolegomenon, otherwise known as introduction. Greek, from neuter present passive participle of *prolegein*, to say beforehand: *pro-*, before; *legein-*, to speak.

Appendix A

Spinor and Dirac Traces Identities

In this Appendix we set the spinor notation and we recall some useful identities pertaining to the spinor helicity formalism which were useful in dealing with Dirac traces.

A.1 Spinor Identities

We work in the metric $g_{\mu\nu} = (1, -1, -1, -1)$. The epsilon tensors with which we raise and lower indices are

$$\epsilon^{\alpha\beta} = \epsilon^{\dot{\alpha}\dot{\beta}} = i\sigma^2 = \begin{pmatrix} 0 & 1 \\ -1 & 0 \end{pmatrix}, \quad (\text{A.1.1})$$

with $\epsilon_{\alpha\beta} = \epsilon^{\alpha\beta} \Rightarrow \epsilon_{\alpha\beta}\epsilon^{\beta\gamma} = -\delta_{\alpha}^{\gamma}$ and

$$\begin{aligned} \sigma^1 &= \begin{pmatrix} 0 & 1 \\ 1 & 0 \end{pmatrix}, \\ \sigma^2 &= \begin{pmatrix} 0 & -i \\ i & 0 \end{pmatrix}, \\ \sigma^3 &= \begin{pmatrix} 1 & 0 \\ 0 & -1 \end{pmatrix}, \end{aligned} \quad (\text{A.1.2})$$

the customarily Pauli matrices, grouped together as $\vec{\sigma}$.

We also have $\sigma_{\alpha\dot{\alpha}}^{\mu} = (1, \vec{\sigma})$, giving

$$\begin{aligned}
P_{\alpha\dot{\alpha}} &= P_{\mu}\sigma_{\alpha\dot{\alpha}}^{\mu} \\
&= \begin{pmatrix} P_0 + P_3 & P_1 - iP_2 \\ P_1 + iP_2 & P_0 - P_3 \end{pmatrix} \\
&= \begin{pmatrix} P^0 - P^3 & -P^1 + iP^2 \\ -P^1 - iP^2 & P^0 + P^3 \end{pmatrix}, \tag{A.1.3}
\end{aligned}$$

and $\bar{\sigma}^{\mu\dot{\alpha}\alpha} = -\sigma^{\mu\alpha\dot{\alpha}} = \epsilon^{\dot{\alpha}\beta}\epsilon^{\alpha\beta}\sigma_{\beta\dot{\beta}}^{\mu} = (1, -\vec{\sigma})$, giving

$$\begin{aligned}
P^{\dot{\alpha}\alpha} &= P_{\mu}\bar{\sigma}^{\mu\dot{\alpha}\alpha} \\
&= \begin{pmatrix} P_0 - P_3 & -P_1 + iP_2 \\ -P_1 - iP_2 & P_0 + P_3 \end{pmatrix} \\
&= \begin{pmatrix} P^0 + P^3 & P^1 - iP^2 \\ P^1 + iP^2 & P^0 - P^3 \end{pmatrix}. \tag{A.1.4}
\end{aligned}$$

For massless particles we can write

$$\begin{aligned}
p_{\alpha\dot{\alpha}} &= \lambda_{\alpha}\tilde{\lambda}_{\dot{\alpha}} \\
&= \begin{pmatrix} \lambda_1 \\ \lambda_2 \end{pmatrix} \begin{pmatrix} \tilde{\lambda}_1 & \tilde{\lambda}_2 \end{pmatrix} \\
&= \begin{pmatrix} \lambda_1\tilde{\lambda}_1 & \lambda_1\tilde{\lambda}_2 \\ \lambda_2\tilde{\lambda}_1 & \lambda_2\tilde{\lambda}_2 \end{pmatrix}, \tag{A.1.5}
\end{aligned}$$

and

$$\begin{aligned}
p^{\dot{\alpha}\alpha} &= -\tilde{\lambda}^{\dot{\alpha}}\lambda^{\alpha} \\
&= -\begin{pmatrix} \tilde{\lambda}^1 \\ \tilde{\lambda}^2 \end{pmatrix} \begin{pmatrix} \lambda^1 & \lambda^2 \end{pmatrix} \\
&= -\begin{pmatrix} \tilde{\lambda}^1\lambda^1 & \tilde{\lambda}^1\lambda^2 \\ \tilde{\lambda}^2\lambda^1 & \tilde{\lambda}^2\lambda^2 \end{pmatrix} \\
&= \begin{pmatrix} \tilde{\lambda}_2\lambda_2 & -\tilde{\lambda}_2\lambda_1 \\ -\tilde{\lambda}_1\lambda_2 & \tilde{\lambda}_1\lambda_1 \end{pmatrix}, \tag{A.1.6}
\end{aligned}$$

which follows from having $\lambda^{\alpha} = (\epsilon^{\alpha\beta}\lambda_{\beta})^T = -\lambda_{\beta}^T\epsilon^{\beta\alpha}$ and $\tilde{\lambda}^{\dot{\alpha}} = (\tilde{\lambda}_{\dot{\beta}}\epsilon^{\dot{\beta}\dot{\alpha}})^T = -\epsilon^{\dot{\alpha}\dot{\beta}}\tilde{\lambda}_{\dot{\beta}}^T$.

The spinor inner product is defined as

$$\begin{aligned}
\langle \lambda \mu \rangle &= \lambda^\alpha \mu_\alpha \\
&= \begin{pmatrix} \lambda^1 & \lambda^2 \end{pmatrix} \begin{pmatrix} \mu_1 \\ \mu_2 \end{pmatrix} \\
&= \epsilon^{\alpha\beta} \lambda_\beta^T \mu_\alpha,
\end{aligned} \tag{A.1.7}$$

and

$$\begin{aligned}
[\tilde{\lambda} \tilde{\mu}] &= \tilde{\lambda}_{\dot{\alpha}} \tilde{\mu}^{\dot{\alpha}} \\
&= \begin{pmatrix} \tilde{\lambda}_1 & \tilde{\lambda}_2 \end{pmatrix} \begin{pmatrix} \tilde{\mu}^{\dot{1}} \\ \tilde{\mu}^{\dot{2}} \end{pmatrix} \\
&= \tilde{\lambda}_{\dot{\alpha}} \tilde{\mu}_{\dot{\beta}}^T \epsilon^{\dot{\beta}\dot{\alpha}}.
\end{aligned} \tag{A.1.8}$$

The Schouten identity is very useful when carrying out algebraic manipulations involving spinors. We recall it below:

$$\begin{aligned}
\langle i j \rangle \langle k l \rangle &= \langle i k \rangle \langle j l \rangle + \langle i l \rangle \langle k j \rangle, \\
[i j] [k l] &= [i k] [j l] + [i l] [k j].
\end{aligned} \tag{A.1.9}$$

A.2 Dirac Traces

To follow, we reproduce some standard formulæ for converting between spinors and Dirac traces. They are

$$\langle i j \rangle [j i] = \text{tr}_+(k_i k_j), \tag{A.2.1}$$

$$\langle i j \rangle [j l] \langle l m \rangle [m i] = \text{tr}_+(k_i k_j k_l k_m), \tag{A.2.2}$$

$$\langle i j \rangle [j l] \langle l m \rangle [m n] \langle n p \rangle [p i] = \text{tr}_+(k_i k_j k_l k_m k_n k_p), \tag{A.2.3}$$

for momenta $k_i, k_j, k_l, k_m, k_n, k_p$ and where the $+$ sign indicates the insertion of $(1 + \gamma_5)/2$:

$$\text{tr}_+(k_i k_j) := \frac{1}{2} \text{tr}_+((1 + \gamma_5) k_i k_j). \tag{A.2.4}$$

We also have

$$\text{tr}_+(k_i k_j) = 2(k_i \cdot k_j), \quad (\text{A.2.5})$$

$$\begin{aligned} \text{tr}_+(k_a k_b k_c k_d) &= 2(k_a \cdot k_b)(k_c \cdot k_d) - 2(k_a \cdot k_c)(k_b \cdot k_d) \\ &+ 2(k_a \cdot k_d)(k_b \cdot k_c) - 2i\varepsilon(k_a, k_b, k_c, k_d). \end{aligned} \quad (\text{A.2.6})$$

Particularly useful were the following identities

$$\text{tr}_+(k_i k_j k_l k_m) = \text{tr}_+(k_m k_l k_j k_i) = \text{tr}_+(k_l k_m k_i k_j), \quad (\text{A.2.7})$$

$$\text{tr}_+(k_i k_j k_l k_m) = 4(k_i \cdot k_j)(k_l \cdot k_m) - \text{tr}_+(k_j k_i k_l k_m), \quad (\text{A.2.8})$$

$$(\text{A.2.9})$$

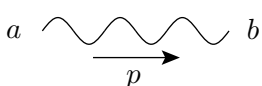
For more on spinor and Dirac traces, the reader is referred to the evergreen [72].

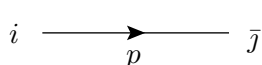
Appendix B

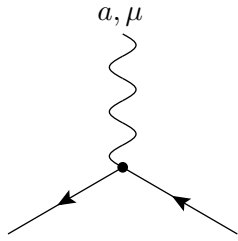
Feynman Rules for a $SU(N_c)$ Gauge Theory

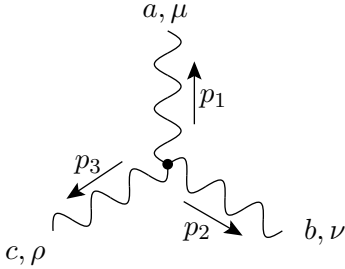
In this Appendix we collect the Feynman rules for a non-abelian $SU(N_c)$ gauge theory. In the below rules it is understood that momentum is conserved at each vertex. We adhere to the convention as adopted in [178]. First, we show the Feynman rules in the form they appear in standard textbook with the *Feynman-'t Hooft* gauge $\xi = 1$ implemented. Then, for comparison, we present the Feynman rules for massless $SU(N_c)$ Yang-Mills theory in the same gauge written in the spinor helicity formalism.

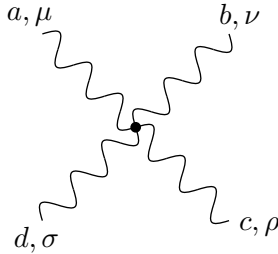
B.1 Feynman Rules

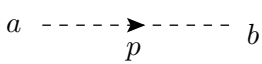
Gauge Boson Propagator: a  b $= \frac{-ig_{\mu\nu}}{p^2 + i\varepsilon} \delta_{ab}$

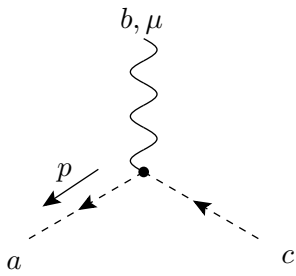
Fermion Propagator: i  \bar{j} $= \frac{i(\not{p} + m)}{p^2 - m^2 + i\varepsilon} \delta_i^{\bar{j}}$

Fermion Vertex:  $= ig\gamma^\mu T^a$

3-Boson Vertex:  $= -gf^{abc}[g^{\mu\nu}(p_1-p_2)^\rho + g^{\nu\rho}(p_2-p_3)^\mu + g^{\rho\mu}(p_3-p_1)^\nu]$

4-Boson Vertex:  $= 2ig^2[f^{abe}f^{ecd}g^{\mu[\rho}g^{\sigma]\nu} + f^{dae}f^{ebc}g^{\mu[\nu}g^{\sigma]\rho} + f^{cae}f^{ebd}g^{\mu[\nu}g^{\rho]\sigma}]$

Ghost Propagator:  $= -\frac{i\delta_{ab}}{p^2}$

Ghost Vertex:  $= gf^{abc}p^\mu$

B.2 Feynman Rules in the Spinor Helicity Formalism

B.2.1 Wavefunctions

In this section we consider all the external states as outgoing. We omit a factor of $\exp(ix_{\beta\dot{\beta}}\lambda^\beta\tilde{\lambda}^{\dot{\beta}})$ which multiplies all the below wavefunctions.

- **Scalar:**

$$\phi = 1 \tag{B.2.1}$$

- **Fermion i , positive helicity:**

$$\psi_i^+ = \tilde{\lambda}_{i\dot{\alpha}} = |i] \tag{B.2.2}$$

- **Fermion i , negative helicity:**

$$\psi_i^- = \lambda_i^\alpha = \langle i| \tag{B.2.3}$$

- **Anti-fermion j , positive helicity:**

$$\bar{\psi}_j^+ = \tilde{\lambda}_j^{\dot{\alpha}} = |j] \tag{B.2.4}$$

- **Anti-fermion j , negative helicity:**

$$\bar{\psi}_j^- = \lambda_{j\alpha} = \langle j| \tag{B.2.5}$$

- **Vector $p = \lambda\tilde{\lambda}$, positive helicity:**

$$\epsilon_{\alpha\dot{\alpha}}^+ = \sqrt{2} \frac{\kappa_\alpha \tilde{\lambda}_{\dot{\alpha}}}{\langle \kappa \lambda \rangle} = \sqrt{2} \frac{|\kappa\rangle [\tilde{\lambda}]}{\langle \kappa \lambda \rangle} \tag{B.2.6}$$

- **Vector $p = \lambda\tilde{\lambda}$, negative helicity:**

$$\epsilon_{\alpha\dot{\alpha}}^- = \sqrt{2} \frac{\lambda_\alpha \tilde{\kappa}_{\dot{\alpha}}}{[\tilde{\kappa} \tilde{\lambda}]} = \sqrt{2} \frac{|\lambda\rangle [\tilde{\kappa}]}{[\tilde{\kappa} \tilde{\lambda}]}, \tag{B.2.7}$$

where κ and $\tilde{\kappa}$ are arbitrary spinors.

B.2.2 Propagators

- Scalars with kinetic term $(\partial\phi)^2/2$:

$$\frac{i}{p^2} \quad (\text{B.2.8})$$

- Fermions with $p = \lambda\tilde{\lambda}$ and kinetic term $\bar{\psi}i\bar{\sigma}^\mu\partial_\mu\psi$:

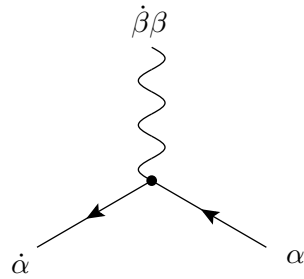
$$\frac{i}{\bar{\sigma}^\mu p_\mu} = \frac{ip_{\alpha\dot{\alpha}}}{2p^2} = \frac{i|\lambda\rangle[\tilde{\lambda}]}{2p^2} \quad (\text{B.2.9})$$

- Vectors with kinetic term $-(\partial A)^2/4$:

$$\frac{-2i\epsilon_{\dot{\alpha}\dot{\beta}}\epsilon_{\alpha\beta}}{p^2} \quad (\text{B.2.10})$$

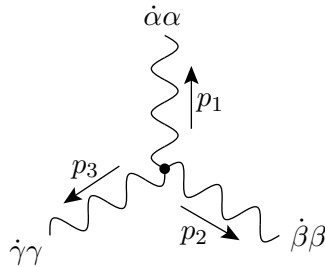
B.3 Vertices

Fermion Vertex:



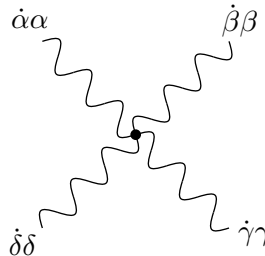
$$= ig\sqrt{2}\delta_{\alpha\dot{\alpha}}\delta_{\dot{\beta}\beta}$$

3-Boson Vertex:



$$= \frac{-g}{2\sqrt{2}}[\epsilon^{\dot{\alpha}\dot{\beta}}\epsilon^{\alpha\beta}(p_1-p_2)^{\dot{\gamma}\gamma} + \epsilon^{\dot{\beta}\dot{\gamma}}\epsilon^{\beta\gamma}(p_2-p_3)^{\dot{\alpha}\alpha} + \epsilon^{\dot{\gamma}\dot{\alpha}}\epsilon^{\gamma\alpha}(p_3-p_1)^{\dot{\beta}\beta}]$$

4-Boson Vertex:



$$= \frac{ig^2}{8}[2\epsilon^{\dot{\alpha}\dot{\gamma}}\epsilon^{\alpha\gamma}\epsilon^{\dot{\beta}\dot{\delta}}\epsilon^{\beta\delta} - \epsilon^{\dot{\alpha}\dot{\delta}}\epsilon^{\alpha\delta}\epsilon^{\dot{\beta}\dot{\gamma}}\epsilon^{\beta\gamma} - \epsilon^{\dot{\alpha}\dot{\beta}}\epsilon^{\alpha\beta}\epsilon^{\dot{\gamma}\dot{\delta}}\epsilon^{\gamma\delta}]$$

Appendix C

Tensor Integrals

In this Appendix we define the one-loop integrals¹ which were used in performing the PV reductions encountered in § 4. Furthermore, we present formulæ for the PV reductions of all tensor bubble, triangle and box integrals appearing in the same chapter. The more complicated three-tensor triangle integral is dealt with separately in Appendix D.

C.1 Bubble Integrals

The bubble integral, is defined by

$$I_2[P(\ell^\mu)] = -i(4\pi)^{2-\epsilon} \int \frac{d^{4-2\epsilon}\ell}{(2\pi)^{4-2\epsilon}} \frac{P(\ell^\mu)}{\ell^2(\ell-K)^2}, \quad (\text{C.1.1})$$

where K is the total outgoing momentum at one side of the bubble and, in the rest of this Appendix, $P(\ell^\mu)$ is some polynomial in the loop momentum ℓ^μ . Evaluation of the scalar bubble integral yields

$$I_2[1] = r_\Gamma \frac{(-Q^2)^{-\epsilon}}{\epsilon(1-2\epsilon)} = r_\Gamma \left[\left(\frac{1}{\epsilon} + 2 - \ln(-Q^2) \right) + \mathcal{O}(\epsilon) \right], \quad (\text{C.1.2})$$

where

$$r_\Gamma = \frac{\Gamma(1+\epsilon)\Gamma^2(1-\epsilon)}{\Gamma(1-2\epsilon)}. \quad (\text{C.1.3})$$

Thus, we see that the difference of two scalar bubbles gives rise to (4.1.9) to $\mathcal{O}(\epsilon^0)$.

¹We followed the convention as given in [21] throughout this thesis. Notice that, although here the integrals are not given in a dimensionally regularised manner, there is no difference up to $\mathcal{O}(\epsilon^0)$ with the ones found in [21].

The PV reduction of the linear and two-tensor bubble integrals are given by

$$I_2[\ell_2^\mu] = -\frac{1}{2}I_2(P^2)P^\mu, \quad (\text{C.1.4})$$

$$I_2[\ell_2^\mu \ell_2^\nu] = \frac{1}{3}I_2(P^2)P^\mu P^\nu - \frac{1}{12}I_2(P^2)P^2 \eta^{\mu\nu}. \quad (\text{C.1.5})$$

C.2 Triangle Integrals

A general tensor triangle integral is defined by

$$I_3[P(\ell^\mu)] = i(4\pi)^{2-\epsilon} \int \frac{d^{4-2\epsilon}\ell}{(2\pi)^{4-2\epsilon}} \frac{P(\ell^\mu)}{\ell^2(\ell - K_1)^2(\ell + K_3)^2}, \quad (\text{C.2.1})$$

where the K_i are sums of the momenta k_i of the external gluons at each vertex. We found that the linear and two-tensor triangle integrals are given by

$$I_3[\ell_2^\mu] = -T^{(1)}P^\mu, \quad (\text{C.2.2})$$

$$I_3[\ell_2^\mu \ell_2^\nu] = \frac{1}{2}T^{(1)}P^\mu P^\nu - \frac{1}{2}P^2 T^{(2)}(P^\mu m^\nu + P^\nu m^\mu), \quad (\text{C.2.3})$$

$$(\text{C.2.4})$$

where only the contributing terms have been written.

C.3 Box Integrals

The box integral is defined by

$$I_4[P(\ell^\mu)] = -i(4\pi)^{2-\epsilon} \int \frac{d^{4-2\epsilon}\ell}{(2\pi)^{4-2\epsilon}} \frac{P(\ell^\mu)}{\ell^2(\ell - K_1)^2(\ell - K_1 - K_2)^2(\ell + K_4)^2}. \quad (\text{C.3.1})$$

For the linear box integral we found

$$I_4[\ell_1^\mu] = \frac{(m_1 \cdot m_2) P^2 I_4 - (m_1 \cdot P) [I_3 + 2 I_4] (m_2 \cdot P)}{2 [(m_1 \cdot m_2) P^2 - 2 (m_2 \cdot P)(m_1 \cdot P)]} P^\mu \quad (\text{C.3.2})$$

$$+ \frac{(m_1 \cdot m_2) P^2 [I_3 - (m_2 \cdot P) I_4] + (m_1 \cdot P)(m_2 \cdot P) [2 I_4(m_2 \cdot P) - I_3]}{2 [(m_1 \cdot m_2) P^2 - 2 (m_2 \cdot P)(m_1 \cdot P)]} m_1^\mu,$$

where we are omitting the m_2 term since it drops out when inserted in (4.2.17). The interested reader is referred to the very helpful Appendices I and II of [21] for a more complete discussion of bubble, triangle and box integrals.

Appendix D

Passarino-Veltman Reduction

In this Appendix we carry out the PV reduction in $D = 4$ dimensions of the three-index tensor triangle integral found in § 4.

The three-index tensor integral in $D = 4$ dimensions

$$\mathcal{I}^{\mu\nu\rho}(m_1, P, Q) = \int d^4\ell_2 \frac{\ell_2^\mu \ell_2^\nu \ell_2^\rho}{\ell_1^2 \ell_2^2 \ell_3^2}, \quad (\text{D.0.1})$$

may be decomposed as

$$\begin{aligned} \mathcal{I}^{\mu\nu\rho} = & a(P^\mu P^\nu P^\rho) + b(P^\mu m^\nu m^\rho + P^\nu m^\mu m^\rho + P^\rho m^\nu m^\mu) + \\ & c(P^\mu P^\nu m^\rho + P^\mu P^\rho m^\nu + P^\nu P^\rho m^\mu) + d(P^\mu \eta^{\rho\nu} + P^\nu \eta^{\mu\rho} + P^\rho \eta^{\mu\nu}) + \\ & e(m^\mu \eta^{\nu\rho} + m^\nu \eta^{\mu\rho} + m^\rho \eta^{\nu\mu}) + f(m^\mu m^\nu m^\rho). \end{aligned} \quad (\text{D.0.2})$$

Taking contractions with all possible momenta then yields

• $P_\mu P_\nu P_\rho$

$$\begin{aligned} \mathcal{I}_1 = \int \frac{(\ell_2 \cdot P)^3}{\ell_1^2 \ell_2^2 \ell_3^2} = & aP^6 + 3b[P^2(m \cdot P)^2] + 3c[(m \cdot P)P^4] + \\ & + 3dP^4 + 3e[(m \cdot P)P^2] + f(m \cdot P)^3, \end{aligned} \quad (\text{D.0.3})$$

• $P_\mu m_\nu m_\rho$

$$\mathcal{I}_2 = \int \frac{(\ell_2 \cdot P)(m \cdot \ell_2)^2}{\ell_1^2 \ell_2^2 \ell_3^2} = a[P^2(m \cdot P)^2] + c(m \cdot P)^3 + 2d(m \cdot P)^2, \quad (\text{D.0.4})$$

• $P_\mu P_\nu m_\rho$

$$\mathcal{I}_3 = \int \frac{(m \cdot \ell_2)(\ell_2 \cdot P)^2}{\ell_1^2 \ell_2^2 \ell_3^2} = a[(m \cdot P)P^4] + b(m \cdot P)^3 + 2c[P^2(m \cdot P)^2] + 3d[P^2(m \cdot P)] + 2e(m \cdot P)^2, \quad (\text{D.0.5})$$

• $P_\mu \eta_{\nu\rho}$

$$\mathcal{I}_4 = \int \frac{(P \cdot \ell_2)}{\ell_1^2 \ell_3^2} = aP^4 + 2b[(m \cdot P)^2] + 3c[P^2(m \cdot P)] + 6dP^2 + 6e(m \cdot P), \quad (\text{D.0.6})$$

• $m_\mu \eta_{\nu\rho}$

$$\mathcal{I}_5 = \int \frac{(\ell_2 \cdot m)}{\ell_1^2 \ell_3^2} = a[(m \cdot P)P^2] + 2c(m \cdot P)^2 + 6d(m \cdot P), \quad (\text{D.0.7})$$

• $m_\mu m_\nu m_\rho$

$$\mathcal{I}_6 = \int \frac{(\ell_2 \cdot m)^3}{\ell_1^2 \ell_2^2 \ell_3^2} = a(m \cdot P)^3. \quad (\text{D.0.8})$$

The integrals take the following values:

$$\begin{aligned} \mathcal{I}_1 = & -\frac{1}{2}(m \cdot P)^2 I_2(Q^2) - \frac{1}{8}P^2 I_3 \\ & -\frac{1}{6}(P \cdot Q)^2 I_2(Q^2) + \frac{1}{24}Q^2 P^2 I_2(Q^2) \\ & -\frac{1}{2}(m \cdot P)(P \cdot Q) I_2(Q^2) + \frac{1}{4}(m \cdot P) I_2(Q^2) \\ & +\frac{1}{8}P^2(P \cdot Q) I_2(Q^2) - \frac{1}{8}P^4 I_2(Q^2), \end{aligned} \quad (\text{D.0.9})$$

$$\mathcal{I}_2 = -\frac{1}{6}(m \cdot Q)^2 I_2(Q^2) - \frac{1}{8}P^2(m \cdot Q) I_2(Q^2) - \frac{1}{8}P^2(m \cdot P) I_2(P^2),$$

$$\begin{aligned} \mathcal{I}_3 = & \frac{1}{2}(m \cdot P)^2 I_2(Q^2) + \frac{1}{6}(P \cdot Q)^2 I_2(Q^2) + \frac{1}{2}(m \cdot P)(P \cdot Q) I_2(Q^2) \\ & - \frac{1}{24}Q^2 P^2 I_2(Q^2) - \frac{1}{6}P^4 I_2(P^2) + \frac{1}{24}P^4 I_2(P^2), \end{aligned}$$

$$\mathcal{I}_4 = (m \cdot P) I_2(Q^2) + \frac{1}{2}(P \cdot Q) I_2(Q^2),$$

$$\mathcal{I}_5 = \frac{1}{2}(m \cdot Q) I_2(Q^2),$$

$$\mathcal{I}_6 = \frac{1}{6}(m \cdot Q)^2 I_2(Q^2) - \frac{1}{6}(m \cdot P)^2 I_2(P^2),$$

Finally, using Mathematica to carry out the algebraic manipulations, we retrieve the

coefficients of the expansion (D.0.2)

$$\begin{aligned}
a &= \frac{I_2(Q^2) - I_2(P^2)}{3Q^2 - 3P^2}, \\
b &= \frac{P^4(I_2(P^2) - I_2(Q^2))}{3(P^2 - Q^2)^3}, \\
c &= \frac{P^2(I_2(Q^2) - I_2(P^2))}{6(P^2 - Q^2)^2}, \\
d &= \frac{Q^2 I_2(Q^2) - P^2 I_2(P^2)}{12(P^2 - Q^2)}, \\
e &= \frac{(Q^4 - 2P^2 Q^2) I_2(Q^2) + P^4 I_2(P^2)}{12(P^2 - Q^2)^2},
\end{aligned} \tag{D.0.10}$$

where we chose not to write the f coefficient as one can easily check that the $m_\mu m_\nu m_\rho$ term vanishes once inserted into the appropriate Dirac trace formulæ appearing in our calculations. Incidentally, the f coefficient is the only place where the I_3 scalar triangle function appears.

Thus, (D.0.1) takes the following form:

$$\begin{aligned}
\int d^4 \ell_2 \frac{\ell_2^\mu \ell_2^\nu \ell_2^\rho}{\ell_1^2 \ell_2^2 \ell_3^2} &= \frac{I_2(Q^2) - I_2(P^2)}{3Q^2 - 3P^2} (P^\mu P^\nu P^\rho) + \frac{P^4(I_2(P^2) - I_2(Q^2))}{3(P^2 - Q^2)^3} (P^\mu m^\nu m^\rho) \\
&+ \frac{P^2(I_2(Q^2) - I_2(P^2))}{6(P^2 - Q^2)^2} (P^\mu P^\nu m^\rho) + \frac{Q^2 I_2(Q^2) - P^2 I_2(P^2)}{12(P^2 - Q^2)} (P^\mu \eta^{\nu\rho}) \\
&+ \frac{(Q^4 - 2P^2 Q^2) I_2(Q^2) + P^4 I_2(P^2)}{12(P^2 - Q^2)^2} (m^\mu \eta^{\nu\rho}).
\end{aligned} \tag{D.0.11}$$

Appendix E

Twistor Space

In this section we report some of the salient features of twistor space. Without pretending to be exhaustive on the topic, we refer the interested reader to the original work [10, 11] and offsprings thereafter.

In order to introduce twistor space, let us consider conformal invariance of $\mathcal{N} = 4$ MHV tree-level amplitudes which we recall are of the form

$$\begin{aligned}\mathcal{A}_{\text{MHV}} &= g(\lambda)\delta^{(4)}\left(\sum_{k=1}^n \lambda_k \tilde{\lambda}_k\right) \\ &= ig^{n-2}(2\pi)^4 \frac{\langle ij \rangle^4}{\prod_{k=1}^n \langle k k+1 \rangle} \delta^{(4)}\left(\sum_{k=1}^n \lambda_k \tilde{\lambda}_k\right),\end{aligned}\tag{E.0.1}$$

and obey the condition

$$\left(\lambda_i^\alpha \frac{\partial}{\partial \lambda_i^\alpha} - \tilde{\lambda}_i^{\dot{\alpha}} \frac{\partial}{\partial \tilde{\lambda}_i^{\dot{\alpha}}}\right) \mathcal{A}_n(\lambda_i, \tilde{\lambda}_i, h_i) = -2h_i \mathcal{A}_n(\lambda_i, \tilde{\lambda}_i, h_i).\tag{E.0.2}$$

Since $\mathcal{N} = 4$ is (super) conformal at tree level, the corresponding tree-level S-matrix must be annihilated by the conformal group. In terms of spinor variables, the conformal

generators are

$$P_{\alpha\dot{\alpha}} = \lambda_{\alpha}\tilde{\lambda}_{\dot{\alpha}}, \quad (\text{E.0.3})$$

$$J_{\alpha\beta} = \frac{i}{2}\left(\lambda_{\alpha}\frac{\partial}{\partial\lambda^{\beta}} + \lambda_{\beta}\frac{\partial}{\partial\lambda^{\alpha}}\right), \quad (\text{E.0.4})$$

$$\tilde{J}_{\dot{\alpha}\dot{\beta}} = \frac{i}{2}\left(\tilde{\lambda}_{\dot{\alpha}}\frac{\partial}{\partial\tilde{\lambda}^{\dot{\beta}}} + \tilde{\lambda}_{\dot{\beta}}\frac{\partial}{\partial\tilde{\lambda}^{\dot{\alpha}}}\right), \quad (\text{E.0.5})$$

$$D = \frac{i}{2}\left(\lambda^{\alpha}\frac{\partial}{\partial\lambda^{\alpha}} + \tilde{\lambda}^{\dot{\alpha}}\frac{\partial}{\partial\tilde{\lambda}^{\dot{\alpha}}} + 2\right), \quad (\text{E.0.6})$$

$$K_{\alpha\dot{\alpha}} = \frac{\partial^2}{\partial\lambda^{\alpha}\partial\tilde{\lambda}^{\dot{\alpha}}}, \quad (\text{E.0.7})$$

where $P_{\alpha\dot{\alpha}}$ is the momentum operator, $J_{\alpha\beta}$ and $\tilde{J}_{\dot{\alpha}\dot{\beta}}$ are the Lorentz operators, D the dilation operator and $K_{\alpha\dot{\alpha}}$ the generator of special conformal transformations. By acting these operators upon a MHV amplitude, we can verify whether the amplitude vanishes or not. It was shown in [10] how a $\mathcal{N} = 4$ MHV tree-level amplitude indeed gets annihilated by the conformal group. Rather than showing the details here, we notice how some generators are represented by differential operators of degree one while others of degree two with the momentum operator just a multiplication operator. If we introduce the transformation [11]¹

$$\tilde{\lambda}_{\dot{\alpha}} \rightarrow i\frac{\partial}{\partial\mu^{\dot{\alpha}}}, \quad (\text{E.0.8})$$

$$\frac{\partial}{\partial\tilde{\lambda}^{\dot{\alpha}}} \rightarrow i\mu_{\dot{\alpha}}, \quad (\text{E.0.9})$$

we are able to recast the conformal generators as

$$P_{\alpha\dot{\alpha}} = i\lambda_{\alpha}\frac{\partial}{\partial\mu^{\dot{\alpha}}}, \quad (\text{E.0.10})$$

$$K_{\alpha\dot{\alpha}} = i\mu_{\dot{\alpha}}\frac{\partial}{\partial\lambda^{\alpha}}, \quad (\text{E.0.11})$$

$$J_{\alpha\beta} = \frac{i}{2}\left(\lambda_{\alpha}\frac{\partial}{\partial\lambda^{\beta}} + \lambda_{\beta}\frac{\partial}{\partial\lambda^{\alpha}}\right), \quad (\text{E.0.12})$$

$$\tilde{J}_{\dot{\alpha}\dot{\beta}} = \frac{i}{2}\left(\mu_{\dot{\alpha}}\frac{\partial}{\partial\mu^{\dot{\beta}}} + \mu_{\dot{\beta}}\frac{\partial}{\partial\mu^{\dot{\alpha}}}\right), \quad (\text{E.0.13})$$

$$D = \frac{i}{2}\left(\lambda^{\alpha}\frac{\partial}{\partial\lambda^{\alpha}} - \mu^{\dot{\alpha}}\frac{\partial}{\partial\mu^{\dot{\alpha}}}\right). \quad (\text{E.0.14})$$

Although we have decided to break the symmetry between λ and $\tilde{\lambda}$ by choosing to transform $\tilde{\lambda}$ rather than λ , we have managed to express the conformal operators in terms of operators of degree one. Furthermore, the scaling properties of λ and μ have

¹There exists a similar transformation for the holomorphic spinor component λ . However, the mathematics is more involved as can be inferred by looking at (E.0.1).

changed from (2.2.9) to

$$(\lambda, \mu) \rightarrow (c\lambda, c\mu), \quad (\text{E.0.15})$$

while (E.0.2) becomes

$$\left(\lambda_i^\alpha \frac{\partial}{\partial \lambda_i^\alpha} + \mu_i^{\dot{\alpha}} \frac{\partial}{\partial \mu_i^{\dot{\alpha}}} \right) \mathcal{A}_n(\lambda_i, \mu_i, h_i) = -(2h_i + 2) \mathcal{A}_n(\lambda_i, \mu_i, h_i), \quad (\text{E.0.16})$$

for a complex number c . In signature $++--$, one can consider λ and μ to be real and independent thus parameterising a copy of \mathbb{R}^4 which under the scaling (E.0.15) reduces to \mathbb{RP}^3 . The familiar Fourier transform

$$\tilde{f}(\mu) = \int \frac{d^2 \tilde{\lambda}}{(2\pi)^2} \exp(i\mu^{\dot{\alpha}} \tilde{\lambda}_{\dot{\alpha}}) f(\tilde{\lambda}), \quad (\text{E.0.17})$$

allows one to switch from an amplitude $\mathcal{A}(\lambda_i, \tilde{\lambda}_i)$ to an amplitude $\tilde{\mathcal{A}}(\lambda_i, \mu_i)$ when λ and μ are real. In Minkowski signature however, it is more natural to regard λ and μ as complex and independent, thus parameterising a copy of \mathbb{C}^4 which reduces to \mathbb{CP}^3 under the scaling (E.0.15). The way to proceed would be to consider (E.0.17) as a contour integral; alternatively, one can make use of the sophisticated machinery of $\bar{\partial}$ cohomology or sheaf cohomology as adopted in [11]. The four-dimensional spaces \mathbb{R}^4 and \mathbb{C}^4 were called *twistor spaces* by Penrose [11] with coordinates λ and μ whilst \mathbb{RP}^3 and \mathbb{CP}^3 are nowadays called *projective twistor spaces*.

An interesting geometrical aspect arises by transforming the scattering amplitude as a function in momentum space to a function in twistor space. Let us observe the fact that MHV amplitudes are holomorphic and, to this end, let us rewrite (E.0.1) using a standard position-momentum representation for the delta function of the momentum conservation as

$$\mathcal{A}_{\text{MHV}} = ig^{n-2} \int d^4 x \exp\left(i x_{\alpha\dot{\alpha}} \sum_{k=1}^n \lambda_k^\alpha \tilde{\lambda}_k^{\dot{\alpha}} \right) f(\lambda_k). \quad (\text{E.0.18})$$

By means of (E.0.8), with some little algebra we can recast (E.0.18) in twistor space

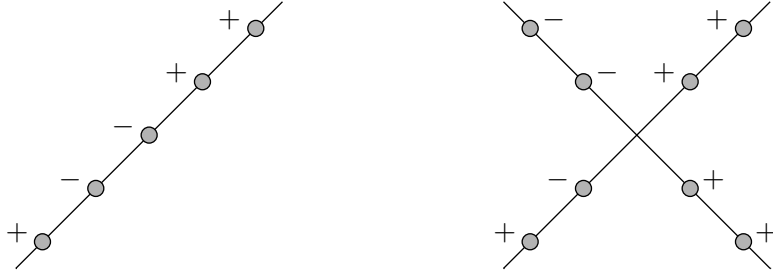


Figure E.1: *Pictorial representation in twistor space of a MHV amplitude (left) and NMHV amplitude (right).*

as

$$\begin{aligned}
 \tilde{\mathcal{A}}_{\text{MHV}}(\lambda, \mu) &= ig^{n-2} \mathcal{A}_{\text{MHV}} \int d^4x \prod_{k=1}^n \int \frac{d^2 \tilde{\lambda}_k}{(2\pi)^2} \exp\left(i \sum_{k=1}^n \mu_{k\dot{\alpha}} \tilde{\lambda}_k^{\dot{\alpha}}\right) \\
 &\times \exp\left(ix_{\alpha\dot{\alpha}} \sum_{k=1}^n \lambda_k^\alpha \tilde{\lambda}_k^{\dot{\alpha}}\right)(\lambda) \\
 &= ig^{n-2} \mathcal{A}_{\text{MHV}}(\lambda) \int d^4x \prod_{i=1}^n \delta^{(2)}(\mu_{i\dot{\alpha}} + x_{\alpha\dot{\alpha}} \lambda_j^\alpha). \quad (\text{E.0.19})
 \end{aligned}$$

Thus, from the last line of (E.0.19), we evince the remarkable fact that MHV tree-level amplitudes in twistor space are localised on curves of degree one which are straight lines in the real case and spheres in the complex case. The localisation properties of many amplitudes have been thoroughly studied [10, 20, 78, 100, 112, 179–183] and it has been found that amplitudes with q negative-helicity gluons localise on curves of degree $q - 1$. Notice that the cases $q = 0, 1$ do not exist thus providing a geometrical interpretation of the vanishing of tree-level amplitudes given in (2.3.10). It has been conjectured in [10] that a generic n -particle scattering amplitude with q negative-helicity gluons localise in twistor space on a curve of degree

$$d = q - 1 + L, \quad (\text{E.0.20})$$

where L is the number of loops.

Bibliography

- [1] T. Stelzer and W. F. Long, *Automatic generation of tree level helicity amplitudes*, Comput. Phys. Commun. **81**, 357 (1994), [hep-ph/9401258](#).
- [2] A. Pukhov *et al.*, *CompHEP: A package for evaluation of Feynman diagrams and integration over multi-particle phase space. User's manual for Version 33*, [hep-ph/9908288](#).
- [3] S. Catani, D. de Florian and M. Grazzini, *Higgs production in hadron collisions: soft and virtual QCD corrections at NNLO*, JHEP **0105**, 025 (2001), [hep-ph/0102227](#).
- [4] R. V. Harlander and W. B. Kilgore, *Next-to-next-to-leading order Higgs production at hadron colliders*, Phys. Rev. Lett. **88**, 201801 (2002), [hep-ph/0201206](#).
- [5] C. Anastasiou and K. Melnikov, *Higgs boson production at hadron colliders in NNLO QCD*, Nucl. Phys. B **646**, 220 (2002), [hep-ph/0207004](#).
- [6] V. Ravindran, J. Smith and W. L. van Neerven, *NNLO corrections to the total cross section for Higgs boson production in Hadron Hadron collisions*, Nucl. Phys. B **665**, 325 (2003), [hep-ph/0302135](#).
- [7] C. Buttar *et al.*, *Les houches physics at TeV colliders 2005, standard model and Higgs working group: Summary report*, [hep-ph/060412](#).
- [8] J. M. Maldacena, *The large N limit of superconformal field theories and supergravity*, Adv. Theor. Math. Phys. **2**, 231 (1998), [Int. J. Theor. Phys. **38**, 1113 (1999)], [hep-th/9711200](#).
- [9] G. 't Hooft, *A planar diagram theory for strong interactions*, Nucl. Phys. B **72**, 461 (1974).
- [10] E. Witten, *Perturbative gauge theory as a string theory in twistor space*, Commun. Math. Phys. **252**, 189 (2004), [hep-th/0312171](#).
- [11] R. Penrose, *Twistor algebra*, J. Math. Phys. **8**, 345 (1967).

- [12] F. Cachazo, P. Svrcek and E. Witten, *MHV vertices and tree amplitudes in gauge theory*, JHEP **0409**, 006 (2004), [hep-th/0403047](#).
- [13] A. Gorsky and A. Rosly, *From Yang-Mills Lagrangian to MHV diagrams*, JHEP **0601**, 101 (2006), [hep-th/0510111](#).
- [14] P. Mansfield, *The Lagrangian origin of MHV rules*, JHEP **0603**, 037 (2006), [hep-th/0511264](#).
- [15] J. H. Eittle and T. R. Morris, *Structure of the MHV-rules Lagrangian*, JHEP **0608**, 003 (2006), [hep-th/0605121](#).
- [16] A. Brandhuber, B. Spence and G. Travaglini, *One-loop gauge theory amplitudes in $\mathcal{N} = 4$ super Yang-Mills from MHV vertices*, Nucl. Phys. B **706**, 150 (2005), [hep-th/0407214](#).
- [17] Z. Bern, L. J. Dixon, D. C. Dunbar and D. A. Kosower, *One-loop n -point gauge theory amplitudes, unitarity and collinear limits*, Nucl. Phys. B **425**, 217 (1994), [hep-ph/9403226](#).
- [18] J. Bedford, A. Brandhuber, B. Spence and G. Travaglini, *A twistor approach to one-loop amplitudes in $\mathcal{N} = 1$ supersymmetric Yang-Mills theory*, Nucl. Phys. B **706**, 100 (2005), [hep-th/0410280](#).
- [19] C. Quigley and M. Rozali, *One-Loop MHV amplitudes in supersymmetric gauge theories*, JHEP **0501**, 053 (2005), [hep-th/0410278](#).
- [20] J. Bedford, A. Brandhuber, B. Spence and G. Travaglini, *Non-supersymmetric loop amplitudes and MHV vertices*, Nucl. Phys. B **712**, 59 (2005), [hep-th/0412108](#).
- [21] Z. Bern, L. J. Dixon, D. C. Dunbar and D. A. Kosower, *Fusing gauge theory tree amplitudes into loop amplitudes*, Nucl. Phys. B **435**, 59 (1995), [hep-ph/9409265](#).
- [22] Carola F. Berger, Z. Bern, L. J. Dixon, D. Forde and D. A. Kosower, *All one-loop maximally helicity violating gluonic amplitudes in QCD*, Phys. Rev. D **75**, 016006 (2007), [hep-ph/0607014](#).
- [23] R. Britto, F. Cachazo and B. Feng, *New recursion relations for tree amplitudes of gluons*, Nucl. Phys. B **715**, 499 (2005), [hep-th/0412308](#).
- [24] R. Britto, F. Cachazo, B. Feng and E. Witten, *Direct proof of tree-level recursion relation in Yang-Mills theory*, Phys. Rev. Lett. **94**, 181602 (2005), [hep-th/0501052](#).
- [25] W. T. Giele and E. W. N. Glover, *Higher order corrections to jet cross-sections in $e^+ e^-$ annihilation*, Phys. Rev. D **46**, 1980 (1992).

- [26] Z. Kunszt, A. Signer and Z. Trocsanyi, *Singular terms of helicity amplitudes at one loop in QCD and the soft limit of the cross-sections of multi-parton processes*, Nucl. Phys. B **420**, 550 (1994), [hep-ph/9401294](#).
- [27] Z. Bern, V. Del Duca, L. J. Dixon and D. A. Kosower, *All non-maximally-helicity-violating one-loop seven-gluon amplitudes in $\mathcal{N} = 4$ super-Yang-Mills theory*, Phys. Rev. D **71**, 045006 (2005), [hep-th/0410224](#).
- [28] S. Catani, *The singular behaviour of QCD amplitudes at two-loop order*, Phys. Lett. B **427**, 161 (1998), [hep-ph/9802439](#).
- [29] J. Bedford, A. Brandhuber, B. Spence and G. Travaglini, *A recursion relation for gravity amplitudes*, Nucl. Phys. B **721**, 98 (2005), [hep-th/0502146](#).
- [30] F. Cachazo and P. Svrček, *Tree level recursion relations in general relativity*, [hep-th/0502160](#).
- [31] Z. Bern, L. J. Dixon and D. A. Kosower, *On-shell recurrence relations for one-loop QCD amplitudes*, Phys. Rev. D **71**, 105013 (2005), [hep-th/0501240](#).
- [32] Z. Bern, L. J. Dixon and D. A. Kosower, *The last of the finite loop amplitudes in QCD*, Phys. Rev. D **72**, 125003 (2005), [hep-ph/0505055](#).
- [33] Z. Bern, L. J. Dixon and D. A. Kosower, *Bootstrapping multi-parton loop amplitudes in QCD*, Phys. Rev. D **73**, 065013 (2006), [hep-ph/0507005](#).
- [34] Z. Bern, N. E. J. Bjerrum-Bohr, D. C. Dunbar and H. Ita, *Recursive calculation of one-loop QCD integral coefficients*, JHEP **0511**, 027 (2005), [hep-ph/0507019](#).
- [35] D. Forde and D. A. Kosower, *All-multiplicity one-loop corrections to MHV amplitudes in QCD*, Phys. Rev. D **73**, 061701 (2006), [hep-ph/0509358](#).
- [36] C. F. Berger, Z. Bern, L. J. Dixon, D. Forde and D. A. Kosower, *Bootstrapping one-loop QCD amplitudes with general helicities*, Phys. Rev. D **74**, 036009 (2006), [hep-ph/0604195](#)
- [37] A. Brandhuber, S. McNamara, B. Spence and G. Travaglini, *Recursion relations for one-loop gravity amplitudes*, JHEP **0703**, 029 (2007), [hep-th/0701187](#).
- [38] C. Anastasiou, Z. Bern, L. J. Dixon and D. A. Kosower, *Planar amplitudes in maximally supersymmetric Yang-Mills theory*, Phys. Rev. Lett. **91**, 251602 (2003), [hep-th/0309040](#).
- [39] Z. Bern, L. J. Dixon and V. A. Smirnov, *Iteration of planar amplitudes in maximally supersymmetric Yang-Mills theory at three loops and beyond*, Phys. Rev. D **72**, 085001 (2005), [hep-th/0505205](#).

- [40] Z. Bern, M. Czakon, D. A. Kosower, R. Roiban and V. A. Smirnov, *Two-loop iteration of five-point $\mathcal{N} = 4$ super-Yang-Mills amplitudes*, Phys. Rev. Lett. **97**, 181601 (2006), hep-th/0604074.
- [41] L. F. Alday and J. M. Maldacena, *Gluon scattering amplitudes at strong coupling*, JHEP **0706**, 064 (2007), 0705.0303 [hep-th].
- [42] J. M. Drummond, G. P. Korchemsky and E. Sokatchev, *Conformal properties of four-gluon planar amplitudes and Wilson loops*, Nucl. Phys. B **795**, 385 (2008), 0707.0243 [hep-th].
- [43] A. Brandhuber, P. Heslop and G. Travaglini, *MHV amplitudes in $\mathcal{N} = 4$ Super Yang-Mills and Wilson loops*, Nucl. Phys. B **794**, 231 (2008), 0707.1153 [hep-th].
- [44] J. M. Drummond, J. Henn, G. P. Korchemsky and E. Sokatchev, *On planar gluon amplitudes/Wilson loops duality*, Nucl. Phys. B **795**, 52 (2008), 0709.2368 [hep-th].
- [45] J. M. Drummond, J. Henn, G. P. Korchemsky and E. Sokatchev, *Conformal Ward identities for Wilson loops and a test of the duality with gluon amplitudes*, 0712.1223 [hep-th].
- [46] Z. Bern, L. J. Dixon, D. A. Kosower, R. Roiban, M. Spradlin, C. Vergu and A. Volovich, *The two-loop six-gluon MHV amplitude in maximally supersymmetric Yang-Mills Theory*, Phys. Rev. D **78**, 045007 (2008), 0803.1465 [hep-th].
- [47] J. M. Drummond, J. Henn, G. P. Korchemsky and E. Sokatchev, *The hexagon Wilson loop and the BDS ansatz for the six-gluon amplitude*, Phys. Lett. B **662**, 456 (2008), 0712.4138 [hep-th].
- [48] J. M. Drummond, J. Henn, G. P. Korchemsky and E. Sokatchev, *Hexagon Wilson loop = six-gluon MHV amplitude*, 0803.1466 [hep-th].
- [49] A. Brandhuber and M. Vincon, *MHV one-loop amplitudes in Yang-Mills from generalised unitarity*, JHEP **0811**, 078 (2008), 0805.3310 [hep-ph].
- [50] D. C. Dunbar, W. B. Perkins and E. Warrick, *The unitarity method using a canonical basis approach*, JHEP **0906**, 056 (2009), 0903.1751 [hep-ph].
- [51] A. Brandhuber, G. Travaglini and M. Vincon, *A note on loop amplitudes in QED*, 0908.1306 [hep-th].
- [52] Z. Komargodski, *On collinear factorization of Wilson loops and MHV amplitudes in $\mathcal{N} = 4$ SYM*, JHEP **0805**, 019 (2008), 0801.3274 [hep-th].
- [53] J. E. Paton and H. M. Chan, Nucl. Phys. B **10** (1969) 519.

- [54] P. Cvitanovic, P. G. Lauwers and P. N. Scharbach, *Gauge invariance structure of quantum chromodynamics*, Nucl. Phys. B **186**, 165 (1981).
- [55] F. A. Berends and W. Giele, *The six gluon process as an example of Weyl-Van Der Waerden spinor calculus*, Nucl. Phys. B **294**, 700 (1987).
- [56] M. L. Mangano, S. J. Parke and Z. Xu, *Duality and multi-gluon scattering*, Nucl. Phys. B **298**, 653 (1988).
- [57] D. Zeppenfeld, *Diagonalization of color factors*, Int. J. Mod. Phys. A **3**, 2175 (1988).
- [58] Z. Bern and D. A. Kosower, *Color decomposition of one loop amplitudes in gauge theories*, Nucl. Phys. B **362**, 389 (1991).
- [59] Z. Bern, L. J. Dixon and D. A. Kosower, *One-loop corrections to two quark three gluon amplitudes*, Nucl. Phys. B **437**, 259 (1995), hep-ph/9409393.
- [60] F. A. Berends, R. Kleiss, P. De Causmaecker, R. Gastmans and T. T. Wu, *Single bremsstrahlung processes in gauge theories*, Phys. Lett. B **103**, 124 (1981).
- [61] P. De Causmaecker, R. Gastmans, W. Troost and T. T. Wu, *Multiple bremsstrahlung in gauge theories at high-energies. 1. General formalism for quantum electrodynamics*, Nucl. Phys. B **206**, 53 (1982).
- [62] R. Kleiss and W. J. Stirling, *Spinor techniques for calculating p anti- $p \rightarrow W^\pm/Z^0 + Jets$* , Nucl. Phys. B **262**, 235 (1985).
- [63] J. F. Gunion and Z. Kunszt, *Improved analytic techniques for tree graph calculations and the $G G Q$ anti- Q lepton anti-lepton subprocess*, Phys. Lett. B **161**, 333 (1985).
- [64] Z. Xu, D. H. Zhang and L. Chang, *Helicity amplitudes for multiple bremsstrahlung in massless nonabelian gauge theories*, Nucl. Phys. B **291**, 392 (1987).
- [65] S. J. Parke and T. R. Taylor, *An amplitude for n gluon scattering*, Phys. Rev. Lett. **56**, 2459 (1986).
- [66] F. A. Berends and W. T. Giele, *Recursive calculations for processes with n gluons*, Nucl. Phys. **B306**, 759 (1988).
- [67] M. T. Grisaru, H. N. Pendleton, and P. van Nieuwenhuizen, *Supergravity and the S matrix*, Phys. Rev. **D15**, 996 (1977).
- [68] M. T. Grisaru and H. N. Pendleton, *Some properties of scattering amplitudes in supersymmetric theories*, Nucl. Phys. **B124**, 81 (1977).
- [69] S. J. Parke and T. R. Taylor, *Perturbative QCD utilizing extended supersymmetry*, Phys. Lett. **B157**, 81 (1985).

- [70] B. S. DeWitt, *Quantum theory of gravity III: Applications of the covariant theory*, Phys. Rev. **162**, 1239–1256 (1967).
- [71] M. L. Mangano and S. J. Parke, *Multi-parton amplitudes in gauge theories*, Phys. Rept. **200**, 301–367 (1991), [hep-th/0509223](#).
- [72] L. J. Dixon, *Calculating scattering amplitudes efficiently*, [hep-ph/9601359](#).
- [73] L. D. Landau, *On analytic properties of vertex parts in quantum field theory*, Nucl. Phys. **13**, 181 (1959).
- [74] S. Mandelstam, *Analytic Properties Of Transition Amplitudes In Perturbation Theory*, Phys. Rev. **115**, 1741 (1959).
- [75] R. E. Cutkosky, *Singularities and discontinuities of Feynman amplitudes*, J. Math. Phys. **1**, 429 (1960).
- [76] R. J. Eden, P. V. Landshoff, D. I. Olive and J. C. Polkinghorne, *The analytic S-Matrix* (Cambridge University Press, 1966).
- [77] G. Passarino and M. J. G. Veltman, *One-loop corrections for $e^+ e^-$ annihilation into $\mu^+ \mu^-$ in the Weinberg model*, Nucl. Phys. B **160**, 151 (1979).
- [78] R. Britto, F. Cachazo and B. Feng, *Generalised unitarity and one-loop amplitudes in $\mathcal{N} = 4$ super Yang-Mills*, Nucl. Phys. B **725**, 275 (2005), [hep-th/0412103](#).
- [79] Z. Bern, L. J. Dixon and D. A. Kosower, *On-shell methods in perturbative QCD*, Annals Phys. **322**, 1587 (2007), 0704.2798 [[hep-ph](#)].
- [80] W. L. van Neerven, *Dimensional regularization of mass and infrared singularities in two-loop on-shell vertex functions*, Nucl. Phys. B **268**, 453 (1986).
- [81] Z. Bern and A. G. Morgan, *Massive loop amplitudes from unitarity*, Nucl. Phys. B **467**, 479 (1996), [hep-ph/9511336](#).
- [82] Z. Bern, L. J. Dixon, D. C. Dunbar and D. A. Kosower, *One-loop selfdual and $\mathcal{N} = 4$ super Yang-Mills*, Phys. Lett. B **394**, 105 (1997), [hep-th/9611127](#).
- [83] A. Brandhuber, S. McNamara, B. Spence and G. Travaglini, *Loop amplitudes in pure Yang-Mills from generalised unitarity*, JHEP **0510**, 011 (2005), [hep-th/0506068](#).
- [84] Z. Bern, L. J. Dixon and D. A. Kosower, *One-loop corrections to five gluon amplitudes*, Phys. Rev. Lett. **70**, 2677 (1993), [hep-ph/9302280](#).
- [85] S. D. Badger, E. W. N. Glover, V. V. Khoze and P. Svrcek, *Recursion relations for gauge theory amplitudes with massive particles*, JHEP **0507**, 025 (2005), [hep-th/0504159](#).

- [86] Z. Bern and D. A. Kosower, *The computation of loop amplitudes in gauge theories*, Nucl. Phys. B **379**, 451 (1992).
- [87] S. D. Badger, E. W. N. Glover and V. V. Khoze, *Recursion relations for gauge theory amplitudes with massive vector bosons and fermions*, JHEP **0601**, 066 (2006), hep-th/0507161.
- [88] Z. Bern, L. J. Dixon and D. A. Kosower, *One-loop amplitudes for $e^+ e^-$ to four partons*, Nucl. Phys. B **513**, 3 (1998), hep-ph/9708239.
- [89] Z. Bern, M. Czakon, L. J. Dixon, D. A. Kosower and V. A. Smirnov, *The four-loop amplitude and cusp anomalous dimension in maximally supersymmetric Yang-Mills Theory*, Phys. Rev. D **75**, 085010 (2007), hep-th/0610248.
- [90] Z. Bern, J. J. M. Carrasco, H. Johansson and D. A. Kosower, *Maximally supersymmetric planar Yang-Mills amplitudes at five loops*, Phys. Rev. D **76**, 125020 (2007), 0705.1864 [hep-th].
- [91] S. J. Bidder, N. E. J. Bjerrum-Bohr, D. C. Dunbar and W. B. Perkins, *One-loop gluon scattering amplitudes in theories with $\mathcal{N} < 4$* , Phys. Lett. B **612**, 75 (2005), hep-th/0502028.
- [92] D. Forde, *Direct extraction of one-loop integral coefficients*, Phys. Rev. D **75**, 125019 (2007), 0704.1835 [hep-ph].
- [93] G. Mahlon, *Multi-gluon helicity amplitudes involving a quark loop*, Phys. Rev. D **49**, 4438 (1994), hep-ph/9312276.
- [94] Z. Bern, G. Chalmers, L. J. Dixon and D. A. Kosower, *One-loop n -gluon amplitudes with maximal helicity violation via collinear limits*, Phys. Rev. Lett. **72**, 2134 (1994), hep-ph/9312333.
- [95] A. Brandhuber, B. Spence, G. Travaglini and K. Zoubos, *One-Loop MHV rules and pure Yang-Mills*, JHEP **0707**, 002 (2007), 0704.0245 [hep-th].
- [96] Z. Bern, L. J. Dixon and D. A. Kosower, *All next-to-maximally-helicity-violating One-Loop amplitudes in $\mathcal{N} = 4$ super Yang-Mills theory*, Phys. Rev. D **72**, 045014 (2005), hep-th/0412210.
- [97] S. J. Bidder, D. C. Dunbar and W. B. Perkins, *Supersymmetric Ward identities and NMHV amplitudes involving gluinos*, JHEP **0508**, 055 (2005), hep-th/0505249.
- [98] S. J. Bidder, W. B. Perkins and K. Risager, *One-loop NMHV amplitudes involving gluinos and scalars in $\mathcal{N} = 4$ gauge theory*, JHEP **0510**, 003 (2005), hep-th/0507170.

- [99] R. Britto, F. Cachazo and B. Feng, *Computing one-loop amplitudes from the holomorphic anomaly of unitarity cuts*, Phys. Rev. D **71**, 025012 (2005), hep-th/0410179.
- [100] S. J. Bidder, N. E. J. Bjerrum-Bohr, L. J. Dixon and D. C. Dunbar, *$\mathcal{N} = 1$ Supersymmetric one-loop amplitudes and the holomorphic anomaly of unitarity cuts*, Phys. Lett. B **606**, 189 (2005), hep-th/0410296.
- [101] R. Britto, E. Buchbinder, F. Cachazo and B. Feng, *One-loop amplitudes of gluons in SQCD*, Phys. Rev. D **72**, 065012 (2005), hep-ph/0503132.
- [102] R. Britto, B. Feng and P. Mastrolia, *The cut-constructible part of QCD amplitudes*, Phys. Rev. D **73**, 105004 (2006), hep-ph/0602178.
- [103] G. Georgiou and V. V. Khoze, *Tree amplitudes in gauge theory as scalar MHV diagrams*, JHEP **0405**, 070 (2004), hep-th/0404072.
- [104] D. A. Kosower, *Next-to-maximal helicity violating amplitudes in gauge theory*, Phys. Rev. D **71**, 045007 (2005), hep-th/0406175.
- [105] G. Georgiou, E. W. N. Glover and V. V. Khoze, *Non-MHV tree amplitudes in gauge theory*, JHEP **0407**, 048 (2004), hep-th/0407027.
- [106] G. Ossola, C. G. Papadopoulos and R. Pittau, *Reducing full one-loop amplitudes to scalar integrals at the integrand level*, Nucl. Phys. B **763**, 147 (2007), hep-ph/0609007.
- [107] N. E. J. Bjerrum-Bohr, D. C. Dunbar and W. B. Perkins, *Analytic structure of three-mass triangle coefficients*, JHEP **0804**, 038 (2008), 0709.2086 [hep-ph].
- [108] Z. Bern, L. J. Dixon and D. A. Kosower, *Dimensionally regulated pentagon integrals*, Nucl. Phys. B **412**, 751 (1994), hep-ph/9306240.
- [109] H. J. Lu and C. A. Perez, *Massless one loop scalar three point integral and associated Clausen, Glaisher and L functions*.
- [110] H. Kawai, D. C. Lewellen and S. H. H. Tye, *A relation between tree amplitudes of closed and open strings*, Nucl. Phys. B **269**, 1 (1986).
- [111] J. M. Drummond, M. Spradlin, A. Volovich and C. Wen, *Tree-level amplitudes in $\mathcal{N} = 8$ supergravity*, 0901.2363 [hep-th].
- [112] Z. Bern, N. E. J. Bjerrum-Bohr and D. C. Dunbar, *Inherited twistor-space structure of gravity loop amplitudes*, JHEP **0505**, 056 (2005), hep-th/0501137.

- [113] N. E. J. Bjerrum-Bohr, D. C. Dunbar and H. Ita, *Six-point one-loop $\mathcal{N} = 8$ supergravity NMHV amplitudes and their IR behaviour*, Phys. Lett. B **621**, 183 (2005), [hep-th/0503102](#).
- [114] A. Hall, *Supersymmetric Yang-Mills and supergravity amplitudes at one loop*, 0906.0204 [[hep-th](#)].
- [115] P. Katsaroumpas, B. Spence and G. Travaglini, *One-loop $\mathcal{N} = 8$ supergravity coefficients from $\mathcal{N} = 4$ super Yang-Mills*, 0906.0521 [[hep-th](#)].
- [116] Z. Bern, L. J. Dixon and R. Roiban, *Is $\mathcal{N} = 8$ supergravity ultraviolet finite?*, Phys. Lett. B **644**, 265 (2007), [hep-th/0611086](#).
- [117] Z. Bern, J. J. Carrasco, L. J. Dixon, H. Johansson, D. A. Kosower and R. Roiban, *Three-loop superfiniteness of $\mathcal{N} = 8$ supergravity*, Phys. Rev. Lett. **98**, 161303 (2007), [hep-th/0702112](#).
- [118] Z. Bern, J. J. Carrasco, D. Forde, H. Ita and H. Johansson, *Unexpected cancellations in gravity theories*, Phys. Rev. D **77**, 025010 (2008), 0707.1035 [[hep-th](#)].
- [119] Z. Bern, J. J. Carrasco, L. J. Dixon, H. Johansson and R. Roiban, *The ultraviolet behavior of $\mathcal{N} = 8$ supergravity at four loops*, 0905.2326 [[hep-th](#)].
- [120] M. B. Green, J. G. Russo and P. Vanhove, *Non-renormalisation conditions in type II string theory and maximal supergravity*, JHEP **0702**, 099 (2007), [hep-th/0610299](#).
- [121] M. B. Green, J. G. Russo and P. Vanhove, *Ultraviolet properties of maximal supergravity*, Phys. Rev. Lett. **98**, 131602 (2007), [hep-th/0611273](#).
- [122] G. Chalmers, *On the finiteness of $\mathcal{N} = 8$ quantum supergravity*, [hep-th/0008162](#).
- [123] N. Berkovits, *New higher-derivative R^4 theorems*, Phys. Rev. Lett. **98**, 211601 (2007), [hep-th/0609006](#).
- [124] Z. Bern, L. J. Dixon, M. Perelstein and J. S. Rozowsky, *Multi-leg one-loop gravity amplitudes from gauge theory*, Nucl. Phys. B **546**, 423 (1999), [hep-th/9811140](#).
- [125] N. E. J. Bjerrum-Bohr, D. C. Dunbar, H. Ita, W. B. Perkins and K. Risager, *The no-triangle hypothesis for $\mathcal{N} = 8$ supergravity*, JHEP **0612**, 072 (2006), [hep-th/0610043](#).
- [126] N. E. J. Bjerrum-Bohr and P. Vanhove, *Explicit cancellation of triangles in one-loop gravity amplitudes*, JHEP **0804**, 065 (2008), 0802.0868 [[hep-th](#)].
- [127] N. Arkani-Hamed, F. Cachazo and J. Kaplan, *What is the simplest quantum field theory?*, 0808.1446 [[hep-th](#)].

- [128] S. Badger, N. E. J. Bjerrum-Bohr and P. Vanhove, *Simplicity in the structure of QED and gravity amplitudes*, JHEP **0902**, 038 (2009), 0811.3405 [hep-th].
- [129] P. Benincasa, C. Boucher-Veronneau and F. Cachazo, *Taming tree amplitudes in general relativity*, JHEP **0711**, 057 (2007), hep-th/0702032.
- [130] N. Arkani-Hamed and J. Kaplan, *On tree amplitudes in gauge theory and gravity*, JHEP **0804**, 076 (2008), 0801.2385 [hep-th].
- [131] T. Binoth, E. W. N. Glover, P. Marquard and J. J. van der Bij, *Two-loop corrections to light-by-light scattering in supersymmetric QED*, JHEP **0205**, 060 (2002), hep-ph/0202266.
- [132] S. G. Naculich, H. Nastase and H. J. Schnitzer, *Two-loop graviton scattering relation and IR behavior in $\mathcal{N} = 8$ supergravity*, Nucl. Phys. B **805**, 40 (2008), 0805.2347 [hep-th].
- [133] A. Brandhuber, P. Heslop, A. Nasti, B. Spence and G. Travaglini, *Four-point amplitudes in $\mathcal{N} = 8$ supergravity and Wilson loops*, Nucl. Phys. B **807**, 290 (2009), 0805.2763 [hep-th].
- [134] A. V. Kotikov, L. N. Lipatov, A. I. Onishchenko and V. N. Velizhanin, *Three-loop universal anomalous dimension of the Wilson operators in $\mathcal{N} = 4$ SUSY Yang-Mills model*, Phys. Lett. B **595**, 521 (2004) [Erratum-ibid. B **632**, 754 (2006)], hep-th/0404092.
- [135] P. Cvitanović and T. Kinoshita, *Sixth order magnetic moment of the electron*, Phys. Rev. D **10**, 4007 (1974).
- [136] P. Cvitanović, *Acceptance speech, 1993 NKH Research Prize in Physics, Dansk Fysisk Selskab Arsmøde*.
- [137] R. Karplus and M. Neuman, *The scattering of light by light*, Phys. Rev. **83**, 776 (1951).
- [138] R. Karplus and M. Neuman, *Non-linear interactions between electromagnetic fields*, Phys. Rev. **80**, 380 (1950).
- [139] Z. Bern, A. De Freitas, L. J. Dixon, A. Ghinculov and H. L. Wong, *QCD and QED corrections to light-by-light scattering*, JHEP **0111**, 031 (2001), hep-ph/0109079.
- [140] G. Mahlon, *One loop multi-photon helicity amplitudes*, Phys. Rev. D **49**, 2197 (1994), hep-ph/9311213.
- [141] G. Mahlon, *Multi-photon production at high-energies in the Standard Model. 2*, Phys. Rev. D **47**, 1812 (1993), hep-ph/9210214.

- [142] T. Binoth, G. Heinrich, T. Gehrmann and P. Mastrolia, *Six-photon amplitudes*, Phys. Lett. B **649**, 422 (2007), hep-ph/0703311.
- [143] C. Bernicot and J. P. Guillet, *Six-photon amplitudes in scalar QED*, JHEP **0801**, 059 (2008), 0711.4713 [hep-ph].
- [144] F. Cachazo, P. Svrček and E. Witten, *MHV vertices and tree amplitudes in gauge theory*, JHEP **0409**, 006 (2004), hep-th/0403047.
- [145] K. J. Ozeren and W. J. Stirling, *MHV techniques for QED processes*, JHEP **0511**, 016 (2005), hep-th/0509063.
- [146] F. Cachazo, M. Spradlin and A. Volovich, *Iterative structure within the five-particle two-loop amplitude*, Phys. Rev. D **74**, 045020 (2006), hep-th/0602228.
- [147] L. F. Alday and J. Maldacena, *Comments on gluon scattering amplitudes via AdS/CFT*, JHEP **0711**, 068 (2007), 0710.1060 [hep-th].
- [148] C. Anastasiou, A. Brandhuber, P. Heslop, V. V. Khoze, B. Spence and G. Travaglini, *Two-loop polygon Wilson loops in $\mathcal{N} = 4$ SYM*, JHEP **0905**, 115 (2009), 0902.2245 [hep-th].
- [149] L. Magnea and G. Sterman, *Analytic continuation of the Sudakov form-factor in QCD*, Phys. Rev. D **42**, 4222 (1990).
- [150] A. H. Mueller, *On the asymptotic behavior of the Sudakov form-factor*, Phys. Rev. D **20**, 2037 (1979).
- [151] J. C. Collins, *Algorithm to compute corrections of the Sudakov form-factor*, Phys. Rev. D **22**, 1478 (1980).
- [152] A. Sen, *Asymptotic behavior of the Sudakov form-factor in QCD*, Phys. Rev. D **24**, 3281 (1981).
- [153] S. V. Ivanov, G. P. Korchemsky and A. V. Radyushkin, *Infrared asymptotics of perturbative QCD: contour gauges*, Yad. Fiz. **44**, 230 (1986), [Sov. J. Nucl. Phys. **44**, 145 (1986)].
- [154] G. P. Korchemsky and A. V. Radyushkin, *Renormalization of the Wilson loops beyond the leading order*, Nucl. Phys. B **283**, 342 (1987).
- [155] G. P. Korchemsky, *Asymptotics of the Altarelli-Parisi-Lipatov evolution kernels of parton distributions*, Mod. Phys. Lett. A **4**, 1257 (1989).
- [156] G. P. Korchemsky and G. Marchesini, *Structure function for large x and renormalization of Wilson loop*, Nucl. Phys. B **406**, 225 (1993), hep-ph/9210281.

- [157] B. Eden and M. Staudacher, *Integrability and transcendentality*, J. Stat. Mech. **0611**, P014 (2006), [hep-th/0603157](#).
- [158] N. Beisert, B. Eden and M. Staudacher, *Transcendentality and crossing*, J. Stat. Mech. **0701**, P021 (2007), [hep-th/0610251](#).
- [159] F. Cachazo, M. Spradlin and A. Volovich, *Four-loop cusp anomalous dimension from obstructions*, Phys. Rev. D **75**, 105011 (2007), [hep-th/0612309](#).
- [160] G. P. Korchemsky, *Double logarithmic asymptotics in QCD*, Phys. Lett. B **217**, 330 (1989).
- [161] S. Catani and L. Trentadue, *Resummation of the QCD perturbative series for hard processes*, Nucl. Phys. B **327**, 323 (1989).
- [162] G. Sterman and M. E. Tejeda-Yeomans, *Multi-loop amplitudes and resummation*, Phys. Lett. B **552**, 48 (2003), [hep-ph/0210130](#).
- [163] G. P. Korchemsky and A. V. Radyushkin, *Loop space formalism and renormalization group for the infrared asymptotics of QCD*, Phys. Lett. B **171**, 459 (1986).
- [164] Z. Bern, V. Del Duca and C. R. Schmidt, *The infrared behavior of one-loop gluon amplitudes at next-to-next-to-leading order*, Phys. Lett. B **445**, 168 (1998), [hep-ph/9810409](#).
- [165] D. A. Kosower and P. Uwer, *One-loop splitting amplitudes in gauge theory*, Nucl. Phys. B **563**, 477 (1999), [hep-ph/9903515](#).
- [166] Z. Bern, V. Del Duca, W. B. Kilgore and C. R. Schmidt, *The infrared behavior of one-loop QCD amplitudes at next-to-next-to-leading order*, Phys. Rev. D **60**, 116001 (1999), [hep-ph/9903516](#).
- [167] A. Brandhuber, B. Spence and G. Travaglini, *From trees to loops and back*, JHEP **0601**, 142 (2006), [hep-th/0510253](#).
- [168] D. Chakrabarti, J. Qiu and C. B. Thorn, *Scattering of glue by glue on the light-cone worldsheet. I: Helicity non-conserving amplitudes*, Phys. Rev. D **72**, 065022 (2005), [hep-th/0507280](#).
- [169] D. Chakrabarti, J. Qiu and C. B. Thorn, *Scattering of glue by glue on the light-cone worldsheet. II: Helicity conserving amplitudes*, Phys. Rev. D **74**, 045018 (2006), [Erratum-ibid. D **76**, 089901 (2007)] [hep-th/0602026](#).
- [170] S. Mandelstam, *Ultraviolet finiteness of the $\mathcal{N} = 4$ model*, In **Miami 1983, Proceedings, High-energy Physics**, 167-177.

- [171] S. Mandelstam, *Light cone superspace and the finiteness of the $\mathcal{N} = 4$ model*, In **La Jolla 1983, Proceedings, Problems in Unification and Supergravity**, 99-108.
- [172] N. E. J. Bjerrum-Bohr, D. C. Dunbar and H. Ita, *Perturbative gravity and twistor space*, Nucl. Phys. Proc. Suppl. **160**, 215 (2006), hep-th/0606268.
- [173] Z. Bern, L. J. Dixon and R. Roiban, *Is $\mathcal{N} = 8$ supergravity ultraviolet finite?*, Phys. Lett. B **644**, 265 (2007), hep-th/0611086.
- [174] Z. Bern, J. J. Carrasco, L. J. Dixon, H. Johansson, D. A. Kosower and R. Roiban, *Three-Loop superfiniteness of $\mathcal{N} = 8$ supergravity*, Phys. Rev. Lett. **98**, 161303 (2007), hep-th/0702112.
- [175] Z. Bern, J. J. M. Carrasco, L. J. Dixon, H. Johansson and R. Roiban, *Manifest ultraviolet behavior for the three-loop four-point amplitude of $\mathcal{N} = 8$ supergravity*, Phys. Rev. D **78**, 105019 (2008), 0808.4112 [hep-th].
- [176] J. M. Drummond, J. Henn, G. P. Korchemsky and E. Sokatchev, *Dual superconformal symmetry of scattering amplitudes in $\mathcal{N} = 4$ super-Yang-Mills theory*, 0807.1095 [hep-th].
- [177] A. Brandhuber, P. Heslop and G. Travaglini, *A note on dual superconformal symmetry of the $\mathcal{N} = 4$ super Yang-Mills S-matrix*, Phys. Rev. D **78**, 125005 (2008), 0807.4097 [hep-th].
- [178] M. E. Peskin and D. V. Schroeder, *An introduction to quantum field theory*. Reading, USA: Addison-Wesley, 1995.
- [179] F. Cachazo, P. Svrček, and E. Witten, *Twistor space structure of one-loop amplitudes in gauge theory*, JHEP **10**, 074 (2004), hep-th/0406177.
- [180] F. Cachazo, P. Svrček, and E. Witten, *Gauge theory amplitudes in twistor space and holomorphic anomaly*, JHEP **10**, 077 (2004), hep-th/0409245.
- [181] I. Bena, Z. Bern, and D. A. Kosower, *Twistor-space recursive formulation of gauge theory amplitudes*, Phys. Rev. **D71**, 045008 (2005), hep-th/0406133.
- [182] R. Britto, F. Cachazo, and B. Feng, *Coplanarity in twistor space of $\mathcal{N} = 4$ next-to-MHV one-loop amplitude coefficients*, Phys. Lett. **B611**, 167-172 (2005), hep-th/0411107.
- [183] I. Bena, Z. Bern, D. A. Kosower, and R. Roiban, *Loops in twistor space*, Phys. Rev. **D71**, 106010 (2005), hep-th/0410054.
- [184] V. P. Nair, *A current algebra for some gauge theory amplitudes*, Phys. Lett. B **214**, 215 (1988).